

Immunity and Arginine Deprivation in Alzheimer's Disease

by

Matthew J. Kan

Department of Immunology  
Duke University

Date: May 11, 2015

Approved:

---

Michael D. Gunn, Supervisor

---

Carol A. Colton, Supervisor

---

Garnett H. Kelsoe, Chair

---

Staci D. Bilbo

---

Michael S. Krangel

---

Mari L. Shinohara

Dissertation submitted in partial fulfillment of  
the requirements for the degree of Doctor  
of Philosophy in the Department of  
Immunology in the Graduate School  
of Duke University

2015

ABSTRACT

Immunity and Arginine Deprivation in Alzheimer's Disease

by

Matthew J. Kan

Department of Immunology  
Duke University

Date: May 11, 2015

Approved:

---

Michael D. Gunn, Supervisor

---

Carol A. Colton, Supervisor

---

Garnett H. Kelsoe, Chair

---

Staci D. Bilbo

---

Michael S. Krangel

---

Mari L. Shinohara

An abstract of a dissertation submitted in partial fulfillment of the requirements for the degree of Doctor of Philosophy in the Department of Immunology in the Graduate School of Duke University

2015

Copyright by  
Matthew J. Kan  
2015

## **Abstract**

The pathogenesis of Alzheimer's disease (AD) is a critical unsolved question, and while recent studies have demonstrated a strong association between altered brain immune responses and disease progression, the mechanistic cause of neuronal dysfunction and death is unknown. We have previously described the unique CVN-AD mouse model of AD, in which immune-mediated nitric oxide is lowered to mimic human levels, resulting in a mouse model that demonstrates the cardinal features of AD, including amyloid deposition, hyperphosphorylated and aggregated tau, behavioral changes and age-dependent hippocampal neuronal loss. Using this mouse model, we studied longitudinal changes in brain immunity in relation to neuronal loss and, contrary to the predominant view that AD pathology is driven by pro-inflammatory factors, we find that the pathology in CVN-AD mice is driven by local immune suppression. Areas of hippocampal neuronal death are associated with the presence of immunosuppressive CD11c<sup>+</sup> microglia and extracellular arginase, resulting in arginine catabolism and reduced levels of total brain arginine. Pharmacologic disruption of the arginine utilization pathway by an inhibitor of arginase and ornithine decarboxylase protected the mice from AD-like pathology and significantly decreased CD11c expression. Our findings strongly implicate local immune-mediated amino acid

catabolism as a novel and potentially critical mechanism mediating the age-dependent and regional loss of neurons in humans with AD.

There is a large interest in identifying, lineage tracing, and determining the physiologic roles of monophagocytes in Alzheimer's disease. While *Cx3cr1* knock-in fluorescent reporting and Cre expressing mice have been critical for studying neuroimmunology, mice that are homozygous null or hemizygous for CX3CR1 have perturbed neural development and immune responses. There is, therefore, a need for similar tools in which mice are CX3CR1<sup>+/+</sup>. Here, we describe a mouse where Cre is driven by the *Cx3cr1* promoter on a bacterial artificial chromosome (BAC) transgene (*Cx3cr1-CreBT*) and the *Cx3cr1* locus is unperturbed. Similarly to *Cx3cr1*-Cre knock-in mice, these mice express Cre in Ly6C<sup>-</sup>, but not Ly6C<sup>+</sup>, monocytes and tissue macrophages, including microglia. These mice represent a novel tool that maintains the *Cx3cr1* locus while allowing for selective gene targeting in monocytes and tissue macrophages.

The study of immunity in Alzheimer's requires the ability to identify and quantify specific immune cell subsets by flow cytometry. While it is possible to identify lymphocyte subsets based on cell lineage-specific markers, the lack of such markers in brain myeloid cell subsets has prevented the study of monocytes, macrophages and dendritic cells. By improving on tissue homogenization, we present a comprehensive protocol for flow cytometric analysis that allows for the identification of several cell

types that have not been previously identified by flow cytometry. These cell types include F4/80<sup>hi</sup> macrophages, which may be meningeal macrophages, IA/IE<sup>+</sup> macrophages, which may represent perivascular macrophages, and dendritic cells. The identification of these cell types now allows for their study by flow cytometry in homeostasis and disease.

## **Dedication**

To my parents, Caroline, Jenny, and Singa, the shaky cat.

# Contents

Abstract .....	iv
List of Tables.....	xi
List of Figures.....	xii
Acknowledgements.....	xiv
1. Introduction.....	1
1.1 Clinical Features of Alzheimer’s Disease.....	4
1.2 Amyloid Cascade Hypothesis.....	6
1.3 The Role of Immunity in AD.....	9
1.4 Mouse Models of Alzheimer’s Disease.....	11
1.5 CVN-AD Mice.....	13
2. Arginine deprivation and immune suppression in a mouse model of Alzheimer’s disease .....	16
2.1 Introduction.....	16
2.2 Materials and Methods.....	18
2.3 Results.....	26
2.3.1 Immune suppression is an early feature of disease progression.....	26
2.3.2 CVN-AD mice show progressive cellular inflammation with CD11c <sup>+</sup> microglia in areas of beta-amyloid deposition.....	30
2.3.3 CD11c <sup>+</sup> microglia show an immunosuppressive phenotype.....	36
2.3.4 CVN-AD pathology is associated with increased arginine utilization and decreased brain arginine bioavailability.....	39
2.3.5 Blockade of arginine utilization reverses memory loss.....	43

2.4 Discussion .....	47
3. Gene targeting of monocytes, microglia, and tissue macrophages with <i>Cx3cr1</i> -BAC-Cre mice.....	55
3.1 Introduction .....	55
3.2 Methods and Materials.....	57
3.3 Results.....	59
3.3.1 Cre is preferentially expressed in Ly6C <sup>low</sup> monocytes in <i>Cx3cr1-CreBT</i> mice ...	59
3.3.2 Cre is expressed in tissue macrophages of <i>Cx3cr1-CreBT</i> mice.....	62
3.3.3. Cre expression in dendritic cells of <i>Cx3cr1-CreBT</i> mice .....	66
3.3.4. Selective depletion of resident monocytes and microglia in <i>Cx3cr1-CreBT:DTR</i> mice .....	69
3.4 Discussion .....	73
4. Comprehensive flow cytometric analysis of immune cells to identify dendritic cells and novel macrophage populations in the murine brain .....	77
4.1 Introduction .....	77
4.2 Materials and Methods.....	79
4.3 Results.....	81
4.3.1 Identification and surface phenotyping of brain immune cells .....	81
4.3.2 <i>Cx3cr1</i> is expressed on all brain myeloid cells.....	86
4.3.3 Blood sampling ability and lineage tracing of brain myeloid cells .....	88
4.4 Discussion .....	92
5. Discussion .....	98
5.1 Arginase in Alzheimer's Disease .....	99

5.2 Arginase in CVN-AD Mice .....	104
5.3 Immune Suppression in Other Models of Alzheimer’s Disease .....	106
5.4 Origin and Functions of CD11c <sup>+</sup> Microglia in CVN-AD mice .....	108
5.5 Applications of Cx3cr1-CreBT Mice .....	114
5.6 Applications of Murine Brain Immune Characterization .....	118
5.7 Concluding Thoughts.....	120
References .....	121
Biography.....	146

## List of Tables

Table 1: Gene expression in CVN-AD CD11c <sup>+</sup> microglia compared to CVN-AD CD11c <sup>-</sup> microglia, C57Bl/6 microglia, and <i>mNos2<sup>-/-</sup></i> microglia.....	37
Table 2: Summary of cell surface marker expression on brain myeloid cells.....	88

## List of Figures

Figure 1: Expression of immune-related genes from whole brain lysates .....	27
Figure 2: CVN-AD amyloid deposition is associated with cells expressing characteristic markers of microglia. ....	33
Figure 3: CD11c <sup>+</sup> cells from CVN-AD brains have a microglial phenotype .....	35
Figure 4: CVN-AD pathology is associated with arginase-1.....	40
Figure 5: CVN-AD brains have decreased total L-arginine bioavailability and increased expression of arginine transporters.....	42
Figure 6: CVN-AD memory deficits and pathology are reversed by an inhibitor of arginine utilization. ....	45
Figure 7: Simplified schematic of arginine catabolism and the actions of difluoromethylornithine (DFMO) to block arginine utilization. ....	51
Figure 8: Flow cytometry gating on peripheral blood cell populations. ....	61
Figure 9: <i>Cx3cr1</i> -BAC-Cre is expressed preferentially in Ly6C <sup>low</sup> monocytes .....	62
Figure 10: <i>Cx3cr1-CreBT</i> :GFP is expressed in tissue macrophages by flow cytometry .....	64
Figure 11: <i>Cx3cr1-CreBT</i> :tdTomato is expressed in tissue macrophages by histology .....	66
Figure 12: Flow cytometry gating on dendritic cell populations.....	67
Figure 13: <i>Cx3cr1-CreBT</i> :GFP is expressed in dendritic cells .....	69
Figure 14: Selective depletion of myeloid cells in <i>Cx3cr1-CreBT</i> -DTR mice .....	71
Figure 15: Flow cytometric analysis of brain immune cells .....	83
Figure 16: MHC-II and CD11c expression in brain macrophages and dendritic cells .....	85
Figure 17: Figure 17: Quantification of brain immune cell subtypes .....	86
Figure 18: Figure 18: Brain myeloid cell expression of GFP in <i>Cx3cr1</i> <sup>GFP/wt</sup> mice .....	87

Figure 19: Figure 19: Blood sampling ability and lineage tracing of brain myeloid cells .90

Figure 20: Fig. 20 Heat map from Agilent microarray analysis of gene expression in monocytes, yolk sac MΦ, and microglia (MG). .....111

Figure 21: Figure 21: *Cx3cr1-CreBT:Csf1<sup>fllox/fllox</sup>* mice lack Ly6C<sup>lo</sup> resident monocytes .....116

## Acknowledgements

Thank you, Dr. Dee Gunn, for your many years of support, for always challenging me to become a better and more rigorous scientist, and for dramatically improving my writing ability. Thank you for helping me become an expert in flow cytometry and for teaching me the skills to answer any question. It has been truly been an honor and privilege to learn from one of the best.

Thanks, Dr. Carol Colton for teaching me how to dream big as a scientist, for the pleasure of participating in this small part of an incredible story, and for your incredible mentorship. You has gone above and beyond to help me further my career, including sending me to a small neuroimmunology conference in Germany when I had no data to present, just so that I could meet and learn from the experts.

I'd like to thank all the members, past and present, of the Gunn Lab: Dr. Andrea Yu, Danielle Hotten, Dr. Min-nung Huang, Dr. Barbara Lipes, and Dr. Emily O'Koren. Andrea and I shared an office for the duration of my PhD, and she has been such an important advisor and confidante to me. She is always willing to share her wisdom, dissuade me conducting from fruitless experiments, and together, we have accomplished some exceedingly difficult experiments. She is an amazing scientist and role model.

In the Colton lab, I have appreciated the support and efforts of Dr. Michael Vitek, Angela Everhart, Joan Wilson, Marilyn Jansen, and Jennifer Lee. Dr. Vitek, in particular, has been a continued source of inspiration, counsel, and entertainment.

Thanks to the Department of Immunology, and in particular, my thesis committee members, who have been instrumental to my education. Dr. Kelsoe very generously invited me to his lab journal club for the duration of my PhD, ensuring that I would not neglect my B cell knowledge while working on innate immunity. Dr. Bilbo, the only other microglial biologist at Duke, has been such a tremendous resource for me. Collaborating with members of her lab has been a privilege. Thanks to Dr. Shinohara for her eagerness to talk about our shared love of innate immunity and for being a great travel companion in Germany. Thanks to Dr. Krangel for running a tight ship for our department, for always helping to make our graduate program stronger, and for his professional counsel, particularly during our time on the search committee.

I thank the phenomenal staff of the Duke Medical Scientist Training Program: Drs. Christopher Kontos, Ann West, and Dona Chikaraishi, and our Assistant Director, Andrea Lanahan. The path of an MD-PhD student is long and treacherous, and I could not have done it without their support and guidance, and the uncountable ways in which they have enriched my career.

Thanks to the Duke Human Vaccine Institute Flow Cytometry Facility, and to Dr. John Whitesides and Patrice McDermott for taking care of the most important resources

for our experiments, and for helping us learn how to sort exceedingly small numbers of cells.

Thanks to Dr. Laura Kus and the GENSAT Program at Rockefeller University for sending us the *Cx3cr1*-CreBT mice.

Lastly, I would like to the Wakeman Endowment and the National Institutes of General Medical Sciences for funding my academic career at Duke, as well as the Frank H. and Eva B. Buck Foundation for their continued support of my education.

# 1. Introduction

I have not had any family members or loved ones with Alzheimer's disease (AD), but AD has been a fixture of my medical and graduate school career. During my first year of medical school, a small group of classmates and I were on call to attend an autopsy. I remember that our autopsy was atypical in that it was scheduled by an outside hospital, so unlike other groups that did not know the cause of death for their patient, we knew from the chart that this elderly woman had passed away from pneumonia secondary to Alzheimer's disease. I read through her records, discovering that she had lived a very healthy lifestyle, eating healthy foods, and even ran regularly with friends until her seventies. Yet, despite these interventions, her memory began to decline and she died from aspiration pneumonia. We observed her autopsy, and later went to neuropathology rounds to see Dr. Christine Hulette perform a gross dissection of her atrophied brain. Upon histologic analysis of brain sections, we observed prominent beta amyloid plaques and she was found to have Alzheimer's disease with Lewy bodies. As we presented to our colleagues about her case and what little knowledge a medical student should know about Alzheimer's disease, I felt intellectual and emotional dissatisfaction. How could it be that she lived such an ideal lifestyle, yet still succumbed to this disease? How could there be no disease modifying treatments?

On my first day of core clinical rotations, I worked at an outpatient clinic in Roxboro, North Carolina. I met a woman who had been brought to the clinic from a

nursing facility for an annual exam. As I interviewed her, she appeared in distress. She said that she could no longer remember events of the last day or week. She knew that her son had come to visit her recently, but when? She could not remember the last time she ate. However, the woman could recall that she used to be prized for her memory. She ran away from an abusive home at the age of 18, joined the military in World War II, and eventually became an aide to General Dwight Eisenhower. The dichotomy between who she once was and who she had become was so upsetting to her that she admitted to me that if not for her Catholic faith, she would end her life. The visit ended on a slightly happier note as she cried, telling me that recalling her youth reminded her of life's worth and helped her reconsider her feelings. Yet, I knew that these she would carry these conflicting emotions for the rest of her life.

At the end of my clinical rotations, I took an elective in palliative care, where I learned the burdens of the caretaker. I was working at a skilled nursing facility, where a husband was visiting his wife with severe memory loss from AD. At first he had tried to take care of her on his own, hoping that familiar environments with loved ones would aid her memory. However, he was also elderly with his own medical ailments, and when her memory regressed, he admitted her to a nursing facility. As is typical in the course of AD, her memory improved and he felt like she could live at home again. Unfortunately, after bringing her home, she rapidly declined, and unable to care for her himself, he returned her to the facility. That day, I saw that she knew her husband loved

her and that he was a safe person. But, she could not recall many details about him or their children. When I asked him how he felt, he took a photo out of his wallet. It was a picture of his wife that he had been carrying for over sixty years. Six decades ago, he lived in Durham, and one evening he walked for four hours to a dance in Hillsborough. Four hours! At that dance, he met his future wife and she gave him photo of herself so that he would remember her. He told me, "How she is today is the only version that you see and know. But when I look at her, even though she does not remember everything, I see her as the beautiful woman that I met over 60 years ago."

When I began graduate school, I was not interested in AD. However, when my advisor, Dr. Gunn asked me what I wanted to study during my PhD, for some reason the first thing that came to mind was that during my first year of medical school I learned about immune cells of unknown tissue origin that could eat large holes in the brain during inflammation. He showed me some preliminary data from an uncharacterized line of mice that suggested that maybe we had a tool to study those cells. Later, in my quest to better understand the different immune cells of the brain, Dr. Gunn introduced me to Dr. Colton, who had been working for some time on a novel mechanism to explain the pathogenesis of AD, but lacked the tools to identify the pathologic cells that she had found. Perhaps due to my lack of preconception in AD pathogenesis, I found her arguments compelling. The work presented here on a novel

theory of disease pathogenesis in AD and new tools to study neuroimmunology are the result of that collaboration.

## **1.1 Clinical Features of Alzheimer's Disease**

Alzheimer's is a disease of aging characterized by a progressive decline in memory and behavior changes that eventually lead to death. There are two major forms of AD. Familial, or early onset, AD represents a small subset of the disease (<5%) and presents around the fifth and sixth decade of life. The majority of patients with familial AD have a mutation in the genes encoding amyloid precursor protein (APP) or presenilin (PSEN) 1 or 2. Late onset AD (LOAD), which encompasses the majority of cases, typically does not develop before the age of 65, and the majority of cases in LOAD are sporadic or idiopathic (Morris et al., 2014). While variations in many genes have been found to increase susceptibility to AD, they have incomplete penetrance. For example, the APOE4 allele (~2% of U.S. population) confers the highest single gene risk for LOAD, yet only 30-50% of individuals who are homozygous for APOE4 develop AD by age 85 (Genin et al., 2011). Instead, it appears that a host of genetic and environmental factors contribute to disease development. The symptoms exhibited in AD are very heterogeneous, and although features of familial and late onset AD are similar, there is some debate as to whether these are diseases with the same etiology.

The clinical diagnosis of Alzheimer's disease is based on symptoms and the ruling out other etiologies of dementia, such as vascular, Lewy body, or fronto-temporal dementia. Gradual decline of memory loss is the earliest symptom and the central feature of Alzheimer's disease. However, a wide range of other behavioral changes may manifest, including language dysfunction and sleep disturbances, and in late stages of disease, symptoms may include loss of executive function, loss of judgment, and personality changes (Webster et al., 2014). A short form of memory assessment is typically done with the Mini-Mental State Examination or Montreal Cognitive Assessment (MoCA) tests (Nasreddine et al., 2005). Eventually, cognitive decline in results in inability to perform tasks associated with daily living, including feeding, cleaning, and dressing, and most AD patients succumb to malnutrition or infection.

Final diagnosis of the disease is made on autopsy based on the presence of beta amyloid ( $A\beta$ ) protein, Braak staging of tau neurofibrillary tangles (NFT), and pathologic score of neuritic plaques. Braak staging is broken into Stage I-II, where NFT are limited to the entorhinal cortex, Stage III-IV, where NFT have spread into the limbic system and medial temporal lobe, and Stage V-VI, where NFT have spread into other cortical areas (Braak et al., 2011). This histologic staging system loosely correlates with clinical symptoms of pre-clinical, early, and late stage AD. As discussed later, the use of these histologic findings, which have no proven causative roles in AD, may confound our understanding the etiology of AD.

There are no disease modifying treatments that alter the progression or reverse clinical outcome for AD. However, there are five FDA approved drugs for the management of symptoms: donepezil, galantamine, memantine, rivastigimine and tacrine. These drugs are all anti-cholinesterases and work to increase acetylcholine in the brain, although they have limited clinical effects (Wang et al., 2015). In addition to lack of treatment, the societal burdens of AD are profound. As alluded to above, the emotional impact of being a caregiver cannot be understated. As human lifespan increases and societies shift towards aging populations, particular in the developing world, the prevalence of AD is expected to grow dramatically. In the United States alone, there are an estimated 5.3 million individuals with AD in 2015, and AD is the sixth leading cause of death (Hebert et al., 2013). There is therefore an urgent need for better understanding of AD to develop therapies that reverse or halt progression of AD.

## ***1.2 Amyloid Cascade Hypothesis***

The mechanism of brain atrophy and neuronal cell loss in AD has not been clearly determined. The major hypothesis in the field, known as the amyloid cascade hypothesis, is that the accumulation of beta amyloid ( $A\beta$ ) peptides within the brain parenchyma or at cerebral blood vessels is toxic and leads to the other key features of AD: neurofibrillary tangles composed of hyperphosphorylated tau, synaptic dysfunction, cognitive loss and neuronal death (Glennner and Wong, 1984; Masters,

1984). This theory was born out of observations from early onset AD, which is associated with mutations in *APP* and *PSEN1* and *PSEN2*. APP is cleaved into smaller fragments by three secretases ( $\alpha$ ,  $\beta$ , and  $\gamma$ ), of which A $\beta$  is one of these fragments. Mutations in *PSEN1* and *PSEN2* result in changes to the catalytic core of  $\gamma$ -secretase. Amyloid plaques are composed largely of A $\beta$  peptides (Levy-Lahad et al., 1995a; Levy-Lahad et al., 1995b; Sherrington et al., 1995). These observations suggested that AD might be caused by improper processing of APP. This was supported by the findings in Down's syndrome, which results from triplication of chromosome 21. The *APP* locus is on chromosome 21 and a large proportion of patients with Down's syndrome go on to develop AD-like symptoms starting in their 40s, although the formation of plaques may begin as early as 8 years of age (Zigman et al., 2008).

The majority of findings that A $\beta$  induces neurotoxicity are derived from *in vitro* experiments. However, the direct relationship of A $\beta$  to neuronal death in humans AD and animal models, has been elusive. As described below, mouse models with transgenic expression of human *APP* or *PSEN1* do not typically develop NFT or neuronal death. Moreover, the mutations found in early onset AD are rare and do not occur in late onset AD, suggesting that other factors may play a role in LOAD. As a result of the focus of the field on this major hypothesis, a number of therapies have been designed to co-opt the immune system to clear A $\beta$  and have reached phase 2 or 3 of clinical trials (Morris et al., 2014). These strategies include active and passive

immunization resulting in anti-A $\beta$  antibodies. While some of these treatments have been effective in decreasing brain levels of A $\beta$  as measured by MRI, these compounds have not been successful in changing clinical outcome. Indeed, some of these attempts have resulted in unintended side effects, such as encephalitis (AN1792, active immunization) (Boche et al., 2010), focal inflammation (gantenerumab) (Ostrowitzki et al., 2012), or even increased cognitive decline (solamezumab) (Doody et al., 2014).

As discussed above, the use of histologic criteria for diagnosis of Alzheimer's disease is potentially confusing when the functions of these proteins are unknown. In fact, ~40% of the non-demented elderly have some form of pathology that meet Braak staging for AD at death (Price et al., 2009). Some non-demented individuals have equivalent levels of A $\beta$ , as measured by MRI, as individuals with AD (Rentz et al., 2010). Moreover, the amyloid cascade hypothesis does not offer a sufficient explanation of the spatial and temporal progression of AD. Amyloid deposition has been shown to plateau in AD (Engler et al., 2006), whereas other findings, such as NFT and the accumulation of microglia, continue to increase with worse cognitive decline (Ingelsson et al., 2004). Together, these findings, along with the observations from clinical trials to remove A $\beta$ , suggest that the role of A $\beta$  in LOAD may not be as direct as previously thought.

### **1.3 The Role of Immunity in AD**

There is overwhelming evidence that brain immunity is profoundly affected in AD. It has long been observed in AD histology that there are reactive immune cells with the morphology of microglia with high expression of MHC-II and CD11c (McGeer et al., 1987). Multiple genome wide association studies (GWAS) have linked sequence variations in specific immune genes to increased risk for AD, including *HLA-DRB5*–*HLA-DRB1*, *CR1*, *CLU*, *INPP5D*, *BIN1*, *IL10*, *CD33*, and *TREM2* (Guerreiro et al., 2013; Jonsson et al., 2013a; Kamboh et al., 2012a; Lambert et al., 2013; Lio et al., 2003). Allelic differences in *APOE*, which encodes apolipoprotein E, have the highest predictive value for development of AD (Strittmatter et al., 1993). There are three alleles for *APOE* (2, 3, and 4), of which homozygosity for *APOE4* confers the highest risk. Despite this association, the role of APOE in AD pathogenesis is unclear. While there is evidence that it may participate in the clearance of beta amyloid as an A $\beta$  binding partner, APOE also plays a role in suppressing TNF production (Laskowitz et al., 1997). Specific ApoE alleles also confer risk for outcome in murine models of sepsis (Wang et al., 2009) and alter the innate immune response (Vitek et al., 2009). An APOE mimetic that suppresses TNF has been used to successfully reverse damage in models of traumatic brain injury, cerebral ischemia, and AD (Hoane et al., 2009; Hoane et al., 2007; Kaufman et al., 2010; Laskowitz et al., 2012; Laskowitz et al., 2007; Tikhovskaya et al., 2009; Vitek et al., 2012), suggesting that ApoE may exert its effects on AD pathogenesis through modulating immunity.

Recently, an integrated analysis comparing gene expression in various brain regions between 376 LOAD and 173 non-demented brain samples demonstrated that immune and microglial gene networks have the strongest association with AD neuropathology. Additionally, it was found that the most central node in immune pathways involves the inhibitory signaling molecule TREM2 and its intracellular adaptor DAP12 (Zhang et al., 2013a). This study also highlighted the complexity of the immune response in the end stage of AD, where there are increased levels of multiple pro- and anti-inflammatory cytokines, chemokines, and members of the complement cascade. These findings support by the most compelling evidence that immunity plays a causative role in AD, as rare sequence variations in TREM2 have been found to confer increased risk for AD (Guerreiro et al., 2013; Jonsson et al., 2013a). The functional outcomes of these variations have yet to be determined, but the study highly implicates a contributory role for immunity in AD pathogenesis.

Despite these findings, we still lack a clear understanding of the precise role that immunity plays in AD pathogenesis (Wyss-Coray, 2006). There is substantial debate as to whether inflammatory cells play a pathologic or protective role in AD, and whether these immune cells are brain resident or recruited. Studies have demonstrated increased expression of classical pro-inflammatory mediators in patients diagnosed with AD, suggesting that A $\beta$  activates immune cells to produce inflammatory mediators that initiate neuronal death. However, as we and others have previously shown, the

immune response in AD is complex. mRNA levels for factors that typically suppress immunity, such as arginase, are increased in human AD (Colton et al., 2006; Hansmannel et al., 2010). In addition, a significant fraction of the genes identified by GWAS, including *Bin1*, *ApoE*, *Cr1*, *Il10* and *CD33*, have anti-inflammatory functions (Kamboh et al., 2012a). How these changes in immunity affect neuronal cell loss and pathology in human AD remains unclear.

#### **1.4 Mouse Models of Alzheimer's Disease**

There has been extensive work in the field to generate mouse models of AD. The constructs, methods of assessment, behavior, and pathologies of these models have been previously reviewed in great detail (Colton et al., 2006; Webster et al., 2014; Wilcock and Colton, 2008; Wilcock et al., 2011b). These models largely rely on the transgenic expression of mutated human *APP*, derived from patients with early onset AD, under a variety of promoters expressed in the brain, such as *PrP*, *PDGF*, and *Thy1*. Differences in the selection of promoters and mutation result in varied levels of relative expression of *hAPP*, ranging from 0.5-18 fold change (Wilcock and Colton, 2008) compared to normal mouse *App*. As a result, these mice exhibit different kinetics and properties in soluble and insoluble amyloid deposition.

In mice, transgenic expression of mutated *hAPP*, by itself, leads to substantial A $\beta$  deposition and behavioral deficits, but does not commonly lead to neuronal cell loss or

tau pathology that are characteristics of humans with AD. As a result, many mouse models of AD have been called “incomplete” models of human AD (Irizarry et al., 1997b; Radde et al., 2008b). Assessment of AD-like symptoms in most disease models is therefore limited to the presence of A $\beta$  or behavior tests, such as assessment of spatial memory, episodic memory, attention, and depression. In an effort to improve upon these phenotypes, mice have been generated with mutations in other proteins that cause early onset AD or fronto-temporal dementia, such as presenilin and tau. These mice include the commonly used APP/PS1, 3xTgAD, and 5xFAD strains (Webster et al., 2014). However, these mice with multiple mutations also exhibit limited expression of tau and no significant neuronal death (Wilcock and Colton, 2008). Additionally, the mutations used to create these mice, which do not co-occur in human disease, have effects independent of beta amyloid processing, which may confound the interpretation of findings in these mice. Mouse models are typically used as pre-clinical models of therapy, but as most of these models do not exhibit neuronal loss, the endpoints of these studies are typically limited to beta amyloid levels and behavior changes. There are few mouse models of AD that do not incorporate a mutation derived from human familial (early onset) AD, and this creates further complications for the assessment of therapies intended for use in late onset AD.

## **1.5 CVN-AD Mice**

We have recently described a mouse model that exploits a critical difference in mouse and human immunity, which results in a more clinically faithful model of AD. Immunity in mice and humans varies in many respects (Mestas and Hughes, 2004b; Seok et al., 2013), particularly in macrophage biology. In response to pro-inflammatory stimuli, such as IFN- $\gamma$  and LPS, mouse macrophages readily express inducible nitric oxide synthase (iNOS; NOS2) and nitric oxide (NO); however, in response to the same mediators, human monocytes and macrophages produce very little iNOS and NO. Due to pre- and post-transcriptional modifications, iNOS protein is repressed in humans, but not in mice, resulting in altered immune responses and lower NO levels (Colton et al., 2008; Geller and Billiar, 1998; Weinberg, 1998; Wink et al., 2011). Additionally, human NOS2 mRNA is actively repressed by miR-939, which is present in both mouse and humans but is only able to bind the 3' untranslated region of human NOS2 (Guo et al., 2012).

These observations in peripheral macrophages are also true for brain-resident microglia (Colton et al., 1996) and we, and others, have reported no significant expression of *Nos2* mRNA in human LOAD (Colton et al., 2006; Zhang et al., 2013a). We have phenocopied human expression of NO by creating mice that express a single transgene for human amyloid precursor protein (APP) on a *Nos2*-deficient background. Specifically, the mice express the human Swedish K670N/M671L vasculotropic

Dutch/Iowa E693Q/D694N mutations in human APP under control of the *Thy1* promoter (*APP<sup>SwDI</sup>*). These *APP<sup>SwDI</sup>-Nos2<sup>-/-</sup>* (CVN-AD) mice develop age-related AD-like pathology, including A $\beta$  plaques, phosphorylated tau protein, spatial memory impairments, and significant hippocampal neuronal death (Colton et al., 2006; Colton et al., 2008; Wilcock et al., 2008). CVN-AD mice also exhibit decreased cortical volume and increased ventricular volume compared to *Nos2<sup>-/-</sup>* controls as measured by MRI (unpublished data). As CVN-AD mice exhibit the major features of AD, we believe that they represent an improved mouse model for investigating the etiology of neurodegeneration.

Here, I present a detailed time-course analysis of the changes in immune responsiveness in CVN-AD mice and describe how this leads to a novel hypothesis of AD pathophysiology. CVN-AD mice develop neuropathology in an age-dependent fashion that mimics the progression of human AD. This neuropathology includes the accumulation of a population of CD11c<sup>+</sup> microglia in the cortex and hippocampus, predominant expression of immunosuppressive genes, and local production of extracellular arginase. Arginase results in decreased arginine bioavailability in the brain, and inhibition of arginine utilization enzymes reverses AD-like pathology and memory impairments in these mice. Together, these findings suggest that AD may be a disease of local immune suppression, rather than pro-inflammatory activation, and that the cause of neuronal death in AD is chronic immune-mediated amino acid catabolism resulting in

nutrient deprivation. Additionally, I describe novel tools for the genetic manipulation and identification of brain immune cells that will potentially allow for novel studies in Alzheimer's disease and neuroimmunology.

## **2. Arginine deprivation and immune suppression in a mouse model of Alzheimer's disease**

### **2.1 Introduction**

Alzheimer's disease (AD) is a disease of aging associated with accumulation of beta amyloid (A $\beta$ ) peptides within the brain parenchyma and cerebral blood vessels and hyper-phosphorylated and aggregated tau within neurons. While the mechanisms causing brain atrophy and neuronal loss are unknown, increasing evidence suggests that immunity plays a critical role in AD pathogenesis. Genome wide association studies (GWAS) have linked immune genes to increased risk for AD (Kamboh et al., 2012b). Recently, an integrated analysis of AD-associated genes demonstrated AD neuropathology has the strongest association with changes in immune and microglial gene networks (Zhang et al., 2013a). Despite this, the specific mechanisms by which immunity contributes to AD pathogenesis have not yet been identified. While some studies have demonstrated increased expression of classical pro-inflammatory mediators in human AD, the inflammatory milieu also includes immunosuppressive components (Colton et al., 2006). These immunosuppressive factors are consistent with the brain's status as an immune privileged site (Carson et al., 2006; Mellor and Munn, 2008; Ransohoff and Cardona, 2010), and the contribution of immunosuppression to neuronal cell loss and other AD pathology remains largely unexplored.

In mice, transgenic expression of mutated human  $\beta$ -amyloid precursor protein (APP), by itself, leads to substantial  $A\beta$  deposition and behavioral deficits, but does not commonly lead to tau pathology or neuronal death. As a result, mouse models of AD have been called “incomplete” models of human AD (Irizarry et al., 1997a; Radde et al., 2008a). In contrast, we have previously reported that CVN-AD mice, which are *mNos2*-deficient and transgenic for the Swedish K670N/M671L vasculotropic Dutch/Iowa E693Q/D694N mutant (APPSwDI) APP, display the cardinal characteristics of AD progression, including  $A\beta$  plaques, phosphorylated tau protein, spatial memory impairments, and significant hippocampal neuronal death (Colton et al., 2008; Colton et al., 2014; Wilcock et al., 2008). The prevention of iNOS protein expression in this model recapitulates the biology of human myeloid cells, which produce relatively little iNOS and nitric oxide (Colton et al., 2008; Geller and Billiar, 1998; Guo et al., 2012; Weinberg et al., 1995; Wink et al., 2011).

Here, we present a detailed time-course analysis of brain immune responses in CVN-AD mice and describe a novel hypothesis for AD pathophysiology. We find that CVN-AD mice develop neuropathology in an age-dependent fashion that mimics the progression of human AD. This neuropathology includes the accumulation of a specific population of activated microglia in the hippocampus and cortex and the predominant expression of immunosuppressive genes that alter utilization of key amino acids. Specifically, we find that arginase-1 is highly expressed in regions of  $A\beta$  accumulation,

suggesting that arginine depletion and nutrient deprivation are responsible for neuronal cell death. In support of this hypothesis, we find that CVN-AD mice have decreased total brain arginine, and pharmacologic inhibition of arginine utilization enzymes reverses amyloid production, immunosuppression, and memory impairments. Together, these findings suggest that AD may be a disease of local immune suppression, rather than pro-inflammatory activation, and that the cause of neuronal death in AD is chronic immune-mediated amino acid catabolism resulting in nutrient deprivation.

## **2.2 Materials and Methods**

**Animals:** All animal experiments were performed in accordance with protocols approved by the Institutional Animal Care and Use committee at Duke University Medical Center under the NIH Guide for the Utilization and Care of Vertebrate Animals Used in Testing, Research and Training.

**CVN-AD mice:** Homozygous *APP<sup>SwDI</sup>/mNos2<sup>-/-</sup>* (CVN; CVN-AD) mice were produced by crossing mice expressing the Swedish K760N/M671L, Dutch E693Q and Iowa D694N human *APP* mutations under control of the Thy-1 promoter (Davis et al., 2004) with *mNos2<sup>-/-</sup>* (B6 129P2NOS2<sup>tau1Lau/J</sup>) mice (Laubach et al., 1998) (Jackson Laboratory, Bar Harbor, ME). *APP<sup>SwDI</sup>* mice were generously provided by Dr. Bill Van Nostrand and Judianne Davis at Stony Brook University Medical Center. Mice were genotyped using standard PCR methods. To determine if mice used in the experiments

expressed the Rd1 mutation in the *Pde68* gene that causes blindness in mice (Carter-Dawson and LaVail, 1979), CVN-AD mice were genotyped and found to be negative for Rd1. All mice were also genotyped for the Rd8 mutation of the *Crb1* gene that, when expressed, causes retinal pathology, but is not associated with blindness (Mattapallil et al., 2012). CVN-AD mice were found to be heterozygous for this gene. Animals were fed standard mouse chow and housed under 12 hour light/12 hour dark cycles at 21±3°C in an IACUC approved barrier facility under IACUC approved animal protocols. Mice were aged to 6, 12, 24, 36, or 52 weeks of age prior to behavioral assays and harvest of tissue. Mixed genders were used in the experiments and gender specific effects were not examined due to the complexity of the experimental protocol and the significantly increased number of mice required. General pathological features of CVN-AD mice include severe cerebral vascular amyloid deposition, tau pathology and neuronal loss associated with a decline in learning and memory as previously described (Wilcock et al., 2008).

**Immunohistochemistry:** After injection with a lethal mixture of ketamine/xylazine, mice were intracardially perfused with 25 mLs of phosphate buffered saline (PBS) to remove intravascular circulating blood cells. Perfused brains were then rapidly removed, bisected in the mid-sagittal plane. The left hemisphere was frozen in liquid nitrogen for use in ELISA and gene expression analysis and the right hemisphere was immersion fixed in 4% paraformaldehyde. For immunohistochemistry,

brains were cryoprotected by sequential passage through 10%, 20%, and 30% sucrose for 24 hrs. Frozen sagittal or coronal sections (25  $\mu$ m) were then cut. Sections equally spaced at 600  $\mu$ m apart were immunostained with standard techniques using the following antibodies: anti-beta amyloid (H31L21; Life Technology, Grand Island, NY) anti-phospho tau (AT8; Thermo Scientific, Waltham, MA), anti-CD45 (YW62.3, AbD Serotec, Raleigh, NC), anti-CD11b (5C6, AbD Serotec), anti-CD11c (N418; AbD Serotec), anti-Iba-1 (polyclonal 01-1941; Wako Pure Chemicals, Osaka, Japan), anti-CD206 (AF2535; R&D Systems, Minneapolis, MN), anti-Arginase-1 (gift from Dr. Sidney Morris, University of Pittsburgh, and commercially available as ABS535; Millipore, Billerica, MA). Secondary antibodies, ABC kit, and DAB kit were purchased from Vector Laboratories (Burlingame, CA).

**Quantitative RT-PCR:** Frozen cryo-pulverized brain samples from CVN-AD; *mNos2<sup>-/-</sup>*, WT, and APPSwDI mice at 6, 12, 24, 36 and 52 weeks of age were used to prepare RNA for analysis of immune gene expression. mRNA was extracted from frozen tissue using the RNeasy Tissue Kit (Qiagen, Valencia, CA) according to manufacturer's instructions. RNA was quantified using a NanoDrop spectrophotometer and cDNA was generated using the cDNA high capacity kit (Applied Biosystems, Inc., Foster City, CA). Real-time PCR was carried out using the Taqman Gene Expression kit (Applied Biosystems), according to the manufacturers instructions and as previously described (Wilcock et al., 2011b). All PCR probe sets were purchased from Applied

Biosystems. Beta-actin served as the internal standard and fold-change in gene expression levels was calculated using the  $2^{-(\Delta\Delta C(T))}$  method (Livak and Schmittgen, 2001). WT mice at the same age were used as the comparator except where delineated.

**Flow Cytometry:** Anesthetized mice were intracardially perfused with PBS and brains were then rapidly harvested, manually dissociated, and digested for 1 hour at 37°C with 1.5 mg/mL collagenase A (Roche Applied Science; Penzberg, Germany) and 0.4 mg/mL DNase I (Roche Applied Science) in 5% fetal bovine serum with 10 mM HEPES. Cells from the digested tissue were then strained through a 70 µm filter and washed with PBS. Cells were centrifuged in a 30% over 70% Percoll (Invitrogen; Carlsbad, CA, USA) in PBS density gradient. Cells from the interface were isolated and red blood cells were lysed with ammonium/chloride/potassium (ACK) lysis buffer (Life Technologies, Grand Island NY). Cells were counted and then stained with Live/Dead Aqua (Invitrogen/Life Technologies, Carlsbad, CA) and the following antibodies (all from eBioscience, San Diego, CA) were used: CD11b FITC; CD11c PE-Cy5.5; CD45 PE-Cy7; CD3ε APC; Ly6G AF700; CD11b APC-Cy7; Ly6C V450 ; IA-IE Qdot655. Flow cytometry was run on a BD™ LSR-II Flow Cytometer (BD Biosciences; Franklin Lakes, NJ) in the Duke Human Vaccine Institute Flow Research Facility and analyzed with FlowJo (Treestar; Ashland, OR).

**Cell isolation by FACS and RNA isolation and amplification:** CVN-AD, *mNos2<sup>-/-</sup>*, and WT (*C57BL/6*) mice (n=4 per genotype) all at 48 weeks of age were anesthetized and intracardially perfused with PBS. Cells were isolated for flow cytometry and described above. Cells were counted and stained with the following antibodies (all from eBioscience, San Diego, CA): CD11c PE-Cy5.5; CD45 PE-Cy7; CD11b APC-Cy7; Ly6G V450. FACS sorting was run on a BD™ FACS Aria II Special Order Research Product (SORP) Flow Cytometer (BD Biosciences; Franklin Lakes, NJ) in the Duke Human Vaccine Institute Flow Research Facility. Cells were gated on Ly6G<sup>-</sup> CD11b<sup>+</sup> CD45<sup>low</sup> microglia for *mNos2<sup>-/-</sup>*, *C57BL/6*, and CVN-AD samples and further sub-gated into CD11c<sup>high</sup> and CD11c<sup>low</sup> populations in CVN-AD samples. 1000 microglia were collected from each *mNos2<sup>-/-</sup>* and *C57BL/6* brain and 1000 CD11c<sup>high</sup> and CD11c<sup>low</sup> microglia were collected per CVN-AD brain and sorted in a volume of 1.0 μL directly into 6.4 μL of SuperAmp™ Lysis Buffer (Miltenyi Biotec, Auburn, CA). Samples were then incubated at 45°C for 10 minutes and frozen at -20°C before shipment to Miltenyi Biotec on dry ice.

**Microarray Analysis:** SuperAmp™ RNA amplification was performed by Miltenyi Biotec based on a global PCR protocol using mRNA-derived cDNA. cDNA integrity was checked via Agilent 2100 Bioanalyzer platform (Agilent Technologies). cDNA was labeled with Cy3 and hybridized to an Agilent Whole Mouse Genome Oligo Microarray 8x60K. After washing and staining, fluorescence signals were detected with

Agilent's Microarray Scanner System. The Agilent Feature Extraction Software was used to read out and process microarray image files (Agilent Technologies). Partek Genomics Suite (Partek Incorporated, St. Louis, MO) was used for data analysis, where we ran an analysis of variance with the four experimental groups to identify significantly differentially expressed genes. Significance threshold for the effect size was set at 2-fold change and false discovery rate at 5% ( $q=0.05$ ).

**Measurement of Brain amino acids:** Amino acids were extracted from cryo-pulverized 20-24 week-old mouse brain tissue ( $n=3$  to 12 mice/strain) using 4% CHAPS/50mM EDTA solution with probe sonication. Stable-isotope labeled internal standards for L-arginine, L-ornithine, and L-citrulline (Cambridge Isotope Laboratories; Andover, MA) were added to the extraction mixture following sonication, and utilized for MS-based quantitation. Samples were clarified with centrifugation, subjected to solid phase extraction purification on Strata-X-C columns (Phenomenex; Torrance, CA), dried under air, and re-suspended in isopropanol/0.2% formic acid. Analytes and their internal standards were then quantified in positive-ion LC-MS/MS mode, using previously described methodology (Brown et al., 2011). Briefly, separations were performed on an Atlantic HILIC column (Waters; Milford, MA) with mobile phases of 75% acetonitrile/25% methanol/0.2% formic acid (mobile phase A) or 0.2% formic acid in water (mobile phase B) at 0.2 ml/min flow rate. Samples were introduced to a 4000 QTrap LC/MS/MS (AB SCIEX; Framingham, MA) via electrospray ionization, and

analytes and internal standards quantified using multiple-reaction monitoring (MRM). Analyte concentrations were calculated from the slope of a calibration curve generated by serial dilutions of internal standards.

**DFMO treatment:** CVN-AD mice at 6 to 8 weeks of age were treated with 10 mg/kg DFMO plus 1 mg/kg putrescine in saline by oral gavage 3 times a week (Mon/Wed/Fri) for 14 weeks (n=8 mice/ group). Control CVN-AD mice were treated on the same schedule using oral gavage with 1 mg/kg putrescine in saline alone (n=7 mice/group). Difluoromethylornithine (DFMO, trade name Eflornithine; pharmaceutical grade) was provided by Dr. Patrick M. Woster, Department of Pharmacology, Wayne State University (Detroit MI) and was stored at -80°C and aliquoted at time of use. Co-treatment with putrescine was used to reduce potential DFMO-mediated damage to the epithelial cells in the gastrointestinal tract. All mice were weighed twice per week and no significant differences in weight were observed between DFMO treated and saline treated mice. After 14 weeks of treatment, mice were tested in the radial arm water maze (RAWM) for learning and memory. On completion of behavioral testing, brains were harvested for pathological assessment and gene analysis.

**Two-day radial arm water maze (RAWM) test for learning and memory:** CVN-AD, WT (*C57BL/6*), and *mNos2<sup>-/-</sup>* mice were tested at the ages indicated using the 2-day radial-arm water maze described in detail previously (Alamed et al., 2006). Briefly, a six-arm maze is submerged in a black plastic pool of water, and a platform is placed at

the end of one arm below the surface. The mouse receives 15 trials per day for 2 days (30 total) and is started in a different arm each trial, while the goal arm containing the platform remains constant for each mouse. Using static visual cues, the mouse learns the position of the escape platform. On the first day, the first 12 trials are considered training and alternate between a visible and a hidden platform, while the final 3 trials use a hidden platform. All trials on day 2 use a hidden platform. The number of errors (incorrect arm entries) is counted over a 1 min period. The errors for each consecutive three trials (1-3, 4-6, 7-9, 10-12, 13-15) are averaged as one block, resulting in 5 blocks per day. After completion of all hidden maze tasks, mice were tested for sensory or motor deficits using the open pool task with visible platform as described (Alamed et al., 2006). Mice that did not perform successfully in the open pool task were excluded from data analysis. All behavioral tests were performed with treatment groups blinded to the investigator.

**Statistical analysis and comparisons between groups:** Average values  $\pm$  SEM was determined for each of the outcome measures at 6, 12, 24, 36, and/or 52 weeks of age in the CVN-AD and control mice. Mixed genders were used in the analyses and gender based-differences were not investigated. Significant differences across age within strain were determined using 1-way ANOVA, while statistical significance between genotypes and age was determined by 2-way ANOVA using the PRISM statistical program

(GraphPad Software, San Diego CA). Significance was set at  $p \leq 0.05$ . Number of mice analyzed ranged from 3-14 mice per group depending on the outcome assay.

## **2.3 Results**

### **2.3.1 Immune suppression is an early feature of disease progression**

CVN-AD mice display characteristic neuropathology resembling human AD as they age, which include the accumulation of  $\beta$ -amyloid ( $A\beta$ ) deposits starting at 6 weeks of age, the presence of hyperphosphorylated and aggregated tau beginning at 12 weeks of age, spatial memory deficits beginning around 24 weeks of age, and neuronal loss at around 36 weeks of age (Colton et al., 2014). We thus reasoned that these mice could be used to identify immune abnormalities that arise early in the course of disease as well as with disease progression during aging. We used qRT-PCR of total brain lysate to measure gene expression for a variety of pro-inflammatory and anti-inflammatory genes implicated in AD in CVN-AD, *mNos2<sup>-/-</sup>* and WT (*C57Bl/6*) mice at 6, 12, 24, 36 and 52 weeks of age. We also examined mRNA expression levels in the parent APPSwDI strain to determine if  $A\beta$  accumulation alone was a factor in the immune changes, as levels of soluble and insoluble  $A\beta$  are not significantly different in APPSwDI versus CVN-AD mice (Wilcock et al., 2008). Since significant neuronal death begins around 36 weeks in CVN-AD mice (Colton et al., 2014), we grouped the genes into 2 major patterns of expression: genes that were up-regulated before 36 weeks (**Figure 1 A-D**) and genes up-

regulated at or after 36 weeks (Figure 1 E-I). We also examined gene expression levels for chemokine receptors and ligands from 6 to 52 weeks of age (Figure 1 J-L).

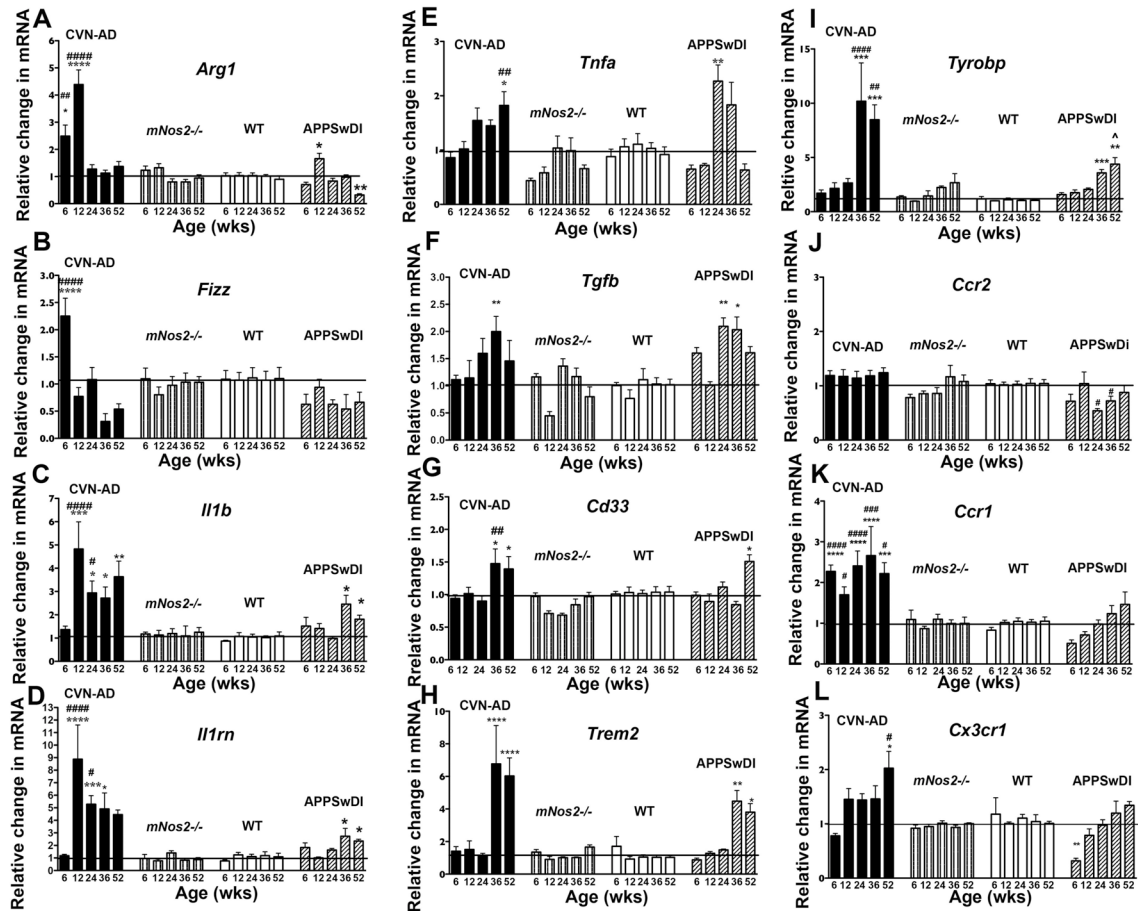


**Figure 1: Expression of immune-related genes from whole brain lysates**

Average values and standard error of the mean for the relative change in mRNA levels are shown for immune related genes from whole brain lysate samples from CVN-AD, *mNos2<sup>-/-</sup>*, WT (*C57Bl/6*) and APPSwDI mice.

**A-D)** Genes that were up-regulated in CVN-AD mice before 36 weeks of age.

**E-I)** Genes that were up-regulated in CVN-AD mice at or after 36 weeks of age.

**J-L)** Gene expression of chemokine receptors. mRNA expression was measured using quantitative RT-PCR and represent the  $2^{-(\Delta\Delta C(T))}$  compared to WT mice. Samples were analyzed by 2-way ANOVA and post-hoc multiple comparison test with

Bonferonni's correction. \* represent comparisons between CVN-AD or APPSwDI and WT, # represent comparisons between CVN-AD and APPSwDI mice. \*p<0.05, \*\*p<0.01, \*\*\*p<0.001, \*\*\*\*p<0.0001; #p<0.05, ##p<0.01, ###p<0.001, ####p<0.0001, n>5 mice per group.

Genes that were up-regulated at the earliest time points in CVN-AD mice were predominately those that have been linked to immune suppression in macrophages (**Figure 1**). This included arginase-1 (*Arg1*), Found in Inflammatory Zone 1 (*Fizz1*), and interleukin 1 receptor antagonist (*Il1rn*). These genes tended to display the highest expression level only transiently, returning toward WT control levels by 24 weeks. Expression of these anti-inflammatory genes was significantly greater in CVN-AD mice compared to the parent APPSwDI strain, with the exception of *Arg1* expression at 12 weeks of age, where a small increase in mRNA level was observed in APPSwDI brain lysates. Interleukin-1 beta (*Il1b*), the classic pro-inflammatory mediator, was also expressed early in CVN-AD mice, beginning at 12 weeks of age. After this initial peak, IL-1 $\beta$  gene expression levels remained significantly elevated throughout the 52 weeks of the study. Compared to APPSwDI mice, which exhibited only slight increases in *Il1b* and *Il1rn* at 24 and 52 weeks, CVN-AD mice had greater expression levels for *Il1b* and *Il1rn* at all time points.

Specific genes that were increased in CVN-AD mice at or after 36 weeks of age included the canonical pro-inflammatory gene *Tnfa*, which was significantly increased only at the latest time point studied (52 weeks), and *Tgfb*, an anti-inflammatory gene

which was increased transiently beginning at 36 weeks of age. Also increased was *Cd33* (Siglec-3), an inhibitory lectin that has been implicated in GWAS studies of AD and that is believed to alter microglial phagocytosis of beta amyloid (Bradshaw et al., 2013; Salminen et al., 2009). Other immunosuppressive genes known to be associated with AD, namely *Trem2* and *Tryobp* (DAP12), were also increased late in disease progression in CVN-AD mice. Data from APPSwDI mice brain showed a similar age-specific pattern of expression for these late genes but no significant changes were found in either *mNos2<sup>-/-</sup>* or wildtype control mice at any age.

Expression of mRNAs for the chemokine receptor, *Ccr2* (**Figure 1J**) and its ligand *Ccl2* (MCP1) (data not shown) were unchanged at all time points in CVN-AD brains. *Ccr2* is expressed on inflammatory monocytes and has been shown to mediate the migration of these cells from the periphery into the brain in mice expressing mutated human APP (El Khoury et al., 2007; Naert and Rivest, 2011), although others have observed that circulating monocytes from humans with AD have depressed CCR2 expression (Zhang et al., 2013b). Expression of *Cxcl1* (KC, GROa), which can mediate neutrophil recruitment and may have a role in neuroprotection, and *Ccl11* (eotaxin 1), a chemoattractive factor for eosinophils, also remained unchanged (data not shown). However, *Ccr1* and *Cx3cr1* expression were significantly increased in CVN-AD mice, but were not observed in any of the control mice, including APPSwDI mice. Increased *Ccr1* expression in CVN-AD mice was observed early and elevated at all ages. CCR1 has

been shown to associate with plaques in the entorhinal cortex and hippocampus, is an early marker for clinical dementia in humans with AD, and has been shown to directly correlate with cognitive decline (Halks-Miller et al., 2003). Expression of *Cx3cr1*, which is expressed primarily by microglia in the brain, increased progressively in CVN-AD brains (**Figure 1L**), consistent with the increasing number of microglia (**Figure 3**). However, gene expression for *Cx3cr1* receptor ligand, *Cx3cl1* (fractalkine), was not increased at any time (data not shown).

### **2.3.2 CVN-AD mice show progressive cellular inflammation with CD11c<sup>+</sup> microglia in areas of beta-amyloid deposition**

To better understand the cellular basis of the altered immune responses found in whole brain lysates of CVN-AD mice compared to control mice, we examined the presence and characteristics of typical immune cells using immunocytochemistry on brain sections through one year of the disease process. Age-matched *mNos2<sup>-/-</sup>* and *C57Bl/6* mice were used as controls. Immune markers that are characteristically up-regulated in tissue sections from autopsied human AD brain include CD45, MHC-II, CD11b, and CD11c (Eikelenboom et al., 2010); (McGeer et al., 1987; Mrazek and Griffin, 2005; Rogers et al., 2002; Rozemuller et al., 1986). Changes in these markers are used as a pathological indicator of the immune response in humans with AD and are also observed in mouse models of AD (Butovsky et al., 2006; Mildner et al., 2011; Nichol et al., 2008; Tambuyzer et al., 2009; Tan et al., 2000). In CVN-AD mice, tissue expression of CD45, Iba-1, and CD11c are correlated with amyloid deposition with aging (**Figure 2**).

A $\beta$  plaques appeared initially in the subiculum of the hippocampus and increased in staining density throughout the cortex and hippocampus with age (**Figure 2 A-D**). A $\beta$  deposition was accompanied in time and spatial location by increased immunoreactivity for CD45 (**Figure 2 E-H**). CD45<sup>+</sup> cells had the morphological features of reactive microglia with bushy, shortened processes (data not shown). To confirm that CD45 cells in CVN-AD brains represent microglia, sections from the same CVN-AD mice were stained with Iba-1, a calcium binding protein that is expressed specifically on microglia in the CNS (**Figure 2 I-L**). Iba-1 stained microglia throughout the brain, as well as cells within the hippocampus and cortex that correlated with the pattern of CD45 staining in these mice.

We also examined the expression pattern of CD11c, which is not commonly found on either resting or reactive microglia in mouse brain, but is found on resting and activated human microglia (Akiyama and McGeer, 1990). An increasing pattern of expression similar to that of CD45 was observed for CD11c (**Figure 2 M-P**), and CD11c expression found to overlap with Iba-1<sup>+</sup> microglia using double labeling techniques (**Figure 2Q**). To further confirm the change in levels of CD11c with age, we also performed qRT-PCR on whole brain lysates. Gene expression levels for *Itgax* (CD11c) increased dramatically from 6 weeks of age, leading to an approximately 100-fold increase at 52 weeks of age (**Figure 2R**). In contrast, the expression levels of *Itgax* mRNA in the APPSwDI parent mouse strain showed a relatively delayed increase in gene

expression levels and were significantly less than the fold changes in mRNA found in CVN-AD mice brain. Similarly, we observed less and delayed CD11c immunostaining at all ages when comparing APPswDI to CVN-AD mice (data not shown). No changes in CD11c mRNA levels were found for *mNos2<sup>-/-</sup>* or WT mice brain lysates at any age studied.

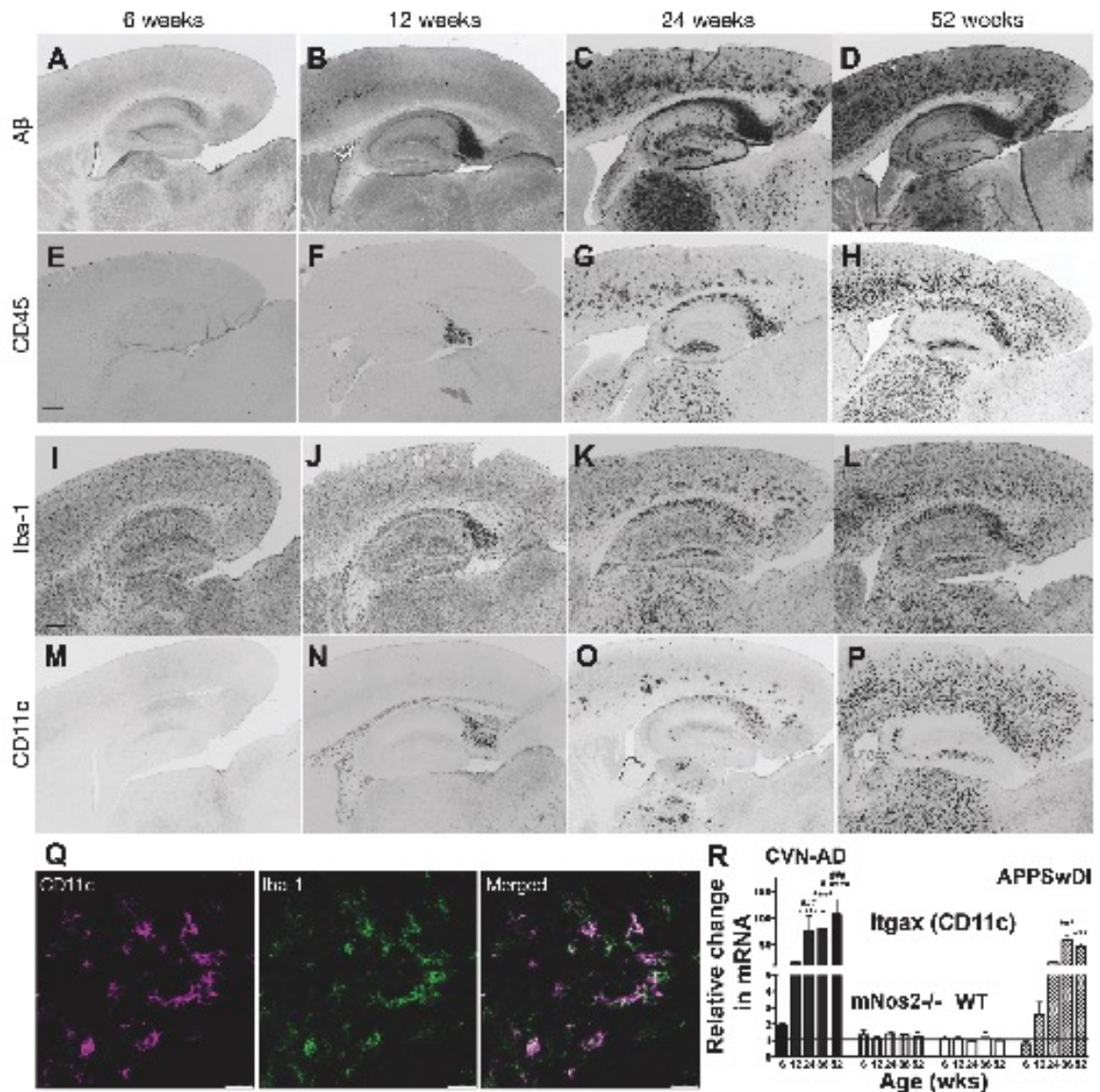


**Figure 2: CVN-AD amyloid deposition is associated with cells expressing characteristic markers of microglia.**

Representative sagittal sections from a CVN-AD mouse at 6, 12, 24, and 52 weeks of age immunostained for beta-amyloid (A-D) CD45 (E-H), Iba-1 (I-L) and for CD11c (M-P). For each age, panels represent sister sections from the same mouse (for example, Panels A, E, I, M are sections from the same 6 week-old mouse). Scale bar, 500  $\mu$ m.

Q) Representative micrographs of CD11c and Iba-1 co-staining in the subiculum of the hippocampus from a 24 week-old CVN-AD mouse. Scale bar, 25  $\mu$ m.

**R)** Increased CD11c immunostaining is associated with increased gene expression of CD11c (*Itgax*). Gene expression levels (mean  $\pm$  SEM) were measured using quantitative RT-PCR and represent the 2(-Delta Delta C(T)) compared to WT mice. Samples were analyzed by 2-way ANOVA and post-hoc multiple comparison test with Bonferonni's correction. \* represent comparisons between CVN-AD or APPSwDI and WT, # represent comparisons between CVN-AD and APPSwDI mice. \*p<0.05, \*\*p<0.01, \*\*\*p<0.001, \*\*\*\*p<0.0001; #p<0.05, ##p<0.01, ###p<0.001, ####p<0.0001, n>5 mice per group.

The above findings suggest that cellular inflammation in CVN-AD mice is primarily due to an increased number of reactive microglial cells that co-express CD45 and CD11c. To confirm the identity of the CD11c<sup>+</sup> cells, we performed 12-color flow cytometric analysis of homogenized whole brains from 42-week old *mNos2<sup>-/-</sup>*, which lack CD11c<sup>+</sup> microglia, and CVN-AD mice (**Figure 3**). Using this technique we found increased total cell numbers in the brains of CVN-AD mice that was caused by a significant increase in the numbers of CD45<sup>low</sup> CD11b<sup>+</sup> microglia, and secondarily, by a trend toward increased numbers of T cells (**Fig. 3B**). The total numbers of B cells, neutrophils, eosinophils, macrophages, Ly6C<sup>low</sup> resident monocytes, and Ly6C<sup>high</sup> inflammatory monocytes, however, were unchanged in CVN-AD brains (**Figure 3B**). CD11c was predominantly expressed by CD45<sup>low</sup> microglia (**Figure 3C**). At 42 weeks of age, approximately 12.2 $\pm$ 2.5% of all microglia were CD11c<sup>+</sup>, compared to 2.24 $\pm$ 0.3% in *mNos2<sup>-/-</sup>* controls, and there was a significant increase in the mean fluorescence intensity of microglial expression of CD11c (**Figure 3D**). Thus, both immunocytochemical and flow cytometric analysis demonstrated that CVN-AD mice develop substantial cellular

inflammation that is caused primarily by the expansion of microglial cells. These microglial cells display a reactive morphology, accumulate specifically in areas of beta-amyloid deposition and can be distinguished from microglia in control mice by their increased expression of CD11c. This pattern of cellular inflammation is consistent with that seen in humans with AD (Akiyama and McGeer, 1990; Dickson et al., 1988).

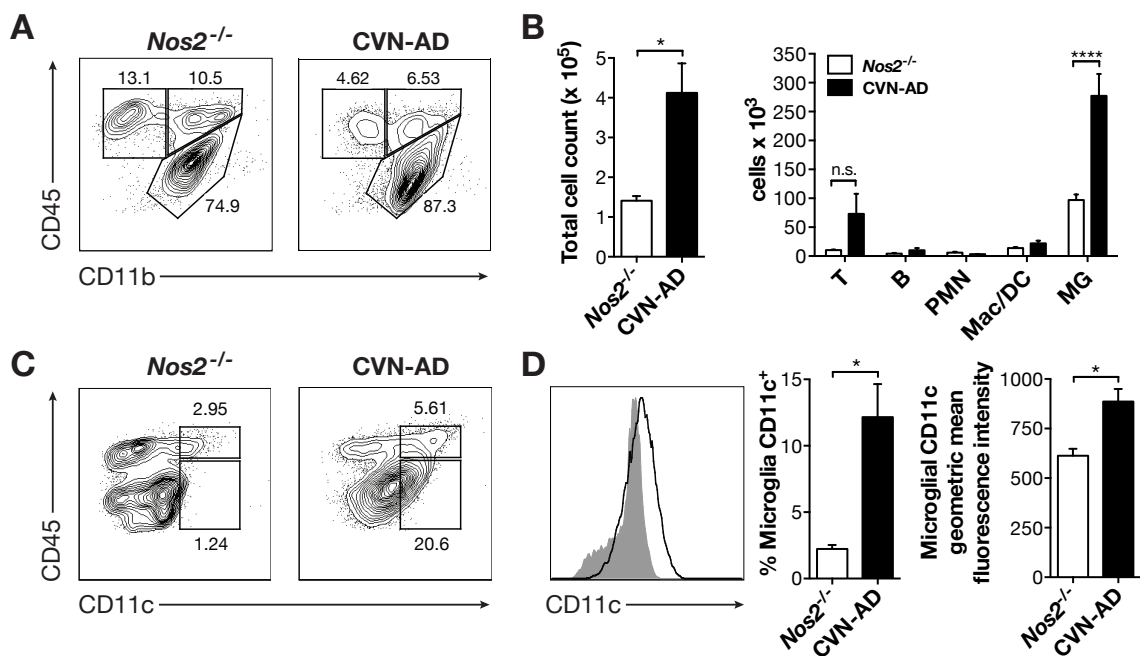


**Figure 3: CD11c<sup>+</sup> cells from CVN-AD brains have a microglial phenotype**

A) Representative flow cytometry plots from aged 48 week-old *mNos2*<sup>-/-</sup> and CVN-AD brains after gating on CD45<sup>+</sup> cells.

B) Quantification of total CD45<sup>+</sup> cells and individual cell types distinguished by FACS in 48 week-old *mNos2*<sup>-/-</sup> and CVN-AD brains, including T lymphocytes (T), B lymphocytes (B), neutrophils (PMN), monocytes/macrophages/DCs (Mac/DC), and microglia (MG) from aged 48 week-old *mNos2*<sup>-/-</sup> and CVN-AD brains.

C) Representative flow plots of CD45 and CD11c expression from aged 48 week-old *mNos2*<sup>-/-</sup> and CVN-AD brains after gating on all CD11b<sup>+</sup> cells.

D) Representative histogram of CD11c expression on *mNos2<sup>-/-</sup>* (closed grey) and CVN-AD (open black) CD11b<sup>+</sup> CD45<sup>low</sup> cells, as well as quantitative summaries of the percentages and geometric mean fluorescence intensities (MFI) of CD11c from *mNos2<sup>-/-</sup>* and CVN-AD CD11b<sup>+</sup> CD45<sup>low</sup> microglia. \*p<0.01; n=4 mice per group.

### 2.3.3 CD11c<sup>+</sup> microglia show an immunosuppressive phenotype

To better understand the potential functional capabilities of the CD11c immunopositive microglia in CVN-AD mice we used flow sorting to isolate this population from whole brain lysates. Mice were used at 48 weeks of age to ensure a large population of cells for the study. Cells were gated on Ly6G<sup>-</sup> CD11b<sup>+</sup> CD45<sup>low</sup> microglia for *mNos2<sup>-/-</sup>*, WT, and CVN-AD brain samples and further sub-gated into CD11c<sup>high</sup> and CD11c<sup>low</sup> populations in CVN-AD mice. Messenger RNA from each collected cell sample then globally amplified using SuperAmp™ to produce cDNA for use in an Agilent Whole Mouse Genome Oligo microarray. Gene expression from the CVN-AD CD11c<sup>+</sup> cells were compared that of the Ly6G<sup>-</sup> CD11b<sup>+</sup> CD45<sup>low</sup> CD11c<sup>-</sup> microglia from CVN-AD, *C57Bl/6*, and *mNos2<sup>-/-</sup>* brains. Analysis of variance with the four experimental groups was used to identify significantly differentially expressed genes. We set the significance threshold for the effect size at 2-fold change and false discovery rate at 5% (q=0.05).

Approximately 375 genes were significantly upregulated and 85 genes down-regulated in CVN-AD CD11c<sup>+</sup> microglia compared to CD11c<sup>-</sup> microglia from CVN-AD, *C57Bl/6*, and *mNos2<sup>-/-</sup>* brains (**Table 1**). Up-regulated genes included those genes that are

used to identify microglia in humans with AD, such as *Itgax* (Cd11c/LeuM5; CR4) and *Cd200r* (Cell surface glycoprotein CD200 receptor 2; OX2R). The 124-fold increase in *Itgax* gene expression verified our previous observations and our FACS isolation process. Strikingly, many of the genes that were upregulated in CVN-AD CD11c<sup>+</sup> microglia, such as *Spp1*, *Wfdc17*, *Gp49a*, *ApoE*, and *Pdcd1* were genes associated with immune suppression and increased arginase activity. Similarly, many of the genes that were downregulated were from pro-inflammatory pathways, such as *ApoBec3*, *Ifngr1*, and *Siglech*, or represent negative regulators of immune suppression, such as *Klf6* (Table 1). Taken together, along with additional genes that were changed significantly (Table 1) we observed that CD11c<sup>+</sup> microglia from CVN-AD mice had a predominantly immunosuppressive phenotype.

**Table 1: Gene expression in CVN-AD CD11c<sup>+</sup> microglia compared to CVN-AD CD11c<sup>-</sup> microglia, C57Bl/6 microglia, and *mNos2<sup>-/-</sup>* microglia.**

Gene	Name	Fold change	p-value	Reported actions	References
<i>Mamdc</i>	MAM domain containing protein 2	515	9.7 x 10 <sup>-7</sup>	Glycosaminoglycan binding, linked to negative regulation of synapses	(Pettem et al., 2013)
<i>Spp1</i>	Secreted phosphoprotein 1; osteopontin	515	5.9 x 10 <sup>-6</sup>	Increased in CSF of AD patients; enhances immunosuppression	(Comi et al., 2010; Sangaletti et al., 2014)
<i>Gpnmb</i>	Glycoprotein - transmembrane nmb ; osteoactivin, Fe65-like1	442	1.5 x 10 <sup>-6</sup>	Tissue repair, M2 state; phagocytic vesicle processing	(Duffield, 2010)
<i>Wfdc17</i>	Whey acidic protein four disulfide core domain 17; AMWAP	136	4.1 x 10 <sup>-5</sup>	Overexpression increases Arg1, reduces IL6, IL-1β;	(Karlstetter et al., 2010)
<i>Itgax</i>	Integrin alpha X (complement component 3 receptor 4 subunit), CD11c	124	5.8 x 10 <sup>-6</sup>	Leucocyte specific integrin; Associated with dendritic cells; phagocytosis of complement-coated particles; found on microglia in AD.	(Akiyama and McGeer, 1990; Becher and Antel, 1996; Butovsky et al., 2007; Tooyama

					et al., 1990),
<b>Gp49a</b>	Glycoprotein 49a; Lirb4	107	$2.8 \times 10^{-4}$	Member of Inhibitory Ig superfamily (ITIMs); Increased IL4; Suppresses LPS; inhibits Fc-gamma-mediated phagocytosis	(Arm et al., 1997; McCormick et al., 1999)
<b>Gng12</b>	Guanine nucleotide binding protein 12	64	$1.7 \times 10^{-4}$	Inhibits LPS-mediated pro-inflammation	(Larson et al., 2010)
<b>Pdcd1</b>	Programmed cell death 1; PD1, CD279	51	$4.1 \times 10^{-6}$	Immunoglobulin superfamily; Shifts microglia to M2 phenotype; Regulates Arg1 activity	(Yao et al., 2014)
<b>Apbb2</b>	Amyloid precursor protein binding protein 2	25.8	$2.4 \times 10^{-4}$	Adaptor protein binds to cytoplasmic domain of APP; polymorphisms associated with dementia in aged population; involved in ECM synthesis by Macs.	(Golanska et al., 2013; Grupe et al., 2006; Wright et al., 2005)
<b>TIMP2</b>	Tissue inhibitor of metallo protease-2	20.7	$3.2 \times 10^{-4}$	Blocks metalloprotease activity; associated with M2 phenotype.	(Ridnour et al., 2007; Wilcock et al., 2011a)
<b>Igf</b>	Insulin like growth factor 1; 2;	27.4	$2.0 \times 10^{-5}$	Found in human microglia, Protects from IL-1 and IFN $\gamma$ mediated damage;	(Trueba-Saiz et al., 2013)
<b>Igf2</b>	somatomedin c	8.0	$2.1 \times 10^{-3}$	promotes A $\beta$ clearance	
<b>ApoE</b>	Apolipoprotein E	20.1	$3.6 \times 10^{-4}$	Strongest single gene risk factor for Alzheimer's disease, suppresses pro-inflammatory cytokines	(Saunders et al., 1996)
<b>CD200r</b>	Cell surface glycoprotein CD200 receptor 2, OX2R	13.8	$3.3 \times 10^{-3}$	Inhibitory immune receptor found on microglia, Marker for M2 activation in human MG, less so in mice	(Denieffe et al., 2013; Walker and Lue, 2013)
<b>Klf6</b>	Kruppel like factor 6	0.12	$4.9 \times 10^{-6}$	Suppression is linked to M2 phenotype	(Date et al., 2014)
<b>ApoBEC3</b>	Apolipoprotein B mRNA editing enzyme, catalytic polypeptide 3	0.18	$4.1 \times 10^{-4}$	Promotes anti-viral immunity through production of neutralizing antibody	(Santiago et al., 2008)
<b>Ifng1</b>	Interferon gamma receptor 1; CD119	0.19	$9.1 \times 10^{-6}$	Encodes ligand binding domain for IFN- $\gamma$ ; down-regulated by TLR2; IFN- $\beta$	(Curry et al., 2004; Kearney et al., 2013)
<b>Siglech</b>	Siglec-H	0.42	$2.6 \times 10^{-4}$	DAP12 signaling molecule, microglial "sosome," decreased with aging	(Hickman et al., 2013)

#### **2.3.4 CVN-AD pathology is associated with increased arginine utilization and decreased brain arginine bioavailability**

The immunosuppressive phenotype observed in CVN-AD mice brain suggested a potential causative role for this immune process in disease progression. In particular, *Arg1*, a critical anti-inflammatory gene that codes for the enzyme arginase-1, was expressed predominantly in young mice in brain areas associated with A $\beta$  deposits but prior to neuronal loss in this model of AD. Arginase-1 regulates the micro-environmental level of arginine, a semi-essential amino acid, by altering arginine catabolism (Bronte and Zanovello, 2005; Gabrilovich and Nagaraj, 2009; Pesce et al., 2009; Tang et al., 2009). Increased usage of arginine results in a drop in tissue levels of arginine (Reeds, 2000), which if not replaced, initiates amino acid deprivation responses in susceptible cells. Sustained arginine deprivation leads to cell death (Kuma and Mizushima, 2010). To determine if induction of *Arg1* may play a role in AD-like pathology in CVN-AD mice, we examined arginase-1 protein expression and its spatial and temporal relationship with A $\beta$  deposition and CD11c<sup>+</sup> microglial at different ages using immunocytochemistry. Arginase-1 protein accumulated in the subiculum and CA1 regions of the hippocampus, areas of primary neuronal loss, starting between 6 to 12 weeks and peaked at 24 weeks (**Figure 4A**), consistent with the onset of behavioral deficits at 24 weeks. In contrast, no arginase-1 staining was observed at any time point in *Nos2*<sup>-/-</sup> brains (Figure 4B and data not shown). Of note, arginase-1 staining in CVN-AD

brains did not primarily localize to cells but instead diffusely stained the hippocampus and subiculum, suggesting that arginase was distributed in the extracellular space surrounding the cells (**Figure 4B**). Additionally, arginase-1 staining in the hippocampus displayed a spatial correlation with that of A $\beta$ , Iba-1, and CD11c (**Figure 4C**), highly suggesting that CD11c<sup>+</sup> microglia are a likely source of arginase-1 production and that expression is associated with A $\beta$ .

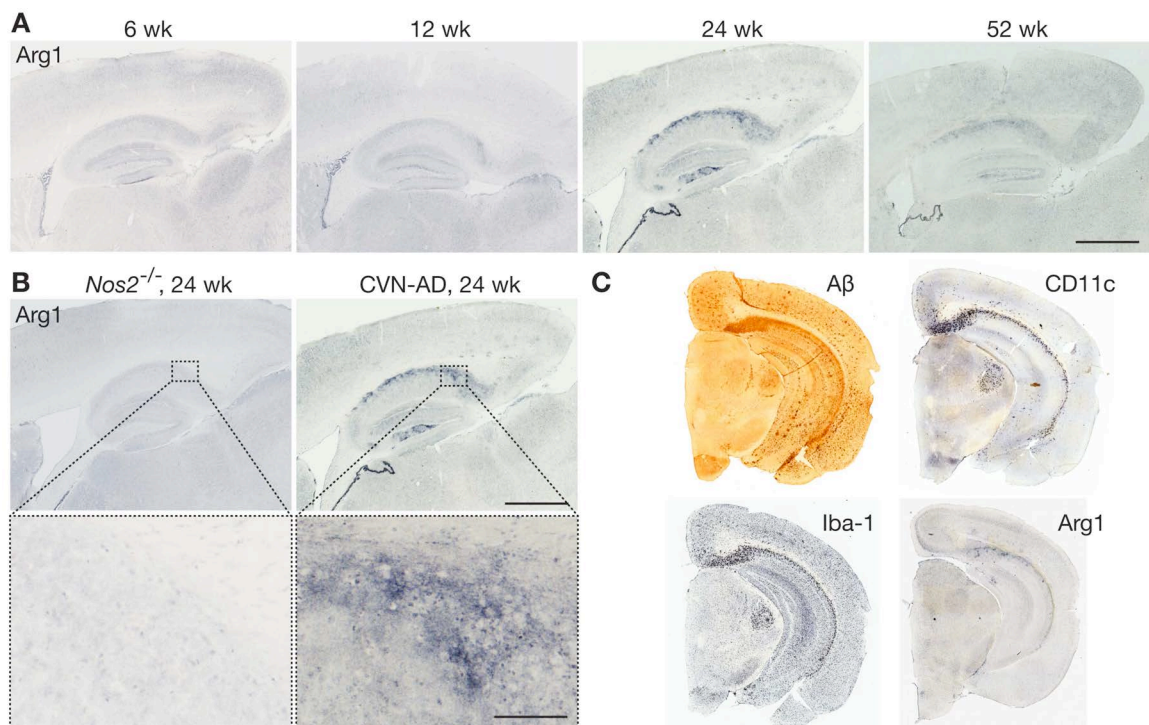


**Figure 4: CVN-AD pathology is associated with arginase-1**

**A)** Representative sagittal sections from CVN-AD mice at 6, 12, 24, and 52 weeks of age stained for arginase-1 in sister sections from the same mice as in Figure 1. Scale bar, 500  $\mu$ m.

**B)** Magnified view of arginase immuno-reactivity in the subiculum. Representative sagittal sections from 24-week old *mNos2<sup>-/-</sup>* and CVN-AD stained for arginase-1. Upper panel scale bar, 500  $\mu$ m; lower panel scale bar, 50  $\mu$ m.

C) Sister coronal sections from the same 52-week old CVN-AD brain stained for A $\beta$ , CD11c, Iba-1 and arginase-1 to show regional associations.

To determine if arginase-1 expression alters brain arginine levels in CVN-AD mice, we examined brain amino acid levels and the compensatory expression of amino acid transporters in these animals. Total brain arginine and arginine metabolites, including ornithine and citrulline, were measured using hydrophilic-interaction chromatography (HILIC) and liquid chromatography-tandem mass spectrometry (LC-MS/MS) (Brown et al., 2011; Morris, 2012). In disease contexts, the global arginine bioavailability ratio (GABR), which is the ratio of arginine to its metabolites ornithine and citrulline (arginine/(ornithine + citrulline)), is often a better indicator of dysregulated arginine metabolism than arginine concentration alone (Tang et al., 2009). Calculating the GABR revealed that, compared to WT, *mNos2<sup>-/-</sup>*, and APPSwDI mice, CVN-AD mice had significantly reduced GABR (**Figure 5A**), indicating that CVN-AD brains exhibited increased arginine catabolism.

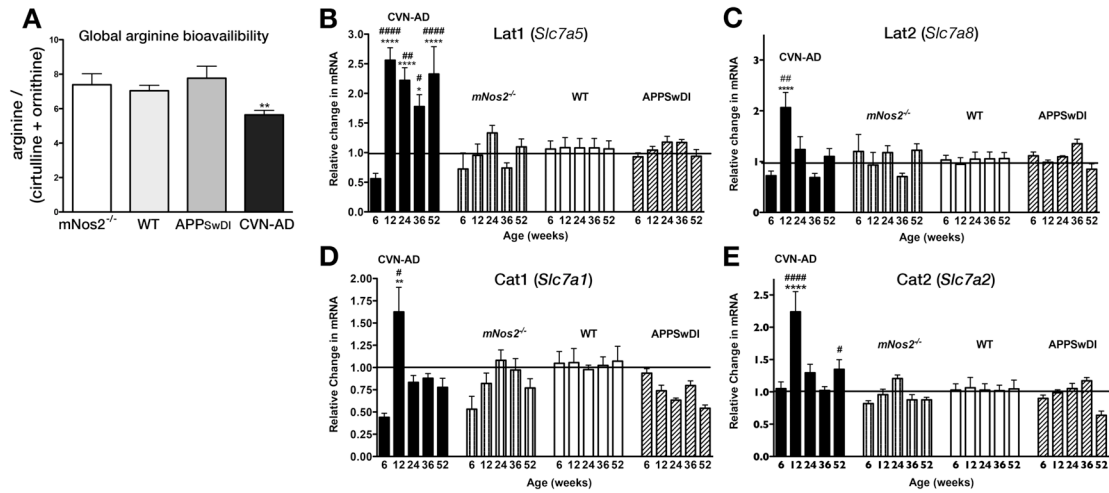


**Figure 5: CVN-AD brains have decreased total L-arginine bioavailability and increased expression of arginine transporters**

**A)** Global arginine bioavailability (arginine/(ornithine + citrulline)) for CVN-AD, *mNos2*<sup>-/-</sup>, WT and APPSwDI mice at 24 weeks of age. Average values (± SEM) per genotype were calculated for individual mice (n=3-12 mice per group). Amino acid levels were measured using HILIC LC-MS/MS. \*\*p<0.01 by 1-way ANOVA.

**B-E)** Relative gene expression (mean ± SEM) was measured in total brain homogenates from CVN-AD, *mNos2*<sup>-/-</sup>, WT and APPSwDI mice for the neutral arginine transporters *Slc7a5* (LAT1) and *Slc7a8* (LAT2) (**B and C**) and for the cationic amino acid transporters *Slc7a1* (CAT1) and *Slc7a2* (CAT2) (**D and E**). Samples were analyzed by 2-way ANOVA and post-hoc multiple comparison test with Bonferonni's correction. \* represent comparisons between CVN-AD or APPSwDI and WT, # represent comparisons between CVN-AD and APPSwDI mice. \*p<0.05, \*\*p<0.01, \*\*\*p<0.001, \*\*\*\*p<0.0001; #p<0.05, ##p<0.01, ###p<0.001, ####p<0.0001, n=4-8 mice per group.

Cells deprived of arginine attempt to compensate by increasing expression of amino acid transporters that regulate the cellular uptake of arginine from the local environment (Broer, 2002; Closs et al., 2006; Hyatt et al., 1997). To determine if such mechanisms were active in CVN-AD brains, we measured whole brain lysate mRNA

levels of cell membrane-bound amino acid transporters that mediate arginine uptake (**Figure 5B-E**). These included cationic amino acid transporter 1 (CAT1; *Slc7A1*), cationic amino acid transporter 2 (CAT2; *Slc7A2*), cationic amino acid transporter 3 (CAT3; *Slc7A3*) and the large neutral amino acid transporters LAT1 (*Slc7A5*) and LAT2 (*Slc7A8*). We observed no significant changes for all of these genes in *Nos2<sup>-/-</sup>*, C57BL/6, and APPSwDI mice (**Figure 5B-E**). In contrast, in CVN-AD brain, we found that LAT1 mRNA was consistently increased from 12 weeks through 52 weeks (**Figure 5B**). We also observed transient increased gene expression for LAT2, CAT1, and CAT2 at 12 weeks of age and returning to baseline expression levels by 24 weeks (**Figure 5 C, D, and E**). CAT3 showed no significant change at any age (data not shown), consistent with its restricted expression on a small number of neuronal populations (Hosokawa et al., 1999). These changes in GABR and arginine transporters indicate that, in comparison to control strains, CVN-AD mice have dysregulated arginine metabolism.

### **2.3.5 Blockade of arginine utilization reverses memory loss**

Our data on arginase expression and arginine depletion in the brains of CVN-AD mice raised the possibility that chronic brain arginine deprivation promotes neurodegeneration. To determine if there is a causal relationship between arginine depletion and the development of pathology and cognitive defects in CVN-AD mice, we reduced the biological effects of arginine catabolism by blocking key enzymes in the arginine utilization pathway (**Figure 6**). We chose to use eflornithine

(difluoromethylornithine, DFMO), an irreversible inhibitor of ornithine decarboxylase (ODC) (Abeloff et al., 1984; Pepin et al., 1987; Seiler, 2003) and a partial inhibitor of arginase that has been previously used to block arginine utilization *in vivo* (Selamnia et al., 1998). Because the polyamine pathway, which is downstream of ODC, is important for cell proliferation particularly in the gastrointestinal system (Buts et al., 1993), we supplemented CVN-AD mice with putrescine to reduce gastrointestinal damage created by decreased polyamine levels (Kameji et al., 1979; Loser et al., 1999).

Two treatment groups were established: CVN-AD mice treated with oral gavage of putrescine alone and CVN-AD mice treated with oral gavage of putrescine plus DFMO. Because increased arginase-1 mRNA and protein levels were observed at the earliest time points in the disease process, treatment was started at 6-8 weeks of age with oral gavage 3 times a week for 14 weeks. Immediately on conclusion of treatment, we tested learning and memory behavior in the putrescine only-treated and DFMO plus putrescine-treated mice. We have previously demonstrated that CVN-AD mice have deficits in spatial memory as measured by radial arm water maze and make significantly more errors than either *mNos2<sup>-/-</sup>* or *C57Bl/6* controls at 24 weeks of age (Colton et al. 2014). CVN-AD mice treated with DFMO plus putrescine demonstrated significantly improved acquisition and recall compared to vehicle (putrescine only)-treated CVN-AD mice (**Figure 6A**), suggesting that blockade of arginine catabolism reverses the behavioral phenotype of memory loss found in CVN-AD mice.

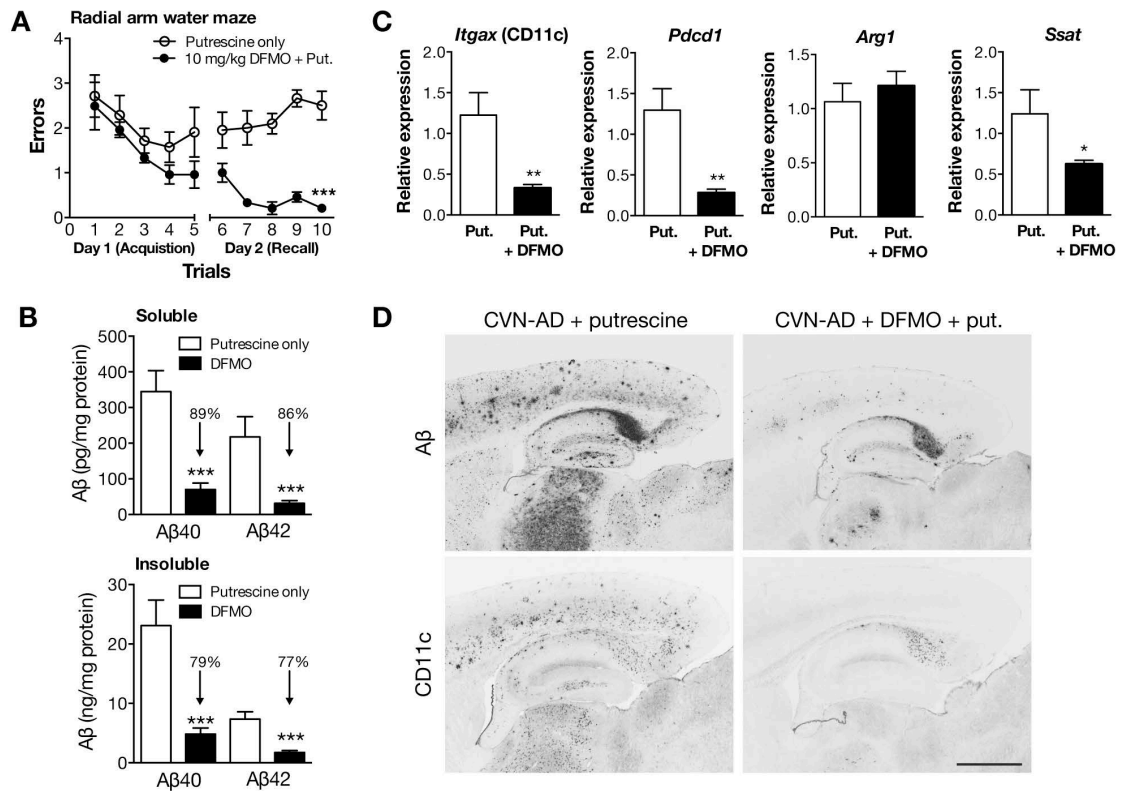


**Figure 6: CVN-AD memory deficits and pathology are reversed by an inhibitor of arginine utilization.**

**A)** Radial arm water maze assessment of spatial memory acquisition and recall in CVN-AD mice treated with putrescine (put.) alone or putrescine and DFMO (10 mg/kg) by oral gavage for 3 days/week for 14 weeks. All mice were naïve to the behavioral procedure and tested on the final 2 days of treatment. Day 1 depicts 5 trial groups for the acquisition phase (learning) and day 2 depicts successive trials for memory recall. Data represent the average number of errors ( $\pm$  SEM) made finding the escape platform for each group of trials. Open circles: CVN-AD mice treated with putrescine and vehicle; closed circles: CVN-AD mice treated with DFMO and putrescine. Data were analyzed by 2-way ANOVA and post-hoc multiple comparison test with Bonferonni's correction. \*\*\* $p < 0.001$ ;  $n=7-8$  mice per group.

**B)** Soluble and insoluble Aβ40 and Aβ42 peptides in total brain homogenates from CVN-AD mice treated with vehicle containing putrescine only or putrescine plus DFMO as measured by ELISA. Data represent average levels ( $\pm$  SEM) of Aβ40 or Aβ42 peptides. \*\*\* $p < 0.001$  for DFMO-treated compared to putrescine/vehicle-treated using an unpaired student's t test.  $n=7-8$  mice/group.

C) DFMO-treatment alters mRNA levels of immune genes. Average mRNA expression levels ( $\pm$  SEM) for *Itgax*, *Pdcd1* (programmed death receptor 1), *Arg1*, and *Ssat* were measured in total brain lysates from CVN-AD mice treated with putrescine in vehicle or putrescine and DFMO. Gene expression levels were measured using quantitative RT-PCR and represent the  $2^{-(\Delta\Delta C(T))}$  with untreated mice as the comparator. Significance between untreated and treated was determined using the unpaired students t test. \* $p < 0.05$ ; \*\* $p < 0.01$ ;  $n=7-8$  mice per group.

D) Representative sagittal sections from CVN-AD mice treated with either putrescine alone or putrescine and DFMO stained for A $\beta$  or CD11c. For each treatment group, panels represent sister sections from the same mouse. Scale bar, 500  $\mu$ m.

To determine whether this reversal was associated with previously identified AD-like pathologies, we measured levels of both soluble and insoluble A $\beta_{40}$  and A $\beta_{42}$  in whole brain lysates. We found that soluble and insoluble A $\beta_{40}$  and A $\beta_{42}$  were significantly reduced by DFMO plus putrescine treatment (**Figure 6B**). To determine if neuronal numbers were altered, the number of neurons in the CA3 region of the hippocampus was counted using unbiased stereology. As we expected, we found no difference in the number of hippocampal neurons between treatment groups of 20-24 week old mice, as CVN-AD mice do not develop significant neuronal loss until around 36 weeks of age (data not shown). We measured mRNA levels for *Itgax* (CD11c) in whole brain lysates from these mice and found that *Itgax* expression was significantly reduced in the DFMO-treated group (**Figure 6C**). We also measured *Pdcd1*, a principal immunosuppressive gene that regulates arginase activity and T-cell activity (Krempski et al., 2011b; Liu et al., 2009) and was highly increased in our gene screen. DFMO treatment significantly reduced *Pdcd1* expression (**Figure 6C**). Genes associated with

arginine utilization were also measured. As expected, *Arg1* mRNA levels did not change, whereas gene expression for spermine synthase s-acetyltransferase (SSAT), which is induced by polyamine activity (Colton et al., 2004) (Krempski et al., 2011a), was significantly decreased by DFMO treatment (**Figure 6C**). IHC staining for A $\beta$  revealed that DFMO treatment in CVN-AD mice resulted in less A $\beta$  plaques, particularly in the cortex and thalamus, and to a lesser extent, in the hippocampus. Similarly, we found that DFMO-treated CVN-AD mice had less CD11c<sup>+</sup> cells in the cortex, thalamus, and hippocampus. Interestingly, treatment with DFMO was less efficacious for reducing A $\beta$  and CD11c in the subiculum of the hippocampus (**Figure 6D**). Taken together, these observations indicate that treatment with DFMO reversed arginine utilization and prevented AD pathology.

## **2.4 Discussion**

Our studies using CVN-AD mice show that CD11c<sup>+</sup> microglia accumulate at sites of Ab deposition, that these microglia show an immunosuppressive phenotype, that extracellular arginase accumulates in these same regions, that global arginine bioavailability significantly decreases, and that inhibition of abnormal arginine utilization results in a marked improvement in pathology and cognitive function. Importantly, CD11c<sup>+</sup> microglial and arginase accumulation in the hippocampus and subiculum in CVN-AD mice correspond to brain areas previously associated with neuronal damage and loss (Colton et al., 2014; Wilcock et al., 2008).

The role of immunity in AD pathogenesis is a critical and unresolved question. One current view proposes that extracellular A $\beta$  peptide activates CNS immune cells, including microglia and perivascular macrophages, to produce inflammatory cytokines such as TNF $\alpha$ , IL-1 $\beta$ , and reactive nitrogen or oxygen species that initiate neuronal death. While this type of response is clearly observed in acute brain diseases, such as bacterial or viral infection and trauma, our data suggest that pro-inflammatory toxicity is not a primary factor in AD pathogenesis and associated neuronal cell loss. While increased pro-inflammatory genes are observed in the CVN-AD mice with increasing age, these changes are late in the course of the disease and counteracted by increased expression of immunosuppressive genes (IL-1Ra, TGF $\beta$ , CD33, TREM2, and DAP12). We propose, instead, that a different type of immune pathology that involves immune suppression leads to neuronal death. In association with A $\beta$  deposition, a subset of resident brain microglia assume a specific immunosuppressive phenotype that includes expression of CD11c and production of extracellular arginase, which acts to deplete brain extracellular arginine levels.

In contrast with other tissues, the brain is particularly susceptible to arginine deprivation as arginine is actively transported into the brain via rate-limiting amino acid transporters (Boado et al., 2004; Closs et al., 2006; Hawkins et al., 2005; Hawkins et al., 2006). While baseline blood arginine levels are approximately 115 mM, whole brain arginine is around 50  $\mu$ M and even lower in the hippocampus (Dawson et al., 2004 ;

Erdely et al., 2010). Furthermore, under inflammatory conditions, endogenous arginine synthesis and transport at the blood brain barrier are decreased. Thus, prolonged and abnormal immune-mediated activation of arginine utilization pathways in susceptible brain regions, such as the hippocampus, may further reduce already low arginine levels, facilitating neuronal damage. When arginine utilization is interrupted by treatment with the arginase and ODC inhibitor DFMO, we show that AD-like pathology is prevented. Further studies will be required to confirm that DFMO improves arginine bioavailability and to determine whether arginase blockade can protect against neuronal death and memory deficit in a therapeutic fashion.

Our findings strikingly reflect previous observations from human AD. CD11c<sup>+</sup> microglia are a well-known feature of human AD pathology, although their functional role has not been explicitly defined (Akiyama and McGeer, 1990; Dick et al., 1997; Tooyama et al., 1990; Walker and Lue, 2005). Direct evidence also supports that dysregulated arginine utilization may contribute to human AD. We, and others, have demonstrated that arginase mRNA expression and enzymatic activity is increased in human AD brain samples (Colton et al., 2006; Hansmannel et al., 2010; Liu et al., 2014). Consistent with increased arginase activity, the frontal cortex of AD patients has significantly decreased levels of L-arginine and L-ornithine (Gueli and Taibi, 2013). Furthermore, others have found increased polyamines (putrescine, spermidine and spermine), the downstream products of arginase activity, in human AD brain (Inoue et

al., 2013). Amino acid starvation leads to GCN2 kinase-mediated phosphorylation of eIF2 $\alpha$ , leading to cell autophagy or apoptosis (Altman and Rathmell, 2012; Young et al., 2009). Indeed, increased phosphorylation of GCN2 kinase has been observed in human AD brain (Ma et al., 2013a), suggesting that the integrated stress response pathway is activated as a result of amino acid deprivation. Collectively, these data support that arginine utilization, which is immune regulated, can be dysfunctional in AD and impact neurodegeneration.

Arginine is the sole substrate of two opposing enzyme systems: the NOS2 pathway and the arginase pathway (**Figure 7**). Both NOS2 and arginase are immune regulated and, in general, NOS2 is associated with the pro-inflammatory phase of an immune response and arginase is associated with the anti-inflammatory phase. NOS2 and arginase are often co-expressed, but competition between these two opposing enzymes favors arginase due to its higher expression level and greater Vmax (Morris, 2007; Wu et al., 2009). In humans, in contrast to *C57BL/6* mice, the competitive advantage is further skewed in favor of arginase. *hNOS2* expression is tightly regulated through promoter differences and post-transcriptional repressors, resulting in less NOS2-mediated NO production in humans compared to mice (Colton et al., 1996; Ganster et al., 2001; Guo et al., 2012; Mestas and Hughes, 2004a). NOS2 transcript, protein, and protein activity are unchanged or even decreased in human AD (Colton et al., 2006; Liu et al., 2014). Low NOS2 enzymatic activity also increases arginase enzyme

activity due to the loss of N-(omega)-hydroxy-L-arginine (NOHA), an intermediate in the L-arginine to NO metabolic pathway and inhibitor of arginase (Boucher et al., 1999; Tenu et al., 1999).

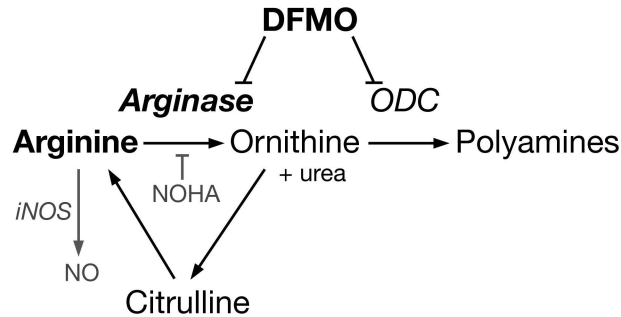


**Figure 7: Simplified schematic of arginine catabolism and the actions of difluoromethylornithine (DFMO) to block arginine utilization.**

Abbreviations: Ornithine decarboxylase (ODC), nitric oxide (NO); inducible nitric oxide synthase (iNOS); N-hydroxyarginine (NOHA). Letters in gray represent a reduction of this protein/product in CVN-AD mice.

Our findings offer one explanation for why most mouse models of AD show abundant A $\beta$  deposition but, despite large increases in pro-inflammatory cytokines, do not show significant neuronal cell loss (Irizarry et al., 1997a; Radde et al., 2008b). By crossing mutant AppSwDI mice onto an *mNos2*-deficient background, we developed a mouse model of AD that more closely mimics the reduced iNOS activity found in humans (Vitek et al., 1997). In contrast to CVN-AD mice, the parent APPSwDI mice had much reduced expression of arginase at all ages and showed no changes in arginine transporter mRNA or global arginine bioavailability. Furthermore, reconstituting the

human *NOS2* gene into the CVN-AD mouse strain resulted in equivalent AD-like pathology as found in CVN-AD mice (Colton et al., 2014), demonstrating that reducing *NOS2* expression to more human-like levels favors arginase in the competition for arginine and highlights the species difference in *NOS2* regulation of arginine utilization. Interestingly, this shift in immune-mediated redox conditions likely accounts for the accelerated and more prominent expression of CD11c, although the mechanisms governing this difference are unknown.

The exact cell type associated with increased arginine consumption remains unclear. Neurons, astrocytes, microglia, and circulating monocytes are all capable of expressing arginase, and thus each (or all) may participate in depletion of extracellular arginine. However, few neurons demonstrate arginase immunoreactivity and the neuronal expression of arginase appears to be limited to specific tracts in the visual cortex and cerebellum (Yu et al., 2001). Astrocytes express a similar profile of arginine transporters to microglia and may actively reduce environmental arginine levels via robust uptake. Future studies are required to understand the kinetics and cellular origin of arginase expression, particularly in human AD pathology. However, we hypothesize that microglia are the primary source for arginine consumption. First, A $\beta$  itself may initiate induction of immunosuppression in microglia (Kurnellas et al., 2013). Secondly, similarly to our observations, human myeloid cells commonly release extracellular arginase under pathologic conditions, as has been observed in glioblastoma and other

tumors (Raychaudhuri et al., 2011). The appearance of CD11c<sup>+</sup> microglia very early in pathology and their tight correlation with AD pathology and extracellular arginase supports a role for this sub-type of microglia in immune-mediated arginase release. Importantly, when we blocked arginase utilization in CVN-AD mice we found significantly decreased expression of CD11c.

Although it cannot be firmly established with the present data, we anticipate that the CD11c<sup>+</sup> cells arise from the brain's endogenous microglial population and not from infiltrating monocytes. Influx of Ly6C<sup>+</sup> inflammatory monocytes into the mouse brain depends largely on expression of CCR2 and its ligands (El Khoury et al., 2007; Mildner et al., 2007) and no change was observed in total brain expression of CCR2 or CCL2 in CVN-AD mice at any age. While infiltrating Ly6C<sup>+</sup> monocytes could comprise a rare cell population, and thus total brain *Ccr2* would be unchanged, we also did not observe any significant increase in brain monocytes at multiple ages by flow cytometry. Supporting these findings, Zhang *et al.* previously demonstrated that monocytes from humans with AD have decreased expression of CCR2 (Zhang et al., 2013b), suggesting decreased capacity for chemotaxis. In concordance with data from human AD, we found increased CCR1 expression in CVN-AD brain, although how CCR1 regulates chemotaxis in AD remains unknown (Halks-Miller et al., 2003). Thus, while our data highly implicate endogenous hippocampal microglia and not peripheral cells, further studies are required to prove this point.

In summary, based on our analysis of CNS immunity during aging in a mouse model of AD, we conclude that, contrary to the predominant paradigm that AD pathology is driven by pro-inflammatory factors, our data support an alternative mechanism for neuronal death in AD. We suggest that immune suppression and arginine catabolism lead to a loss of arginine, a critical semi-essential amino acid, and this nutrient deprivation is followed by cell death. This is a novel and potentially critical mechanism that may explain the temporal and spatial induction of the slow and persistent loss of neurons in humans with AD.

### **3. Gene targeting of monocytes, microglia, and tissue macrophages with *Cx3cr1*-BAC-Cre mice**

One of our future goals is to definitively demonstrate that neuronal death in CVN-AD mice is caused by microglial-derived arginase-1 by selectively deleting *Arg1* from microglia. This has required the development of a mouse model allowing for the deletion of *Arg1* in microglia, but not neurons, astrocytes, or oligodendrocytes, and where CNS immunity is not perturbed. Here, we describe a novel mouse model that when mated onto the CVN-AD background will allow us to conduct these critical experiments.

#### **3.1 Introduction**

There has been a recent intense focus on the function and origin of mononuclear phagocytes, which includes blood monocytes, tissue macrophages, and dendritic cells. The use of mice expressing tissue-specific Cre recombinase has been invaluable in this effort by enabling the lineage tracing of myeloid cells and the ability to delete or force expression of genes. Many of these mice have employed the *Cx3cr1* locus to drive Cre expression as the chemokine receptor CX<sub>3</sub>CR1 is differentially expressed on many myeloid cell populations. These mice have allowed for the manipulation of tissue

macrophage populations, such as brain microglia and blood monocytes (Parkhurst et al., 2013; Yona et al., 2013).

Currently, all available *Cx3cr1* Cre and/or fluorescent reporter mice are knock-in mice (Ellmeier et al., 2000; Parkhurst et al., 2013; Yona et al., 2013), meaning that these mice are haploinsufficient in the *Cx3cr1* gene. While it had long been thought that deficiency or heterozygosity of *Cx3cr1* had a negligible phenotype, both *Cx3cr1*-deficient and heterozygote mice have been demonstrated to have a variety of functional differences from wild-type mice, including differences in neural development and spatial memory, development of experimental atherosclerosis, and the induction of oral tolerance (Combadiere et al., 2003; Mazzini et al., 2014; Moatti et al., 2001; Rogers et al., 2011). These observations suggest that in certain contexts, *Cx3cr1* gene dosage can have important effects on biological outcomes and that caution should be taken when *Cx3cr1* knock-in reporter or Cre mice are used.

We have characterized a line of *Cx3cr1*-Cre mice developed by the GENSAT BAC Transgenic Project (Gong et al., 2003), in which Cre is driven by the *Cx3cr1* promoter in a bacterial artificial chromosome (BAC) transgene. This transgene was not targeted to a particular gene locus. These Tg(*Cx3cr1*-cre)MW123Gsat (*Cx3cr1*-CreBT) mice thus carry two copies of the endogenous *Cx3cr1* gene while demonstrating a Cre expression pattern that is very similar to that of previously described *Cx3cr1*-Cre knock-in (*Cx3cr1*-CreKI) mice. Similar to *Cx3cr1*-CreKI mice, *Cx3cr1*-CreBT mice preferentially express Cre in

Ly6C<sup>low</sup> resident monocytes, but not Ly6C<sup>high</sup> inflammatory monocytes. Cre is expressed in a variety of tissue macrophages, including kidney macrophages, liver Kupffer cells, skin Langerhans' cells, and brain microglia. We find that Cre is also expressed in the vast majority of dendritic cells. Lastly, we demonstrated that these mice can be used for preferential gene targeting with fluorescent reporters and inducible diphtheria toxin receptor cell ablation. The *Cx3cr1*-CreBT mouse line is thus a novel tool for constitutive Cre targeting of myeloid cell populations without perturbing the *Cx3cr1* locus.

### **3.2 Methods and Materials**

**Mice and diphtheria toxin treatments.** C57BL/6 mice were purchased from Charles River Laboratories (Wilmington, MA). Tg(*Cx3cr1*-Cre)MW123GSat mice were generated and provided by the L. Kus (GENSAT BAC Transgenic Project, Rockefeller University, New York, NY) and backcrossed over 12 generations on a C57BL/6 background. *Cx3cr1*<sup>GFP/GFP</sup> mice were provided by D. Littman (New York University, New York, NY) or purchased from Jackson Laboratories (Bar Harbor, ME) and crossed with C57BL/6 mice to produce *Cx3cr1*<sup>+GFP</sup> mice. *Rosa26*-GFP mice were provided by F. Wang (Duke University), and *Rosa26*-tdTomato and *Rosa26*-DTR mice were purchased from Jackson Laboratories. All mice used for experiments were between 8 and 12 weeks old. Diphtheria toxin (DT) (List Biological Laboratories, Inc., Campbell, CA) was

resuspended in PBS and mice were injected *i.p.* with 10 ng/g or 150 ng/g DT in 100  $\mu$ L of PBS every 24 hours for 3 days. Body weight of DT-treated mice was monitored daily. All animal experiments were conducted in accordance with National Institutes of Health guidelines and protocols approved by the Animal Care and Use Committee at Duke University.

**Flow Cytometric Analysis.** Blood was collected from isoflurane-anesthetized mice with a 27G insulin syringe and immediately resuspended in 5% fetal bovine serum with 10 mM HEPES. Mice were intracardially perfused with PBS and tissues were then rapidly harvested, manually dissociated, and digested for 1 hour at 37°C with 1.5 mg/mL collagenase A (Roche Applied Science; Penzberg, Germany) and 0.40 mg/mL DNase I (Roche Applied Science). Cells from the digested tissue were then strained through a 70  $\mu$ m filter and washed with PBS. Red blood cells were lysed with ammonium/chloride/potassium (ACK) lysis buffer and then cells were counted and stained with LIVE/DEAD Aqua (Invitrogen/Life Technologies, Carlsbad, CA) in PBS. Samples were blocked in 5% rat serum, 5% mouse serum, 1% Fc Block (eBioscience, San Diego, CA) and stained for 30 minutes at 4°C with the following antibodies (eBioscience, San Diego, CA): CD11c PE-Cy5.5; F4/80 PE-Cy7; CD3e APC; Ly6G AF700; CD11b APC-Cy7; Ly6C V450; CD45 Qdot605; IA-IE Qdot655. Cells were analyzed on a BD™ LSR-II Flow Cytometer (BD Biosciences; Franklin Lakes, NJ) in the Duke Human Vaccine

Institute Flow Research Facility and data was analyzed with FlowJo (Treestar; Ashland, OR).

**Immunohistochemistry.** Mice were anesthetized with isoflurane and then intracardially perfused with phosphate buffered saline (PBS). Perfused brains were then rapidly removed, bisected in the mid-sagittal plane and cryoprotected by sequential passage through 10%, 20%, and 30% sucrose for 24 hrs. Frozen sagittal sections (25  $\mu\text{m}$ ) were then prepared by microtome. Sections equally spaced at 600  $\mu\text{m}$  apart were immunostained with anti-Iba-1 (Wako Pure Chemical Industries, Osaka, Japan) and AlexaFlour-488 donkey anti-rabbit secondary antibody (Invitrogen, Carlsbad, CA).

**Statistics.** All numerical data are presented as mean  $\pm$  standard error of the mean (SEM). All data are analyzed by two-way ANOVA or unpaired Student's *t* tests using GraphPad Prism (La Jolla, CA) software, as indicated in the figure legends.

### **3.3 Results**

#### **3.3.1 Cre is preferentially expressed in Ly6C<sup>low</sup> monocytes in *Cx3cr1-CreBT* mice**

We characterized three lines of *Cx3cr1-CreBT* mice from the GENSAT BAC Transgenic Program, and the line presented here (Tg(Cx3cr1-Cre)MW123GSat) was selected as it exhibited the least off-target expression in CX3CR1<sup>-</sup> cell populations and the highest efficiency of expression in CX3CR1<sup>+</sup> cell populations (data for other strains not shown). Of note, this strain is distinct from a previously described GENSAT *Cx3cr1-*

*CreBT* line (Abram et al., 2014). We first assessed Cre expression in various immune cell subsets in the peripheral blood (see **Figure 8** for flow gating) of *Cx3cr1-CreBT* mice by mating them to Cre-inducible *Rosa-GFP<sup>flox/flox</sup>* reporter mice (F. Wang, unpublished), in which GFP is produced only by Cre-expressing cells, to generate *Cx3cr1-CreBT:GFP<sup>flox/wt</sup>* mice. We found that in *Cx3cr1-CreBT:GFP<sup>flox/wt</sup>* mice, GFP was expressed in the vast majority of Ly6C<sup>low</sup> resident monocytes, but GFP was expressed in only ~30% of Ly6C<sup>high</sup> inflammatory monocytes (**Figure 9A and 9B**). Approximately 25% of natural killer (NK) cells expressed GFP, and there was minimal (<10%) GFP expression in eosinophils, neutrophils, T cells, and B cells, which was similar to GFP expression in *Cx3cr1<sup>GFP/wt</sup>* mice (**Figure 9**).

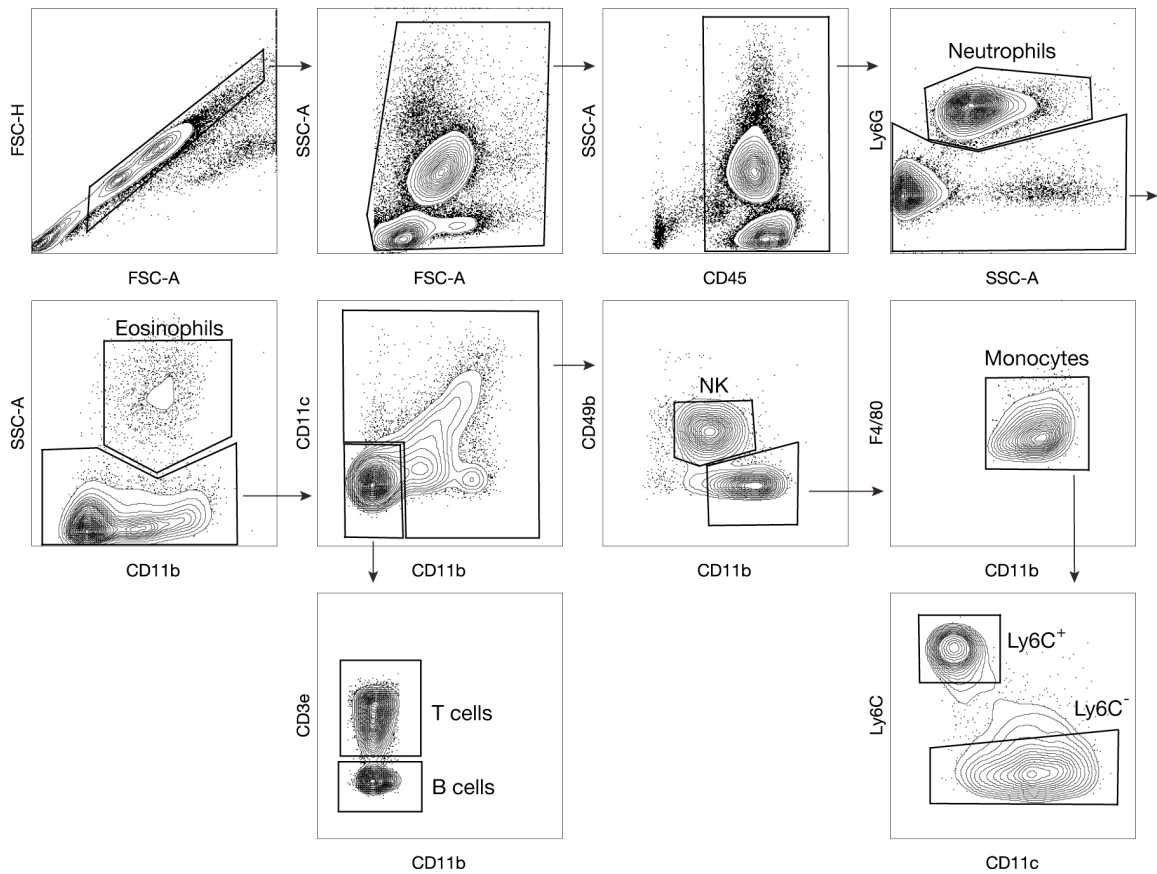


**Figure 8: Flow cytometry gating on peripheral blood cell populations.**

Gating strategy for flow cytometric identification of peripheral blood populations, including neutrophils, eosinophils, natural killer (NK) cells, T and B lymphocytes, and Ly6C<sup>hi</sup> inflammatory monocytes and Ly6C<sup>lo</sup> resident monocytes.

As a comparator, we analyzed GFP expression in *Cx3cr1*<sup>GFP/wt</sup> mice, which have GFP knocked in to the *Cx3cr1* locus (Jung et al., 2000). In *Cx3cr1*<sup>GFP/wt</sup> mice, almost all monocytes, including Ly6C<sup>low</sup> and Ly6C<sup>high</sup> monocytes, express GFP. Only 20% of natural killer (NK) cells express GFP, and there is minimal GFP expression in eosinophils, neutrophils, T cells, and B cells (**Figure 9B**). In sum, unlike the *Cx3cr1*<sup>GFP/wt</sup>

mice, which express GFP in all monocytes, *Cx3cr1-CreBT* mice preferentially express Cre recombinase in Ly6C<sup>low</sup> resident monocytes and have limited expression in Ly6C<sup>high</sup> inflammatory monocytes. This expression pattern is very similar to that previously described in *Cx3cr1-CreKI* mice, which also preferentially express Cre-inducible fluorescent reporters in Ly6C<sup>low</sup> (~60% YFP<sup>+</sup>) but not Ly6C<sup>high</sup> monocytes (<10% YFP<sup>+</sup>) (Yona et al., 2013).

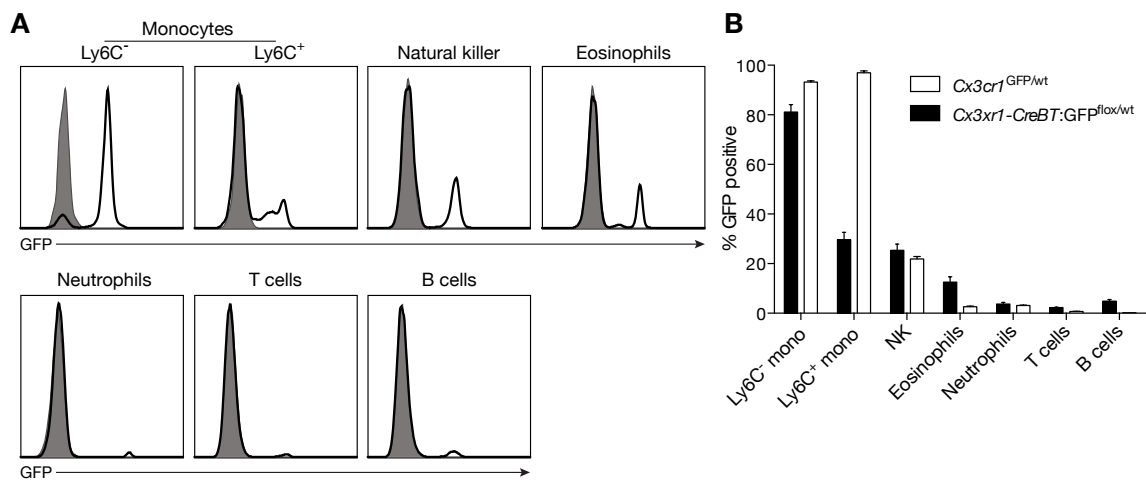


**Figure 9: *Cx3cr1*-BAC-Cre is expressed preferentially in Ly6C<sup>low</sup> monocytes**

**A)** Histograms of GFP expression as determined by flow cytometry in *Cx3cr1*<sup>GFP/wt</sup> and *Cx3cr1-CreBT:GFP*<sup>lox/wt</sup> peripheral blood subsets, representative of more than 30 animals and 6 experiments.

**B)** Quantitative summary of percent GFP expression by flow cytometry of *Cx3cr1*<sup>GFP/wt</sup> (n=9) and *Cx3cr1-CreBT:GFP*<sup>lox/wt</sup> (n=15) peripheral blood immune cells.

### 3.3.2 Cre is expressed in tissue macrophages of *Cx3cr1-CreBT* mice

We also characterized GFP expression in a variety of tissue macrophage populations of *Cx3cr1-CreBT:GFP*<sup>lox/wt</sup> mice relative to that seen in *Cx3cr1*<sup>GFP/wt</sup> mice and

non-Cre expressing GFP<sup>fllox/wt</sup> negative controls (**Figure 10**). In adult *Cx3cr1*<sup>GFP/wt</sup> mice, GFP expression was limited to CD11b<sup>+</sup> CD45<sup>low</sup> brain microglia and CD11b<sup>+</sup> F4/80<sup>high</sup> kidney macrophages, with little or no GFP expression detected in Kupffer cells, splenic macrophages or lung alveolar macrophages. In contrast, GFP expression was found in almost all tissue macrophage populations of *Cx3cr1-CreBT*:GFP<sup>fllox/wt</sup> mice, although this expression was limited to 60% of alveolar macrophages. GFP was expressed in the majority of E10.5 yolk sac macrophages (DeFalco et al., 2014) and negligible GFP expression was observed in non-myeloid populations or CD45<sup>-</sup> populations (data not shown).

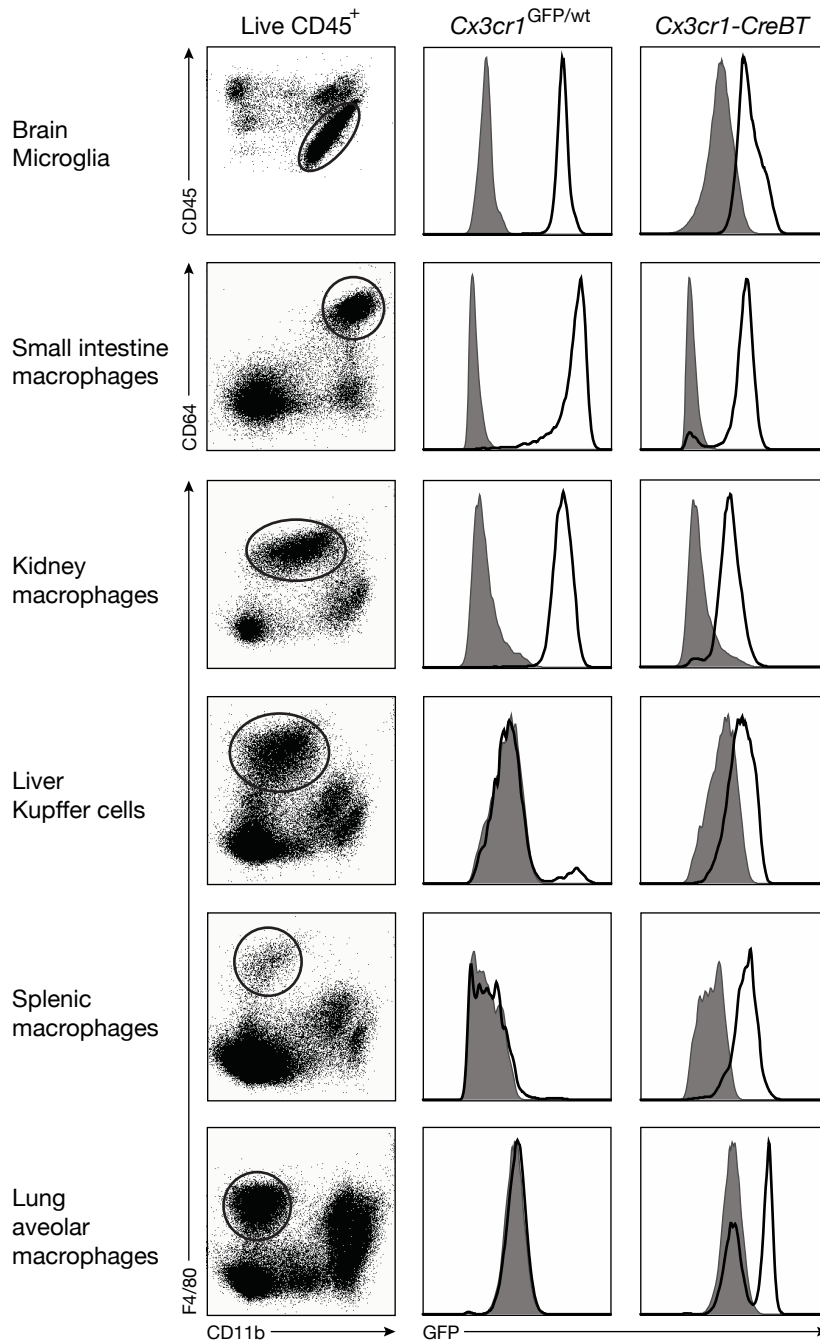


**Figure 10: *Cx3cr1-CreBT*:GFP is expressed in tissue macrophages by flow cytometry**

Histograms of GFP expression in tissue macrophage populations after gating on live CD45<sup>+</sup> cells. Tissue macrophages were identified as depicted in the left panels, and

GFP expression in those macrophages in *Cx3cr1*<sup>GFP/wt</sup> and *Cx3cr1-CreBT*:GFP<sup>flox/wt</sup> mice are shown. Closed grey histogram: *Rosa26*-GFP<sup>flox/wt</sup> control; open black histogram: *Cx3cr1*<sup>GFP/wt</sup> or *Cx3cr1-CreBT*:GFP<sup>flox/wt</sup> mouse. Representative of over 15 animals and 4 experiments.

In some tissues of *Cx3cr1-CreBT*:GFP<sup>flox/wt</sup> mice, such as the brain, liver, and spleen, GFP expression displayed considerable overlap with the GFP<sup>flox/wt</sup> negative control despite a total shift in the curve (**Figure 10**). To determine if this limited expression of GFP was due to poor Cre expression or to characteristics of the reporter strain used, we mated *Cx3cr1-CreBT* mice to *Rosa26*-tdTomato reporters (Madisen et al., 2010) to generate *Cx3cr1-CreBT*:tdTomato<sup>flox/wt</sup> mice and analyzed individual tissues by fluorescent microscopy. In the brains of *Cx3cr1-CreBT*:tdTomato<sup>flox/wt</sup> mice, all parenchymal microglia expressed tdTomato in a pattern that overlapped staining for Iba-1, a calcium-binding adaptor protein that is expressed on microglia (**Figure 11A**). The tdTomato reporter and Iba-1 were also expressed in other brain macrophage populations known to express CX3CR1, such as meningeal macrophages (**Figure 11A, arrows**). No tdTomato expression was observed in non-myeloid populations, including neurons, astrocytes, and oligodendrocytes. In *Cx3cr1-CreBT*:tdTomato<sup>flox/wt</sup> mice, tdTomato was expressed in patterns consistent with those of liver Kupffer cells (**Figure 11B**), splenic red pulp macrophages (**Figure 11C**), and lung alveolar macrophages (**Figure 11D**).

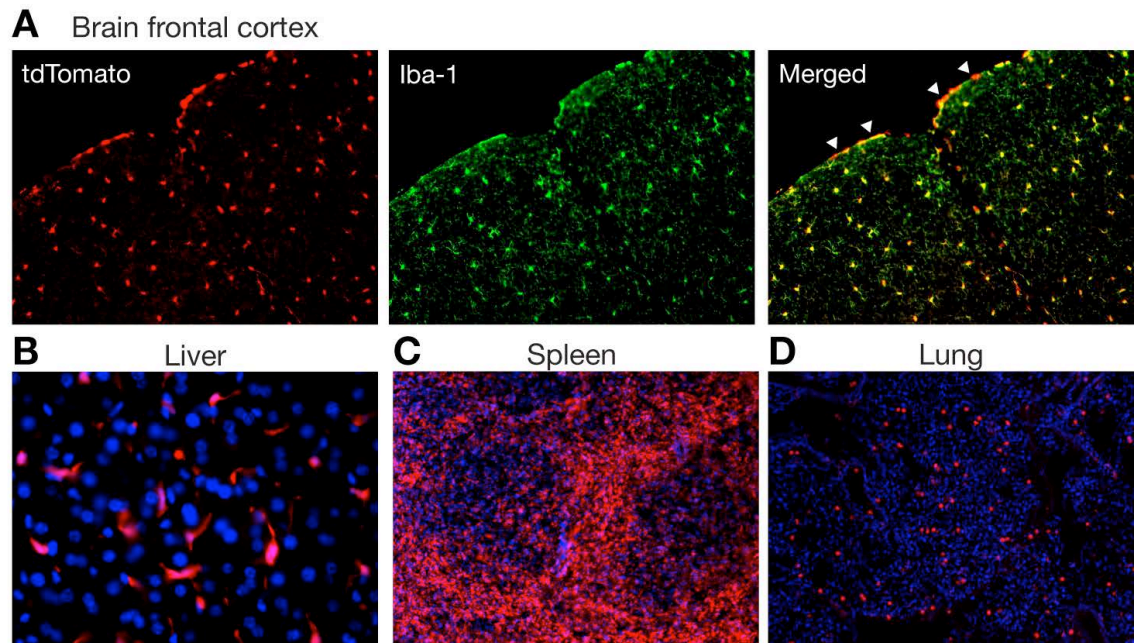


**Figure 11: *Cx3cr1-CreBT:tdTomato* is expressed in tissue macrophages by histology**

- A) Frontal cortex of a 6 week-old *Cx3cr1-CreBT: tdTomato*<sup>fl<sup>ox</sup>/wt</sup> mouse showing tdTomato, Iba-1, and merged markers.
- B) Liver of a 6 week-old *Cx3cr1-CreBT: tdTomato*<sup>fl<sup>ox</sup>/wt</sup> mouse showing tdTomato (red) and DAPI (blue).
- C) Spleen of a 6 week-old *Cx3cr1-CreBT: tdTomato*<sup>fl<sup>ox</sup>/wt</sup> mouse showing tdTomato (red) and DAPI (blue).
- D) Lung of a 6 week-old *Cx3cr1-CreBT: tdTomato*<sup>fl<sup>ox</sup>/wt</sup> mouse showing tdTomato (red) and DAPI (blue).

### 3.3.3. Cre expression in dendritic cells of *Cx3cr1-CreBT* mice

CX3CR1 has been previously described to be expressed on subsets of both migratory and resident lymph node dendritic cells (DC) (Becker et al., 2014), and is upregulated on DC with maturation (Kanazawa et al., 1999; Papadopoulos et al., 1999).

To determine if Cre is expressed in dendritic cells (DC) of *Cx3cr1-CreBT* mice, we performed flow cytometric analysis in *Cx3cr1-CreBT:GFP<sup>lox/wt</sup>* mice for lymph node DC populations (see **Figure 12** for flow gating).

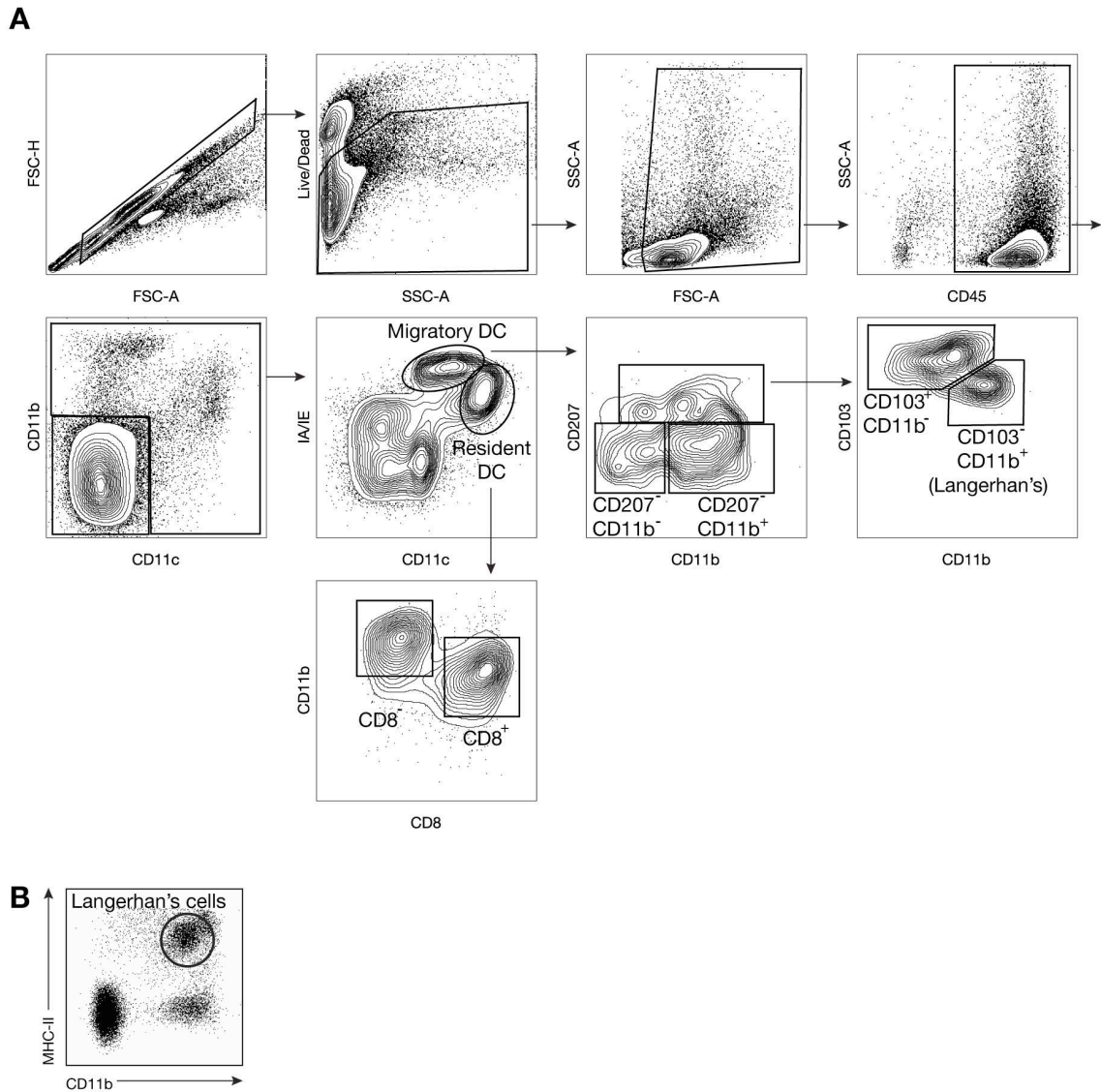


**Figure 12: Flow cytometry gating on dendritic cell populations**

A) Gating strategy for flow cytometric identification of lymph node dendritic cell (DC) populations.

**B) Gating strategy for flow cytometric identification of skin Langerhan's cells, after gating on live CD45<sup>+</sup> cells.**

Among the migratory DC populations, we found that the vast majority of CD11b<sup>+</sup> DC expressed GFP, including both CD207<sup>-</sup> and CD207<sup>+</sup>CD103<sup>-</sup> (Langerhan's) CD11b<sup>+</sup> DC (**Figure 13A**). While there was heterogeneous GFP expression in migratory CD11b<sup>-</sup> DC populations (**Figure 13A**), as well as CD8<sup>+</sup> and CD8<sup>-</sup> lymph node resident DC (**Figure 13B**), the majority of these DC populations also expressed GFP. To confirm these findings in a peripheral tissue, we examined GFP expression in skin Langerhan's cells (see **Figure 12** for flow gating). As we observed with the CD11b<sup>+</sup>CD207<sup>+</sup>CD103<sup>-</sup> Langerhan's DC in the lymph node, most skin Langerhan's cells were GFP<sup>+</sup> (**Figure 13C**). While reporter expression has not been assessed in depth in *Cx3cr1*-CreKI mice for DC populations, Langerhan's cells have been reported to be positive for a Cre-inducible fluorescent reporter in *Cx3cr1*-CreKI mice, whereas Langerhan's cells are GFP<sup>-</sup> in *Cx3cr1*<sup>GFP/wt</sup> mice (Yona et al., 2013).

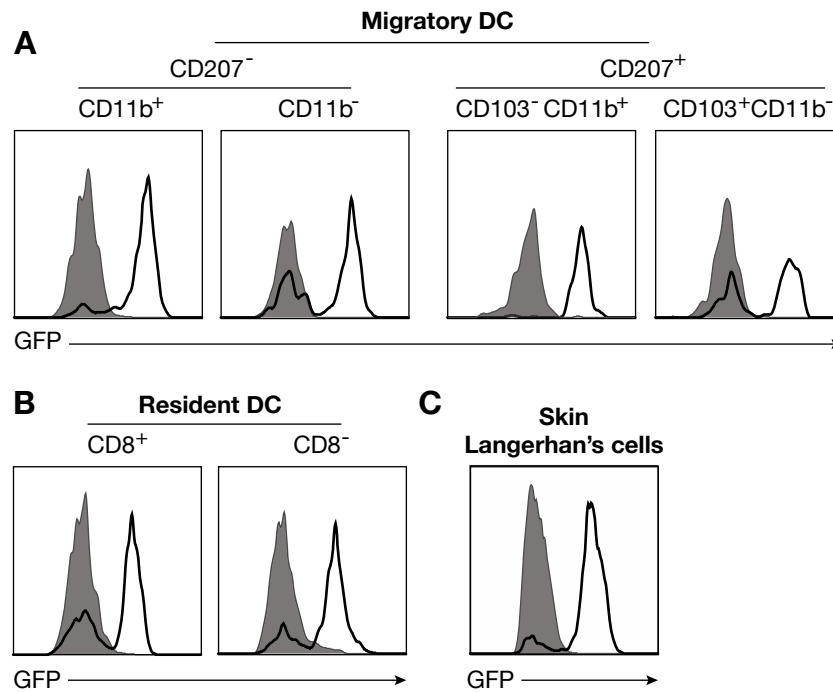


**Figure 13: *Cx3cr1-CreBT:GFP* is expressed in dendritic cells**

**A)** Histograms of GFP expression as determined by flow cytometry in dendritic cell populations in lymph nodes from *Cx3cr1*<sup>GFP/wt</sup> and *Cx3cr1-CreBT:GFP*<sup>flox/wt</sup> mice. Closed grey histogram: *GFP*<sup>flox/wt</sup> control; open black histogram: *Cx3cr1*<sup>GFP/wt</sup> or *Cx3cr1-CreBT:GFP*<sup>flox/wt</sup> mouse. Representative of 10 mice over 3 experiments.

**B)** Histograms of GFP expression as determined by flow cytometry in skin Langerhan's cells from *Cx3cr1*<sup>GFP/wt</sup> and *Cx3cr1-CreBT:GFP*<sup>flox/wt</sup> mice. Closed grey histogram: *GFP*<sup>flox/wt</sup> control; open black histogram: *Cx3cr1*<sup>GFP/wt</sup> or *Cx3cr1-CreBT:GFP*<sup>flox/wt</sup> mouse. Representative of over 12 mice and 4 experiments.

### 3.3.4. Selective depletion of resident monocytes and microglia in *Cx3cr1-CreBT:DTR* mice

To confirm the pattern of Cre expression in *Cx3cr1-CreBT* mice, we mated these mice to mice expressing the Cre-inducible diphtheria toxin receptor (*Rosa26-DTR*) (Buch et al., 2005) to generate *Cx3cr1-CreBT:Rosa26-DTR*<sup>flox/wt</sup> (*Cx3cr1-CreBT-DTR*) mice. In the

*Rosa26*-DTR mice, a stop codon preventing translation of the diphtheria toxin receptor is excised in the presence of Cre. Thus, Cre-expressing cells are able to bind and internalize diphtheria toxin (DT) and thereby be specifically ablated. The treatment of *Cx3cr1-CreBT*-DTR mice with DT (10 ng/g *i.p.* daily for 3 days) resulted in a dramatic reduction in Ly6C<sup>low</sup> resident monocytes as a percentage of total blood cells (**Figure 14A and B**). In non-Cre expressing *Rosa26*-DTR<sup>flx/flx</sup> control mice, resident monocytes were unaffected by DT treatment (**Figure 14A and B**). Despite their low level of Cre expression, Ly6C<sup>hi</sup> inflammatory monocytes were not ablated in DT-treated *Cx3cr1-CreBT*-DTR mice, resulting in an increase in the percentage of these cells among total blood cells (**Figure 14A and B**).

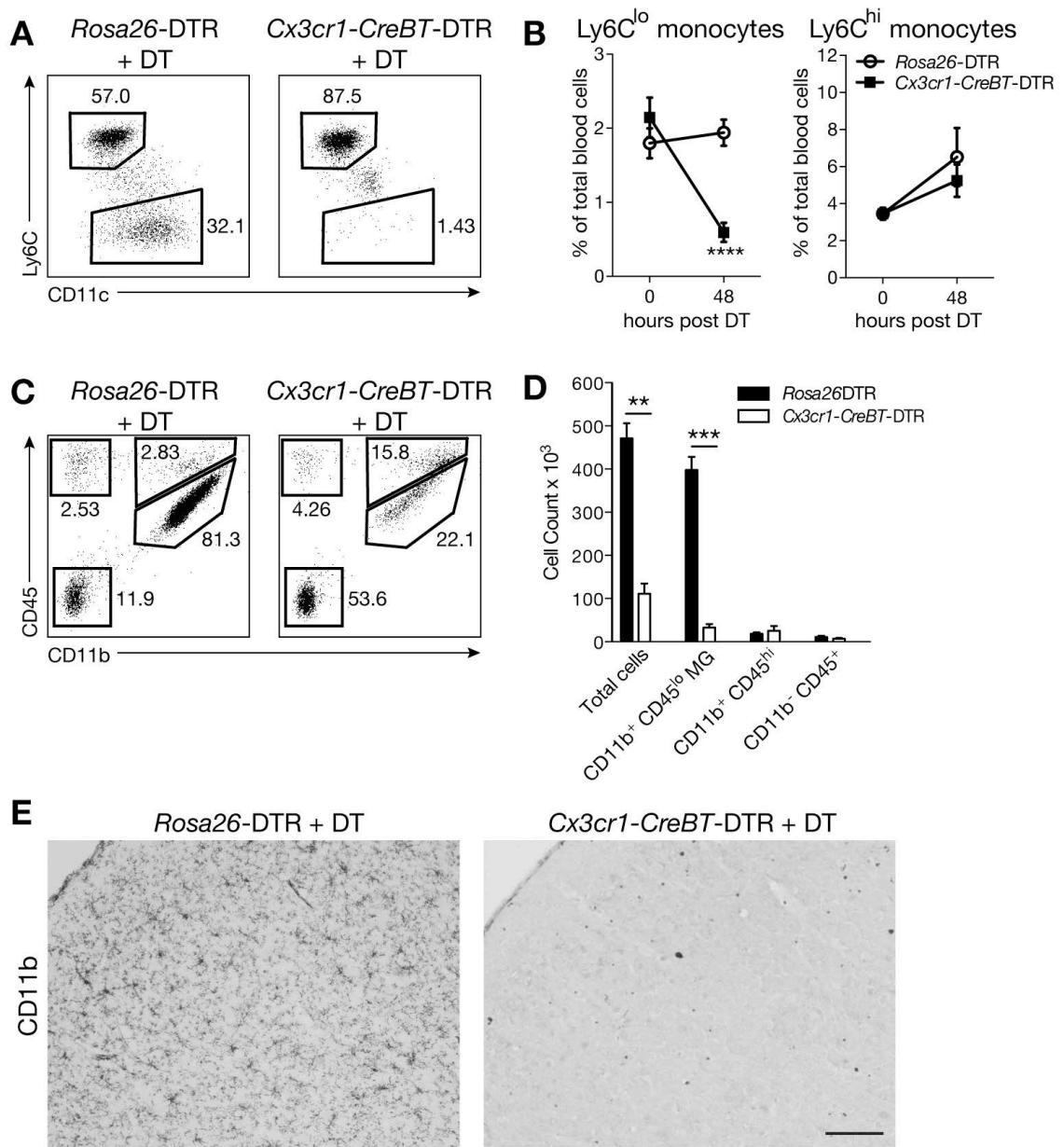


**Figure 14: Selective depletion of myeloid cells in *Cx3cr1-CreBT-DTR* mice**

**A)** Peripheral blood monocytes as determined by flow cytometry in *Rosa26-DTR* and *Cx3cr1-CreBT-DTR* mice 48 hours after treatment with 10 ng/kg of diphtheria toxin (DT) *i.p.* Plots are gated on total monocytes and further subgated into Ly6C<sup>hi</sup> inflammatory and Ly6C<sup>low</sup> resident monocytes. Representative of 5 experiments with at least 5 mice each.

**B)** Quantification of Ly6C<sup>low</sup> resident monocytes and Ly6C<sup>hi</sup> inflammatory as a percentage of total blood cells in *Rosa26-DTR* and *Cx3cr1-CreBT-DTR* mice before treatment and 48 hours after treatment with 10 ng/kg of diphtheria toxin (DT). n=3, representative of 5 experiments.

**C)** Total brain leukocytes as determined by flow cytometry in *Rosa26-DTR* and *Cx3cr1-CreBT-DTR* mice 24 hours after treatment with 50 ng/kg DT *i.p.* daily for 3 days. Plots are gated on total live CD45<sup>+</sup> cells and subgated into microglia (CD11b<sup>+</sup> CD45<sup>low</sup>), myeloid (CD11b<sup>+</sup> CD45<sup>high</sup>), lymphoid (CD11b<sup>-</sup> CD45<sup>high</sup>), and non-immune (CD45<sup>-</sup>) cells. Representative of 5 experiments with at least 3 mice each.

**D)** Quantification of absolute number of cells after treatment as described in C. n=3, representative of 5 experiments. \*\*p<0.01, \*\*\*p<0.001 by Student's t test.

**E)** CD11b immunohistochemical staining in the frontal cortex of *Rosa26-DTR* and *Cx3cr1-CreBT-DTR* mice after DT treatment as described in C. Scale bar: 100  $\mu$ m. Representative of 3 experiments with at least 3 mice each.

To determine if tissue macrophage populations could be depleted in *Cx3cr1-CreBT-DTR* mice, these mice were treated with a much higher dose of DT (150 ng/g *i.p.* daily for 3 days). This treatment dramatically reduced the number of microglia in the CNS (**Figure 14C and D**). On histologic examination, DT-treated *Cx3cr1-CreBT-DTR* mice demonstrated a dramatic reduction in the presence of parenchymal CD11b<sup>+</sup> microglia while control mice were unaffected by DT treatment (**Figure 14E**). After DT treatment, *Cx3cr1-CreBT-DTR* mice did not exhibit any neurological or behavioral symptoms for the first 3-4 days. However, after 5 days, the majority of these mice began to lose body weight, developed ataxia, and had to be sacrificed due to a failure to thrive of unknown etiology. Thus, while we could not utilize this particular model to study the biological outcomes of DT depletion of microglia as has been done by previous groups

(Parkhurst et al., 2013), these results establish the proof of concept that *Cx3cr1-CreBT* mice can be used for Cre-mediated gene targeting in resident monocytes and tissue macrophages.

### **3.4 Discussion**

Our studies characterizing *Cx3cr1-CreBT* mice demonstrate that Cre recombinase is expressed primarily in Ly6C<sup>-</sup> but not Ly6C<sup>+</sup> blood monocytes, the vast majority of tissue macrophages, including microglia, and the majority of dendritic cells. We have established proof of concept that *Cx3cr1-CreBT* mice can be used for selective gene targeting in these populations using the Cre-inducible diphtheria toxin receptor to demonstrate cell-specific DT depletion. Cre-dependent fluorescent reporting in *Cx3cr1-CreBT* mice is consistent with the patterns observed in previously described constitutive *Cx3cr1-CreKI* lines, with the benefit that, unlike knock-in fluorescent reporting or Cre-expressing mice, *Cx3cr1-CreBT* mice express both copies *Cx3cr1*.

*Cx3cr1* knock-in reporter and Cre expressing mice have been invaluable tools for lineage tracing and gene deletion in monophagocytes. As the ontogenic relationships between monocytes and tissue macrophages in homeostasis have become more clearly defined, studies are increasingly focused on understanding the physiologic roles of these populations in inflammation. However, *Cx3cr1* knock-in mice present a barrier to studying the physiologic function of monophagocytes because CX3CR1 itself plays a

role in organismal development, immune responses, and disease pathogenesis in a gene dose-dependent fashion. For example, *Cx3cr1* has been demonstrated to be important for cognitive function in a gene-dosage-dependent manner, where both *Cx3cr1<sup>-/-</sup>* and *Cx3cr1<sup>+/-</sup>* mice exhibiting decreased hippocampal neurogenesis and associative and spatial memory formation when compared to *Cx3cr1<sup>+/+</sup>* mice (Rogers et al., 2011). In humans, the CX3CR1 I249 allele, which significantly decreases CX3CL1 binding sites on monocytes, is an independent risk factor for coronary artery disease (Moatti et al., 2001). This observation has been replicated in mice, as both *Cx3cr1<sup>-/-</sup>* and *Cx3cr1<sup>+/-</sup>*, but not *Cx3cr1<sup>+/+</sup>*, mice on an ApoE-deficient background were both protected from atherosclerosis (Combadiere et al., 2003). In mice, the induction of oral tolerance has been demonstrated to be dependent on CX3CR1<sup>+</sup> intestinal macrophages, which pass antigen to CD103<sup>+</sup> dendritic cells through gap junctions. This phenomenon is dependent on CX3CR1, as *Cx3cr1<sup>GFP/GFP</sup>* and *Cx3cr1<sup>GFP/wt</sup>* mice have impaired induction of oral tolerance (Mazzini et al., 2014). In sum, these studies suggest that *Cx3cr1<sup>+/-</sup>* mice have altered development and immune responses and should be chosen with care for experimental design.

The major finding of this study is that, despite the use of a BAC transgene, *Cx3cr1*-CreBT mice have a phenotype that is virtually identical to that of a previously described *Cx3cr1*-CreKI mouse, which also selectively expresses Cre in tissue macrophages and Ly6C<sup>-</sup> but not Ly6C<sup>+</sup> blood monocytes (Yona et al., 2013). This is

highlighted in the monocyte populations, as >95% of both Ly6C<sup>+</sup> and Ly6C<sup>-</sup> monocyte populations are GFP<sup>+</sup> in *Cx3cr1*<sup>GFP/wt</sup> reporter mice, but demonstrate dichotomous expression in fluorescent-reporting *Cx3cr1*-CreKI mice (Yona et al., 2013). We found a similar pattern of expression, in that GFP was expressed in ~80% of Ly6C<sup>+</sup> monocytes and only ~35% of Ly6C<sup>-</sup> monocytes, and this was reflected in different susceptibilities to inducible diphtheria toxin ablation, where only Ly6C<sup>-</sup> monocytes were depleted with DT. These findings demonstrate that *Cx3cr1*-CreBT mice are a useful tool for understanding the different physiological roles of Ly6C<sup>+</sup> and Ly6C<sup>-</sup> monocytes. *Cx3cr1*-*CreBT* mice also have a very similar pattern fluorescent reporting compared to previously described constitutive *Cx3cr1*-CreKI mice in tissue macrophages. We found that the majority of dendritic cells were GFP<sup>+</sup> in *Cx3cr1*-*CreBT* mice, but DC expression of Cre in *Cx3cr1*-CreKI mice has not been previously described.

The description of Cre expression in this *Cx3cr1*-*CreBT* mouse may be used as a reference, but the phenotype of every Cre-flox mouse cross is unique. The induction or deletion of a floxed target gene should be examined and demonstrated in specific cell populations, as Cre-mediated DNA excision of floxed alleles is dependent on the timing of Cre expression, simultaneous accessibility of the floxed gene locus, and the rate of cell turnover. For example, the *LysM*-Cre mouse was described to express Cre in both macrophage and neutrophil populations (Clausen et al., 1999), but when mated to the *Rosa26*-DTR mouse, diphtheria toxin administration had no significantly effect on

neutrophils (Goren et al., 2009). Similarly, we have observed that when the *Cx3cr1-CreBT* mouse is mated to certain strains of floxed mice that we see robust target gene deletion and decreased protein expression in tissue macrophages but not in DC populations (unpublished data), despite widespread expression of GFP expression in the DC of *Cx3cr1-CreBT:GFP<sup>flox/wt</sup>* mice. These data suggest that every unique Cre-flox mouse strain should describe cell type-specific gene deletion and protein expression in order to contextualize subsequent physiologic studies.

In sum, *Cx3cr1-CreBT* mice represent a novel tool that express Cre similarly to *Cx3cr1-CreKI* mice without perturbing the *Cx3cr1* locus. These mice are useful for gene targeting in Ly6C<sup>-</sup> resident monocytes, dendritic cells, tissue macrophages, and microglia.

## **4. Comprehensive flow cytometric analysis of immune cells to identify dendritic cells and novel macrophage populations in the murine brain**

### **4.1 Introduction**

It was once believed that the central nervous system (CNS) is fully “immune privileged” and that the access of immune cells to the brain is severely restricted. It is now known that there are many immune cell types present in the brain that actively regulate local immune responses. We now understand that brain-resident immune cells play a role in the pathogenesis of a variety of neuroinflammatory and neurodegenerative diseases, including multiple sclerosis, cerebrovascular accidents, traumatic brain injury, amyotrophic lateral sclerosis, and Alzheimer’s disease (Ransohoff and Cardona, 2010). Recent studies have also demonstrated that immune cells facilitate brain development, as microglia regulate the numbers of neural precursors (Cunningham et al., 2013), and may even contribute to neuropsychiatric illnesses such as bipolar disorder, schizophrenia, and major depressive disorder (Beumer et al., 2012). Flow cytometry has been employed to understand the cellular players involved in mouse models of these pathologies, but the identities of brain immune cells have been poorly defined. In general, brain immune cells have been largely classified as CD11b<sup>+</sup> CD45<sup>lo</sup> microglia, and CD45<sup>hi</sup> cells, which represent a heterogeneous population of leukocytes (Cardona et al., 2006a)

As microglia are the predominant immune cell of the CNS, the focus in the field has been to identify a molecular signature that is unique to microglia (Hickman et al., 2013). Substantial work has also been done to characterize the lymphocytes of the CNS. This has been aided by the fact that T and B cells exhibit lineage-specific surface markers, and CNS-resident T cells, in particular, have been phenotyped to the level of the individual T cell receptor (Baruch and Schwartz, 2013). However, less work has been done to describe non-microglial myeloid cells of the brain. This is in part because commonly used markers to identify myeloid cells in lymphoid organs lack specificity in non-lymphoid organs. For example, the identification of dendritic cells (DC) by the use of MHC-II and CD11c, which is sufficient in lymphoid organs, also includes macrophage and monocyte populations in non-lymphoid organs (Misharin et al., 2013; Zaynagetdinov et al., 2013). Brain myeloid cells, including monocytes, macrophages, and dendritic cells, are increasingly being recognized as important contributors to brain development, homeostasis, inflammation, and disease pathology, yet there are no tools to specifically distinguish between these cell types.

In this study, we present a detailed strategy based on flow cytometry to identify all brain immune cell types. We highlight a novel method to unambiguously distinguish microglia, monocytes, dendritic cells, and two novel populations of macrophages: F4/80<sup>hi</sup> macrophages and IA/IE<sup>+</sup> macrophages. We demonstrate that expression of the chemokine receptor CX3CR1 is not restricted to microglia, but rather is expressed on all

brain myeloid cells. IA/IE<sup>+</sup> macrophages are demonstrated to survey the blood, whereas F4/80<sup>hi</sup> macrophages appear to be restricted by the blood-brain barrier. Lastly, we find that while brain dendritic cells are a transient population derived from bone-marrow precursors, F4/80<sup>hi</sup> macrophages and IA/IE<sup>+</sup> macrophages are long-lived or self-renewing populations. The detailed identification of these cell subtypes provides a framework for future studies of brain development, homeostasis, and inflammation.

## **4.2 Materials and Methods**

**Mice, PKH26PCL treatment, and bone marrow chimeras.** C57BL/6 mice were purchased from Charles River Laboratories (Wilmington, MA). *Cx3cr1*<sup>GFP/GFP</sup> mice were provided by D. Littman (New York University, New York, NY) or purchased from Jackson Laboratories (Bar Harbor, ME) and crossed with C57BL/6 mice to produce *Cx3cr1*<sup>+GFP</sup> mice. CD45.1 mice were purchased from Jackson Laboratories. PKH26PCL and Diluent B vehicle were prepared as described by manufacturer for *in vivo* labeling (Sigma-Aldrich, St. Louis, MO). C57BL/6 mice were treated retro-orbitally (*r.o.*) with 200  $\mu$ L of either PKH26PCL or Diluent B vehicle. Expression of PKH26PCL was determined by flow cytometry 6 days after administration. For bone marrow chimeras, C57BL/6 mice were treated with 25 mg/kg busulfan in PBS *i.p.* daily for 2 consecutive days. 48 hours after the last busulfan injection, mice were transferred 5x10<sup>6</sup> whole bone marrow cells *r.o.* from CD45.1 congenic donors. Mice were observed and weighed daily to

monitor health. All animal experiments were conducted in accordance with National Institutes of Health guidelines and protocols approved by the Animal Care and Use Committee at Duke University.

**Tissue Processing.** Blood was collected from isoflurane-anesthetized mice with a 27G insulin syringe and immediately resuspended in 5% fetal bovine serum (FBS) with 10 mM HEPES. Mice were intracardially perfused with PBS and brains were then rapidly harvested and stored on ice in PBS. Brains were gently teased apart and digested for 1 hour at 37°C in a 50 mL conical tube with 1.5 mg/mL collagenase A (Roche Applied Science; Penzberg, Germany) and 0.40 mg/mL DNase I (Roche Applied Science) in 5% FBS and 10mM HEPES in HBSS. Every 15 minutes, brain suspensions were passed through increasingly narrow Pasteur pipettes (made manually by glass flaming) and then tubes were vigorously vortexed every 15 minutes. Cells were then washed with PBS, resuspended in 30% Percoll in PBS, and centrifuged for 20 minutes at 600g. Supernatant was discarded and the pellet was washed in PBS. Red blood cells were lysed with ammonium/chloride/potassium (ACK) lysis buffer and then cells were resuspended in 5% FBS and 10mM HEPES in HBSS.

**Flow cytometric analysis.** Cells were counted and  $2 \times 10^6$  cells were stained with LIVE/DEAD Aqua (Invitrogen/Life Technologies, Carlsbad, CA) in PBS. Samples were

blocked in 5% rat serum, 5% mouse serum, 1% Fc Block (eBioscience, San Diego, CA) and stained for 30 minutes at 25°C with the following antibodies: CD11c PE-Cy5.5, F4/80 PE-Cy7, Ly6G AF700, CD11b APC-Cy7, Ly6C V450, CD45 Qdot605, IA-IE Qdot655 (eBioscience, San Diego, CA), CD64 APC, CD206 APC, CD45 BV605, CD24 BV711 (Biolegend, San Diego, CA). Cells were analyzed on a BD™ LSR-II Flow Cytometer (BD Biosciences; Franklin Lakes, NJ) in the Duke Human Vaccine Institute Flow Research Facility and data was analyzed with FlowJo (Treestar; Ashland, OR).

## **4.3 Results**

### **4.3.1 Identification and surface phenotyping of brain immune cells**

In order to develop a way to comprehensively examine immune cells in the mouse central nervous system (CNS), we improved upon existing methods of CNS tissue processing for flow cytometry (Cardona et al., 2006a; Garcia et al., 2014; Nguyen et al., 2011). Mice were first terminally anesthetized and perfused through the left ventricle with PBS to ensure that circulating blood cells had been removed. Brains were removed and rather than direct mechanical digestion, such as the use of mortar and pestle, cell strainers, razors, and frosted glass slides, which we find induce cell death (data not shown), brains were gently teased apart with forceps and then enzymatically digested in collagenase and DNase. Enzymes such as papain and dispase should be avoided as we

have determined that they result in undesired cleavage of cell surface proteins (data not shown). During the enzymatic digestions, the brain pieces were periodically agitated with increasingly stringent Pasteur pipettes, which were manually flamed to produce progressively smaller apertures. After an hour, the resulting solution was washed with PBS. We and others have previously utilized density gradients (commonly layering a 30% over 70% Percoll solution or Optiprep gradients) to isolate immune cells (Cardona et al., 2006a; Nguyen et al., 2011). However, we have found that density gradients decrease cell yield and remove certain immune cell subsets. Instead, we resuspended and centrifugated cells in 30% Percoll, which removes myelin debris and results in a cell pellet, with about a 5-10-fold increase in cell yield over Percoll gradients (data not shown).

We have previously described a method of comprehensively identifying immune cells in non-lymphoid tissues by flow cytometry (Yu et al., in submission). We have applied this general strategy to the CNS, which has unique cell populations, as shown in **Figure 15**. We first gated on singlet events larger than cell debris (FSC-H vs. FSC-A) and then selected for live cells, which are negative for the LIVE/DEAD discriminator. We then gated on CD45<sup>+</sup> cells, which comprise approximately 35% of the cells following our brain digestion protocol. While we have not systematically characterized the CD45<sup>-</sup> cells, of which most are likely neurons, astrocytes, and oligodendrocytes, we have determined that approximately 10% of CD45<sup>-</sup> cells are endothelial cells (data not shown). After

gating on CD45<sup>+</sup> cells, neutrophils can be identified as Ly6G<sup>+</sup> SSC<sup>hi</sup> cells. After gating out neutrophils, the remaining cells can be generally classified as lymphoid (CD11b<sup>-</sup>CD11c<sup>-</sup>) or myeloid (CD11b<sup>+</sup> and/or CD11c<sup>+</sup>). Lymphocytes can be further classified into T cells (IA/IE<sup>-</sup> CD24<sup>+</sup>) or B cells (IA/IE<sup>+</sup> CD24<sup>+</sup>), and we have confirmed the identities of these cell populations by their expression of CD3ε and CD19 (data not shown).

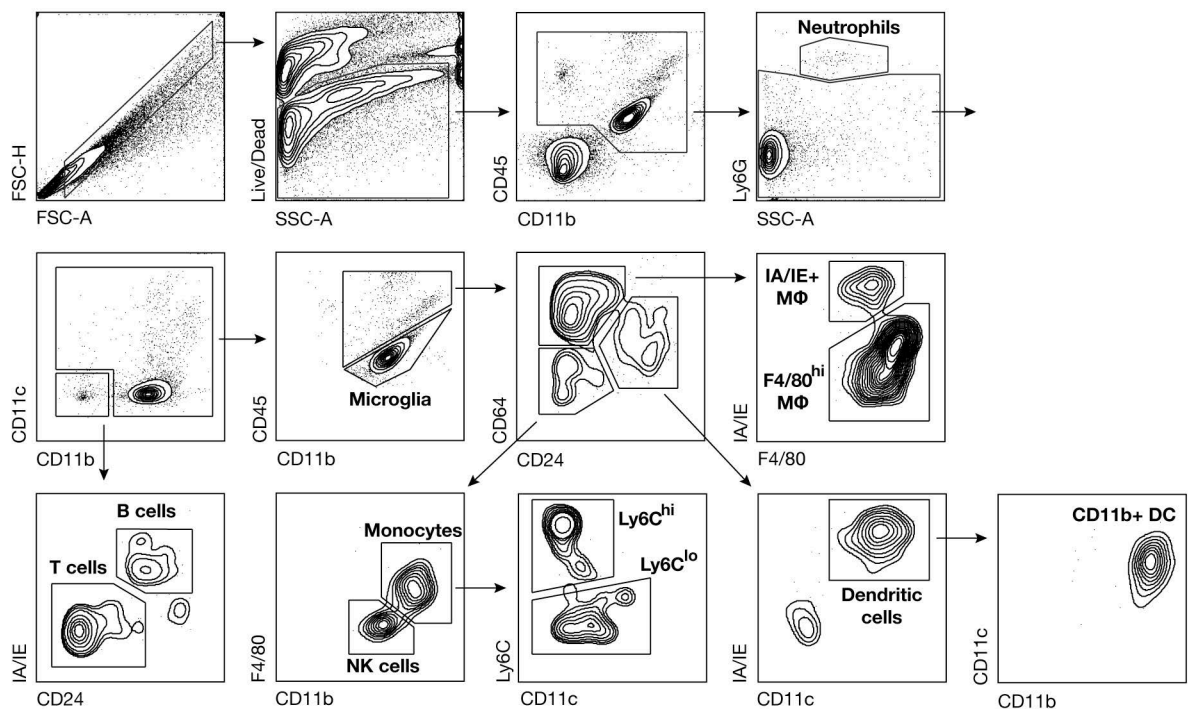


**Figure 15: Flow cytometric analysis of brain immune cells**

Flow cytometric gating strategy for identifying lymphocytes (T and B cells), NK cells, neutrophils, microglia, monocytes (Ly6C<sup>hi</sup> inflammatory and Ly6C<sup>lo</sup> resident), macrophages (IA/IE<sup>+</sup> macrophages and F4/80<sup>hi</sup> macrophages), and dendritic cells.

Representative of 4 experiments with at least 3 mice each.

Among the predominantly myeloid cell populations, we separate microglia, which are CD11b<sup>+</sup> CD45<sup>lo</sup>, from other myeloid subsets, which are CD11b<sup>+</sup> and express higher levels of CD45. CD45<sup>hi</sup> myeloid cells can be separated into 3 major populations based on their expression of CD64 and CD24. CD64<sup>+</sup> CD24<sup>-</sup> cells represent mature macrophage populations, which can be further subdivided into two populations based on their expression of IA/IE and F4/80. We have termed these two populations IA/IE<sup>+</sup> macrophages and F4/80<sup>hi</sup> macrophages. The CD64<sup>-</sup> CD24<sup>-</sup> cells are made up of F4/80<sup>-</sup> CD11b<sup>lo</sup> natural killer (NK) cells and CD11b<sup>+</sup> F4/80<sup>lo</sup> monocytes. Monocytes can be further subdivided into Ly6C<sup>hi</sup> CD11c<sup>-</sup> inflammatory monocytes and Ly6C<sup>lo</sup> CD11c<sup>lo</sup> resident monocytes. The CD64<sup>lo</sup> CD24<sup>+</sup> population is primarily composed of IA/IE<sup>+</sup> CD11c<sup>+</sup> dendritic cells, of which almost all are CD11b<sup>+</sup> (**Figure 15**). Of note, in the brain, dendritic cells cannot be identified solely by MHC-II and CD11c, as the IA/IE<sup>+</sup> macrophage population exhibits heterogeneous expression of CD11c, and thus the two populations cannot be separated by IA/IE and CD11c alone (**Figure 16**).

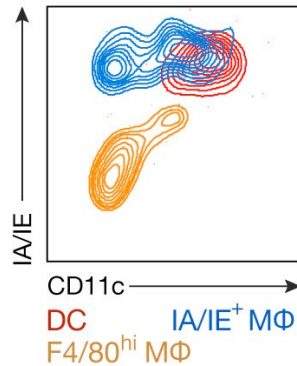


**Figure 16: MHC-II and CD11c expression in brain macrophages and dendritic cells**

Overlay of MHC-II and CD11c expression as determined by flow cytometry in dendritic cells (red), IA/IE<sup>+</sup> macrophages (blue), and F4/80<sup>hi</sup> macrophages (orange). Representative of 5 experiments with at least 3 mice each.

After identifying these cell populations, we sought to quantitate their frequencies relative to all CD45<sup>+</sup> brain immune cells (**Figure 17**). Microglia, which make up ~93% of CD45<sup>+</sup> cells, are the most predominant. The second largest population of cells are F4/80<sup>hi</sup> macrophages, ~2.6%. The remaining cell populations are relatively rare, each making up ~1% or less of total immune cells, and their frequencies are shown in **Figure 17**.

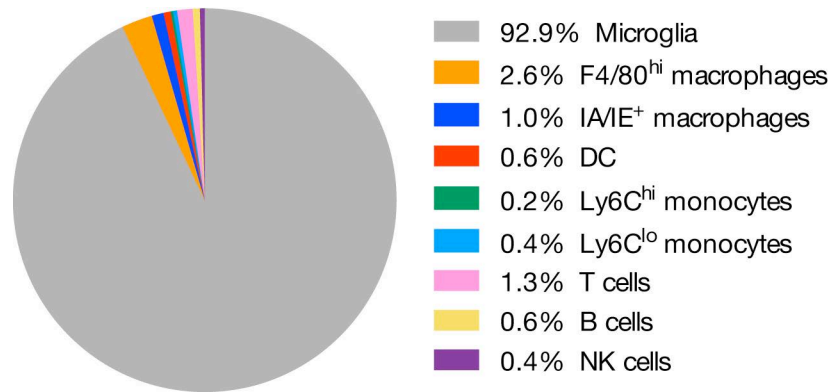


**Figure 17: Figure 17: Quantification of brain immune cell subtypes**

Quantification of immune cell types as a percentage of total CD45<sup>+</sup> brain immune cells as identified in Figure 15. Data represent the mean percentages of 8 mice pooled from 2 experiments.

#### 4.3.2 *Cx3cr1* is expressed on all brain myeloid cells

The chemokine receptor CX3CR1 is important for the regulation of microglial activation (Cardona et al., 2006b) and is commonly used as a marker for microglia within the CNS. It is increasingly described as a molecule that, within the CNS, is expressed exclusively on microglia (Wolf et al., 2013), and mouse strains making use of the *Cx3cr1* promoter and locus have become invaluable tools for tracing and manipulating microglia (Parkhurst et al., 2013; Yona et al., 2013). Previous studies have been unable to study the expression of CX3CR1 on other myeloid cells in the CNS due to an inability to specifically identify non-microglial myeloid cell types. As anti-CX3CR1 antibodies have been found to sometimes bind non-specifically, we assessed CX3CR1 expression on CNS myeloid populations using *Cx3cr1*<sup>GFP/wt</sup> mice (Jung et al., 2000), which

have GFP knocked into the *Cx3cr1* locus. In concordance with previous observations, we found that the vast majority of microglia in *Cx3cr1*<sup>GFP/wt</sup> mice expressed GFP (**Figure 18**). We also found high levels of GFP expression in F4/80<sup>hi</sup> macrophages, IA/IE<sup>+</sup> macrophages, dendritic cells, and Ly6C<sup>lo</sup> monocytes, with slightly lower but still positive GFP expression in Ly6C<sup>hi</sup> monocytes (**Figure 18**). We found minimal expression of GFP in brain T cells, B cells, NK cells, and neutrophils, which is consistent with our findings in peripheral populations (data not shown). These findings demonstrate that *Cx3cr1*, as reported by GFP, is expressed not just in microglia, but in all brain myeloid cells.

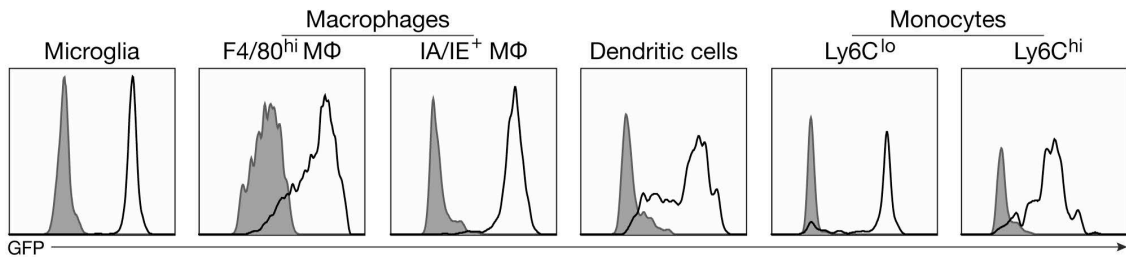


**Figure 18: Brain myeloid cell expression of GFP in *Cx3cr1*<sup>GFP/wt</sup> mice**

Histograms of GFP expression as determined by flow cytometry in microglia, F4/80<sup>hi</sup> and IA/IE<sup>+</sup> macrophages, dendritic cells, and Ly6C<sup>lo</sup> and Ly6C<sup>hi</sup> monocytes from the brains of *Cx3cr1*<sup>GFP/wt</sup> mice. Open black histogram, *Cx3cr1*<sup>GFP/wt</sup> mice; closed grey histogram, *C57BL/6* littermate. Representative of 4 experiments with at least 3 mice each.

In addition to *Cx3cr1*, we assessed other markers commonly used to distinguish myeloid cells, including CD206 (mannose receptor) and SSC-A (granularity). We found that F4/80<sup>hi</sup> macrophages are unique from other brain myeloid cell populations in that

they express higher levels of CD206 and are also more granular (SSC-A<sup>hi</sup>). Brain myeloid cell expression patterns of cell surface molecules are summarized in **Table 2**.

**Table 2: Summary of cell surface marker expression on brain myeloid cells.**

– negative, lo = low positive expression, + positive expression, ++ very high expression

	CD45	CD11b	CD11c	F4/80	CD206	IA/IE	CD64	CD24	Cx3cr1	SSC-A
<b>Microglia</b>	lo	+	lo	+	-	-	+	-	++	lo
<b>F4/80<sup>hi</sup> MΦ</b>	+	+	-	++	++	-	+	-	++	hi
<b>IA/IE<sup>+</sup> MΦ</b>	++	++	lo/+	+	lo	+	+	-	++	lo
<b>DC</b>	++	++	+	lo	-	+	lo	+	++	lo
<b>Ly6C<sup>hi</sup> monocyte</b>	++	++	-	+	-	-/+	lo	-	+	lo
<b>Ly6C<sup>lo</sup> monocyte</b>	++	++	+	+	-	-	lo	-	++	lo

#### **4.3.3 Blood sampling ability and lineage tracing of brain myeloid cells**

In order to better understand the physiologic functions of the dendritic cell and macrophage populations as we have identified them, we sought to determine their relationship to the blood brain barrier through the ability to phagocytose and retain factors from the blood. We treated mice with an intravascular injection of PKH26PCL, a fluorescent dye that is selectively phagocytosed by monocytes, macrophages, and dendritic cells, and can be retained and detected for over 21 days (Maus et al., 2001). 7 days after injection, we sacrificed the mice and assessed the expression of PKH26PCL in brain immune cells by flow cytometry. We found that the majority of DC and IA/IE<sup>+</sup>

macrophages retained PKH26PCL, whereas most microglia and F4/80<sup>hi</sup> macrophages did not (**Figure 19A**). These results suggest that DC and IA/IE<sup>+</sup> macrophages have access to the vasculature, while microglia and F4/80<sup>hi</sup> macrophages are unable to ingest the dye due to the blood brain barrier. To ensure that these results were not affected by differential ability to retain dye, we also performed a similar experiment where brain immune cells were analyzed 24 hours after injection, and we observed very similar results (data not shown). PKH26PCL was retained only in monophagocytes, as we did not observe positive dye staining in T, B, or NK cells (data not shown).

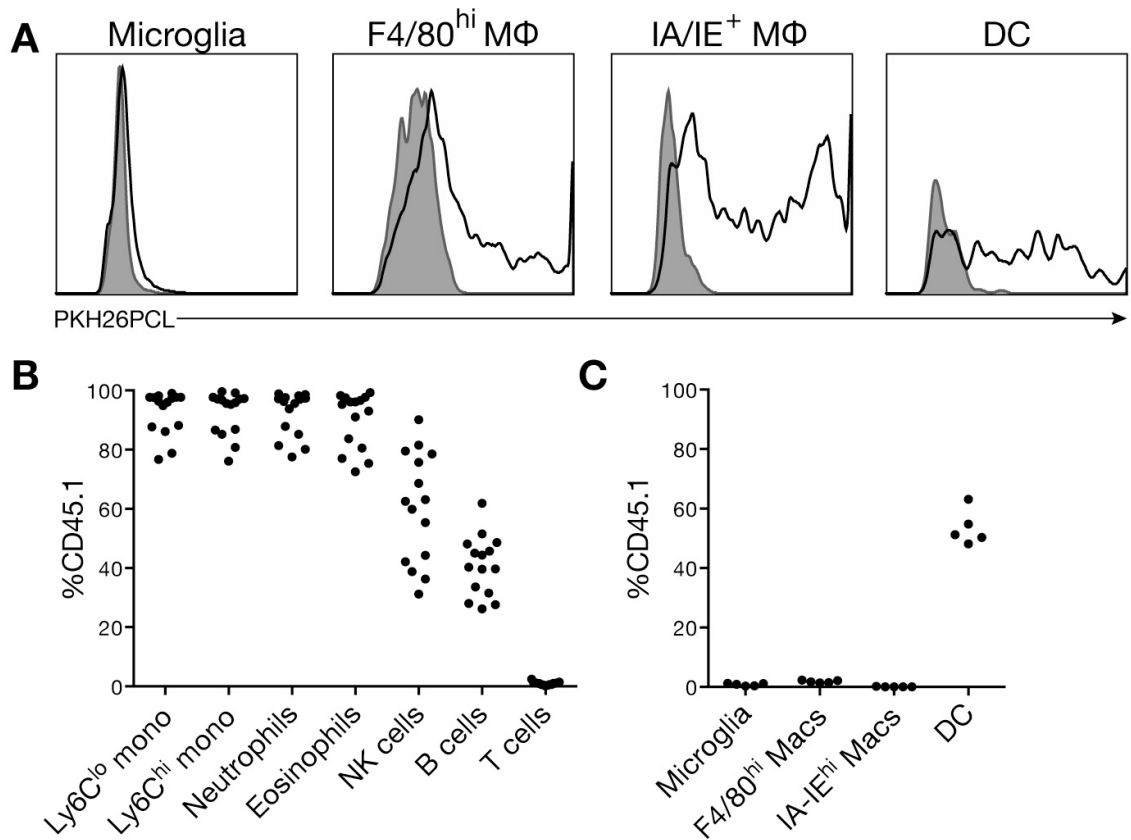


**Figure 19: Figure 19: Blood sampling ability and lineage tracing of brain myeloid cells**

**A)** Histograms of PKH26PCL expression as determined by flow cytometry in brain microglia, F4/80<sup>hi</sup> macrophages, IA/IE<sup>+</sup> macrophages, and dendritic cells 6 days after *i.v.* administration of vehicle control (closed grey histogram) or PKH26PCL (open black histogram). Representative of 2 experiments with 4 mice per treatment.

**B)** Quantification of percentage of donor-derived (CD45.1) cells in peripheral blood 3 weeks after adoptive bone marrow transfer. Representative of 4 experiments with 15 mice per group.

**C)** Quantification of percentage of donor-derived (CD45.1) cells in brain microglia, F4/80<sup>hi</sup> macrophages, IA/IE<sup>+</sup> macrophages, and dendritic cells 6 weeks after adoptive bone marrow transfer. Representative of 3 experiments with 5 mice each.

These findings suggested that that DC and IA/IE<sup>+</sup> macrophages might be situated outside of the brain parenchyma and the blood brain barrier, or that they might be derived from a blood-borne precursor that had already phagocytosed PKH26PCL. In order to assess the longevity and cellular origin of brain macrophages and DC, we transferred congenic CD45.1 bone marrow into C57BL/6 mice after busulfan conditioning. Busulfan, a myeloablative DNA chelating agent, has been previously used to generate highly efficient bone marrow chimeras with high survival and minimal perturbation of the blood brain barrier compared to irradiation (Kierdorf et al., 2013). We treated 4 week-old C57BL/6 mice daily for 2 days with 25 mg/kg busulfan *i.p.* before transferring 5x10<sup>6</sup> CD45.1 bone marrow 48 hours after the last injection. All mice survived the procedure with <5% acute decrease in body weight (data not shown).

3 weeks after bone marrow transfer, we assessed the mice for peripheral blood cell chimerism (see **Figure 8** for gating strategy) and found that 80-100% of all monocytes, neutrophils, and eosinophils were donor-derived (CD45.1) (**Figure 19B**). 6 weeks after bone marrow transfer, we sacrificed the mice and assessed chimerism in brain macrophages and DC. The vast majority of microglia, F4/80<sup>hi</sup> macrophages, and IA/IE<sup>+</sup> macrophages did not express CD45.1, meaning that they were not bone-marrow derived and instead derive from local self-renewing populations (**Figure 19C**). ~60% of DC were CD45.1, suggesting that brain DC are replenished by circulating precursors

(Figure 19C). The observations that IA/IE<sup>+</sup> macrophages are able to uptake PKH26PCL but are not derived from bone marrow precursors suggests that these cells have greater access to the vasculature than F4/80<sup>hi</sup> macrophages. These findings also support our differential identification of IA/IE<sup>+</sup> macrophages from DC by flow cytometry, as these two cell types clearly derive from different precursors.

#### **4.4 Discussion**

Here, we have presented the development of a novel brain homogenization technique and flow cytometry staining strategy that allows for the identification of all major cell types in the murine brain. This strategy allows, for the first time, the unambiguous identification of brain resident dendritic cells and macrophages and the characterization of two novel macrophage subsets, the F4/80<sup>hi</sup> macrophages and IA/IE<sup>+</sup> macrophages. Additionally, we are able to distinguish both resident and inflammatory monocytes from macrophage populations. The ability to properly identify these cell populations allows us to quantify their relative frequencies, to examine cell surface expression of commonly used myeloid markers, and to begin to assess the functional properties of these cell types.

The identification of these different cell types is critical for studying immunity in the CNS and greatly extends our knowledge beyond the typical classification of brain myeloid cells as CD45<sup>hi</sup> and CD45<sup>lo</sup>. While our findings have yet to be conducted under

mouse models of CNS inflammation, such as traumatic brain injury, experimental autoimmune encephalitis, and Alzheimer's disease, our identification of these cell types at the steady state provides a foundation for identifying the cell types that may be important in the context of disease. Our studies with bone marrow chimeras also provide insight into the cellular origin of the cell types that we have identified. In concordance with previous studies, we find that microglia are not derived from bone marrow precursors (Ajami et al., 2011; Ajami et al., 2007; Ginhoux et al., 2010; Schulz et al., 2012), and we also observe that F4/80<sup>hi</sup> macrophages and IA/IE<sup>+</sup> macrophages are not derived from bone marrow precursors in the adult animal and may locally renew. Further studies will be needed to address whether these two macrophages populations are also derived from yolk-sac macrophages or *Myb*-dependent hematopoietic precursors and determine when they take up residence in the brain during development.

While we have yet to identify the anatomical locations of brain F4/80<sup>hi</sup> macrophages and IA/IE<sup>+</sup> macrophages, which will require the examination of multiple markers as we have described by fluorescent imaging, these cell populations have similarities to previously described cell types by histology. The differential ability of F4/80<sup>hi</sup> macrophages and IA/IE<sup>+</sup> macrophages to uptake a dye from the vasculature implies that these two cell types are situated on opposite sides of the blood brain barrier. There has been a long-standing observation that there are MHC-II<sup>+</sup> cells with the

morphology of macrophages in the perivascular spaces of the brain (Hickey and Kimura, 1988; Perry, 1998; Sasaki et al., 1996) as well as and within the choroid plexus of the lateral ventricles (Prodinger et al., 2011), which are the interface between the blood and the CSF fluid. Perivascular macrophages have also been described to be long-lived (Bechmann et al., 2001) and extend processes through the endothelium to sample blood antigens (Prodinger et al., 2011). Based on our findings that IA/IE<sup>+</sup> macrophages are able to phagocytose PKH26PCL from the vasculature, we believe that IA/IE<sup>+</sup> macrophages are similar to perivascular and choroid plexus macrophages. CD206<sup>+</sup> macrophages have been described in the meninges and perivascular spaces of the brain (Galea et al., 2005). We find that F4/80<sup>hi</sup> macrophages, which are also CD206<sup>hi</sup>, have minimal ability to phagocytose PKH26PCL, which would be consistent with localization to the meninges, where they would have less access to the vasculature and instead be associated with cerebral spinal fluid (CSF). IA/IE<sup>+</sup> macrophages are CD206<sup>lo</sup>, but not CD206<sup>-</sup> like microglia, which may explain why histologically some have described perivascular macrophages to express CD206. Further studies will be required to support these associations.

The ability to identify dendritic cells by flow cytometry improves upon previous methods, which included the treatment of mice with exogenous Flt3L and the use of CD11c-EYFP reporter mice, which are not always compatible with *in vivo* experiments (Anandasabapathy et al., 2011) Previous attempts to identify brain DC by flow

cytometry have utilized their high expression of MHC-II and CD11c (Anandasabapathy et al., 2011), although we now know that the use of these two markers are insufficient identifiers as IA/IE<sup>+</sup> macrophages can exhibit a similar phenotype. As we describe here, the usage of CD64 and CD24 allows for the unambiguous identification of IA/IE<sup>+</sup> macrophages from DC. This is a strategy that has been previously utilized to distinguish macrophages from dendritic cells in other peripheral tissues, including the lung, peritoneum, and intestines (Langlet et al., 2012; Tamoutounour et al., 2012). Of note, it is important to first gate out B cells and neutrophils, which also express high levels of CD24 (data not shown). The majority of brain DC as we have described are all CD11b<sup>+</sup>. Furthermore, in line with previous observations that brain DC are a mobile population that have a brain half-life of 5-7 days (Anandasabapathy et al., 2011), our studies with PKH26PCL and bone marrow chimeras suggest that brain DC have a higher rate of turnover than microglia and other brain macrophages. Previously, it has been suggested that brain DC reside in the meninges and choroid plexus, although these were based on the use of a CD11c-EYFP reporter (Anandasabapathy et al., 2011). Further studies will be required to determine the anatomical niches of brain DC and to trace their migration after egress from the brain.

Some of the cell types that we were able to identify, such as neutrophils, monocytes, T cells, B cells, and NK cells, likely are present due to incomplete perfusion, as the brain is highly vascularized, or perhaps are adherent to the brain endothelium.

The vast majority of these cells are donor-derived during bone marrow chimera studies and are present in higher percentages when the mice are not perfused (data not shown). We did not assess subsets of lymphocytes, such as T cells, which have been previously described in detail, where choroid plexus-resident T cells are mostly effector memory CD4<sup>+</sup> with specificity for brain antigens presented on MHC (Baruch et al., 2013).

Although the relative frequencies of the non-microglial immune cell types described here are low, they may be vital to brain homeostasis and inflammation. For example, T cells have been demonstrated to play an important role in CNS development, as T cell-deficient mice have impaired neurogenesis, which is corrected with adoptive transfer of T cells (Kipnis et al., 2012; Ziv et al., 2006). It is still unclear whether the activity of T cells on brain development occur directly within the CNS or are secondary to effects peripheral to the brain, but our findings suggest that there are two populations of cells in the brain, IA/IE<sup>+</sup> macrophages and dendritic cells, that may mediate antigen presentation and modulate CD4<sup>+</sup> T cell activity within the CNS.

In the CNS, the chemokine receptor CX3CR1 has been described to be exclusively expressed on microglia, while its ligand CX3CL1 is expressed both on the cell surface and as a secreted protein by neurons (Mizutani et al., 2012; Wolf et al., 2013). We find that, in addition to microglia, *Cx3cr1* is also expressed on resident monocytes, inflammatory monocytes, F4/80<sup>hi</sup> macrophages, IA/IE<sup>+</sup> macrophages, and dendritic cells by the *Cx3cr1*<sup>GFP/wt</sup> reporter. These findings suggest that CX3CR1 is an important

chemokine for all CNS myeloid cells and the functional ramifications of CX3CR1 expression on microglia may also extend to other cell populations. Furthermore, these findings demonstrate that while microglia are the predominant cell type expressing CX3CR1, the use of this chemokine receptor to specifically identify microglia is insufficient. Studies identifying microglia by CX3CR1 should be evaluated carefully, and studies utilizing *Cx3cr1* promoter-driven constructs, such as fluorescent reporters or Cre recombinase, may also affect other brain macrophages and dendritic cells.

In conclusion, this study provides a foundation for the comprehensive identification of immune cells in the brain. These findings allow for the study of previously unidentifiable cell populations in the brain, particularly monocytes, macrophage subpopulations, and dendritic cells. We hope the detailed descriptions of these cell types will provide insight into the complex cellular milieu in mouse models of brain inflammation and be useful for finding correlates in the human brain.

## 5. Discussion

In this dissertation, I present a novel mechanism for neuronal death in the CVN-AD mouse model of Alzheimer's disease, where neuronal death is preceded by the presence of CD11c<sup>+</sup> microglia and extracellular arginase-1, resulting in decreased brain arginine bioavailability. Blockade of arginase-1 with the partial arginase antagonist DFMO was able to reverse AD-like pathology and memory loss. I describe a novel strain of *Cx3cr1-CreBT* mice, which express Cre recombinase under the control of the *Cx3cr1* promoter without disturbing the *Cx3cr1* locus. These mice allow for genetic manipulation of resident monocytes, microglia, and tissue macrophages without the defects in development and inflammation that are seen with *Cx3cr1* knock-in Cre mice. Lastly, I presented a comprehensive protocol for the flow cytometric analysis of immune cell types in the brain, which allows the identification of several cell types that have not been previously identified by flow cytometry. These cell types include brain dendritic cells, F4/80<sup>hi</sup> macrophages, which may represent meningeal macrophages, and MHC-II<sup>+</sup> macrophages, which may be perivascular macrophages, by flow cytometry. Together, this work encompasses both a novel potential theory for the pathogenesis of Alzheimer's disease and the tools that are likely to be needed to extend upon this theory.

## **5.1 Arginase in Alzheimer's Disease**

A major concern for any observations made in a mouse models of AD is that the findings may not have relevance in human AD. Because the mouse model that we use has been demonstrated to have multiple similarities to human AD, including the age dependent development of amyloid plaques, spontaneously hyper-phosphorylated tau, memory deficits, and neuronal death (Colton et al., 2008; Colton et al., 2014; Wilcock et al., 2008), we believe that it accurately models events that occur in human disease. Additional support for the conclusion that our findings have are relevant to human disease is provided by the finding that changes in both arginase and arginine levels are observed in human AD brain autopsy tissue. Specifically, we and others have previously demonstrated that both *ARG1* or *ARG2* mRNA levels are increased in AD frontal cortex (Colton et al., 2006; Hansmannel et al., 2010). Arginase protein levels and activity are increased in human AD compared to age-matched controls (Liu et al., 2014). A study of amino acids and metabolites in AD brain revealed decreased arginine and increased urea, a product of arginase activity, leading the authors to speculate that arginase activity might be increased in human AD (Gueli and Taibi, 2013). Additionally, increased polyamines, the downstream products of the arginase pathway, are upregulated in AD brain (Inoue et al., 2013). In addition, the rs742869 allele of arginase-2 has been associated with an increased risk for AD in men and an earlier onset of symptoms in men and women (Hansmannel et al., 2010). In contrast to reports in other

mouse models of AD, we and others have found that *NOS2* mRNA is unchanged in AD, and that *NOS2* protein and activity are unchanged or even decreased in AD (Colton et al., 2006; Liu et al., 2014). Lastly, there is evidence that the integrated stress response pathway, which responds under amino acid deprivation, is activated in human AD through phosphorylation of GCN2 kinase and eIF2 $\alpha$  (Ma et al., 2013b). Taken together, these findings provide substantial evidence that arginine metabolism is altered in human AD and suggest that the pathologic mechanism of immune-mediated arginine deprivation that we describe in CVN-AD mice is relevant to human AD. These findings also suggest that, as a model, CVN-AD mice accurately recapitulate events that occur in humans and therefore represent an improvement over other mouse models of amyloid overexpression.

The depletion of arginine or other amino acids by immune cells is not unique to Alzheimer's disease and is an ancient strategy used by the immune system. This phenomenon was first demonstrated almost 40 years ago, when arginase produced by peritoneal macrophages was demonstrated to suppress lymphocyte activity *in vitro* (Kung et al., 1977), leading to the prediction that arginase serves the dual functions of suppressing lymphocyte activity as well as inhibiting the growth of tumors, parasites, bacteria, and viruses (Schneider and Dy, 1985). Indeed, neonatal erythroid cells in mice and humans produce arginase-2 to inhibit intestinal lymphocytes from reacting against colonizing gut microbiota (Elahi et al., 2013). Arginase is utilized by macrophages to

protect against nematode parasites (Anthony et al., 2006), shistosomiasis (Hesse et al., 2001), and trypanosomiasis (Gobert et al., 2000). This process has been also coopted by cancer cells to inhibit the activity of tumor infiltrating effector T cells within tumors (Serafini et al., 2006).

It remains to be determined which isoform of arginase predominates in human AD, as mRNA of both isoforms of this enzyme are increased in human AD brain tissues (Colton et al., 2006; Hansmannel et al., 2010). Arginase-1 and arginase-2 share ~60% sequence homology and have the same capacity to perform the same catalytic reaction. In both humans and mice, arginase-1 is expressed predominantly in the liver, where it participates as the first enzyme in the urea cycle (Jenkinson et al., 1996). In humans, arginase-2 is expressed primarily in the prostate, kidney, and brain (Vockley et al., 1996). In mice, arginase-1 is the isoform that is increased in activated macrophages and dendritic cells (Munder et al., 1999). In rodents, arginase-1 is generally localized to the mitochondria and cytosol, whereas arginase-2 is associated with mitochondria (Jenkinson et al., 1996). However, in humans, this subcellular localization may not be as distinct, and both isoforms appear to be used interchangeably. Indeed, there is precedence for the extracellular release of arginase in human disease. Arginase-1 is released into the blood by human hepatocytes in endotoxemia (Miki et al., 2009) and in malaria, arginase is released by erythrocytes, resulting in hypoargininemia, which is correlated with poor outcome (Weinberg et al., 2008; Yeo et al., 2008a; Yeo et al., 2008b).

Increased arginase is present in the serum of patients with glioblastoma (Raychaudhuri et al., 2011), and arginase-2 is released into the blood by blast cells in acute myeloid leukemia, resulting in pancytopenia and T cell suppression (Mussai et al., 2013).

Another issue that should be addressed in a potential explanation for the pathogenesis of AD involves the characteristic spatial and temporal aspects of the disease. Patients with late onset AD typically do not exhibit symptoms until the seventh or eighth decade of life. The disease also generally manifests first in the hippocampus before spreading slowly into other areas of the cortex. There is some evidence in mice that aging is associated with a natural increase in arginase in the choroid plexus (Baruch et al., 2013). The choroid plexuses are particularly developed in the lateral ventricles and, in humans, they line the hippocampus and entorhinal cortex. Additionally, the effects of extracellular arginase are limited to their local microenvironment. If certain subpopulations of microglia do in fact produce arginase, then the localization of these microglia to the hippocampus and cortex may explain why these regions are differentially affected. Furthermore, arginine is actively transported into the brain across the blood brain barrier, and specific brain regions differ in their arginine concentrations (Dawson et al., 2004). It has been previously observed that the concentration of arginine in the hippocampus is far lower than that of the cortex (Dawson et al., 2004). While it is unknown whether this is due to limited ability to deliver arginine or increased requirement for arginine in the hippocampus, this suggests that the hippocampus would

be more sensitive to arginine deprivation than other brain regions. Additionally, there is evidence that low arginine levels may also have a deleterious effect on non-neuronal populations, such as endothelial cells, that may contribute to AD pathogenesis (Yi et al., 2009).

Explanations for AD should also address the heterogeneity of amyloid plaques, as some individuals develop AD with few plaques, and others may develop plaques, but never exhibit symptoms of AD. In the CVN-AD mouse model, the presence of mutated hAPP is required for the induction of arginase-1, as *Nos2*-KO mice do not exhibit increased arginase-1. However, APP is not mutated in the vast majority of late-onset AD, and the relationship between A $\beta$  and arginase remains to be determined in human disease. Interestingly, arginine is important for protein solubility and folding, and it prevents the aggregation of hydrophobic proteins (Arakawa et al., 2011; Kudou et al., 2011). While the mechanism by which this occurs is unclear, this property of arginine has been exploited for drug delivery, as in cases where poly-arginine moieties are appended to proteins to allow passage across the cell membrane (Macewan and Chilkoti, 2012). Thus, levels of brain arginine may result in decreased protein solubility and increased precipitation of hydrophobic peptides, such as A $\beta$ .

The immune system also makes use of and is affected by the manipulation of other amino acids, such as tryptophan (MacIver et al., 2013). We have found that in CVN-AD mice, indoleamine 2,3-dioxygenase (IDO), which catabolizes tryptophan, is

upregulated by astrocytes (unpublished data), suggesting that other amino acids may be similarly manipulated in AD. In collaboration with the Duke Proteomics and Metabolomics Shared Resource Facility, future studies will utilize LC-MS/MS of whole brain lysate from CVN-AD mice to generate a metabolic profile of arginine, arginine metabolites, and other essential amino acids. The evolutionary manipulation of amino acids suggests that our findings may have relevance in other neurodegenerative diseases, such as Huntington's disease and Parkinson's disease. They may have particular application to Down's syndrome, as the extra copy of chromosome 21 results in triplication of the *APP* locus, and patients with Down's syndrome sometimes experience an early form of dementia similar to AD (Zigman et al., 2008).

## **5.2 Arginase in CVN-AD Mice**

Although the presence of extracellular arginase-1 and the appearance of CD11c<sup>+</sup> microglia in CVN-AD mice are spatially and temporally associated, we have not yet demonstrated that CD11c<sup>+</sup> microglia are the cellular source of arginase-1. Because, as visualized by confocal microscopy, arginase-1 appears predominately in the extracellular space, its cellular origin cannot be determined (data not shown). To address this issue, we are currently performing fluorescent *in situ* hybridization studies to identify cells that express *Arg1* mRNA.

We have demonstrated that pre-treatment of CVN-AD mice with DFMO prevents the development of several AD-like pathologies, including A $\beta$  deposition, accumulation of CD11c<sup>+</sup> cells, and memory loss. Despite this, we believe that additional studies will be required to definitively prove our hypothesis that AD pathologies are caused by arginine depletion. For example, although we have demonstrated that DFMO treatment prevents the upregulation of *Ssat* (spermine synthase s-acetyltransferase), which is downstream of and therefore an indicator of arginase and polyamine activity, we have not directly demonstrated that DFMO treatment reverses arginine deprivation. Further studies will be required to demonstrate that DFMO directly increases arginine bioavailability. Additional studies will also be required to determine if the administration of DFMO as a therapy after the development of memory and neuronal loss is efficacious, and identify DFMO analogs that may have better CNS penetration and fewer off-target effects. In addition, although our use of DFMO provided an excellent proof of concept, this treatment results in a general blockade of ornithine decarboxylase (ODC), arginase-1 and arginase-2 in CVN-AD mice and is therefore not entirely specific. Proof that *Arg1* production by microglia is the primary mechanism of neuronal death will likely require the generation of CVN-AD mice in which *Arg1* is specifically deleted in microglia, as we discuss below.

It should be noted that the therapeutic blockade of arginase is not without potential side effects and risks. While there have been no described mutations in human

arginases that cause increased function in arginase, rare autosomal recessive mutations in *ARG1* exist in humans that cause arginase-1 deficiency, resulting in hyperargininemia and hyperammonia. Humans with arginase deficiency exhibit developmental defects, seizures, muscle spasms, mental retardation, early dementia, and eventually, death (Iyer et al., 1998). These observations suggest that the use of arginase inhibitors may have potentially devastating consequences and must be considered in design of future study.

Importantly, the AD-like pathology in CVN-AD mice is not an artifact of *Nos2* deletion. We have also produced a version of the CVN-AD mouse that carries a transgene for human *NOS2*. *hNOS2*<sup>tg+/+</sup> CVN-AD mice demonstrate very similar AD-like pathology to CVN-AD mice, in that they develop amyloid plaques, hyperphosphorylated tau, memory deficits, and hippocampal neuronal death, demonstrating the relevance of species difference in NOS regulation (Colton et al., 2014). Future studies will explore the role of immunity in *hNOS2*<sup>tg+/+</sup> CVN-AD mice and *mNos2*<sup>-/-</sup> *hNOS2*<sup>tg+/+</sup> mice, which do not harbor alleles associated with early onset AD, crossed onto other backgrounds.

### **5.3 Immune Suppression in Other Models of Alzheimer's Disease**

The potential involvement of arginase in AD pathophysiology has been previously demonstrated in other models of AD. A single *i.c.v.* injection of A $\beta$ <sub>25-35</sub> in rats resulted in decreased NOS expression and increased arginase-2 protein expression and

arginase activity in the CA2 and CA3 regions of the hippocampus (Liu et al., 2011), suggesting that A $\beta$  may induce the production of arginase. In a study of the brain vasculature in aged wildtype and *ApoE*<sup>-/-</sup> mice, it was observed that aged *ApoE*<sup>-/-</sup> mice have increased lipid deposition in the cortical blood vessels and increased permeability of the blood brain barrier. Aged *ApoE*<sup>-/-</sup> mice also exhibited astrogliosis and increased brain tissue arginase levels, particularly in blood vessels (Badaut et al., 2012). These findings suggest a functional link between ApoE and arginase, and may shed light on the contribution of ApoE genotype to the development of AD. It has also been demonstrated in mice that administration of A $\beta$  *i.p.* is able to prevent and reverse paralysis in experimental autoimmune encephalitis. In this system, A $\beta$  peptides and other amyloidogenic molecules can directly inhibit lymphocyte activation and cell proliferation (Grant et al., 2012; Kurnellas et al., 2013). Further work will be required to demonstrate if this has relevance for brain-resident immune cells.

Recently, there has been renewed interest in the role of other immunosuppressive mediators in AD. CX3CR1 is thought to inhibit the activity of microglia, and deletion of *Cx3cr1* in APP/PS1 mice results in decreased A $\beta$  (Fuhrmann et al., 2010). Polymorphisms in the anti-inflammatory cytokine IL-10 have previously been demonstrated to increase the risk of AD in certain populations (Lio et al., 2003). Recently, two groups tested the role of IL-10 in mouse models of AD. One group overexpressed IL-10 with an adeno-associated virus (AAV) vector in the TgCRND8 and

Tg2576 transgenic amyloid models, finding that increased IL-10 production increased A $\beta$  concentration and the number and size of plaques (Chakrabarty et al., 2015). The other study generated APP/PS1 mice on an *Il10*<sup>-/-</sup> background, finding that IL-10 deficiency partially improved cognitive function and resulted in increased phagocytosis of A $\beta$ . This group also found increased IL-10R $\alpha$  levels in the hippocampi of AD patients, suggesting that IL-10 signaling is increased in AD (Guillot-Sestier et al., 2015). There has also been interest in TREM2, a DAP12 inhibitory signaling molecule present on the surface of microglia, as TREM2 variants have been demonstrated to confer risk for Alzheimer's disease (Guerreiro et al., 2013; Jonsson et al., 2013b). While the biological effects of these variants in human alleles have yet to be described, APP/PS1 *Trem2*<sup>-/-</sup> mice were found to have fewer plaques than APP/PS1 mice (Jay et al., 2015), suggesting a contributory role for this immunosuppressive signaling molecule. While these mouse models do not address the species differences in iNOS, they do suggest that multiple mediators of immune suppression may play a role in AD pathogenesis.

#### **5.4 Origin and Functions of CD11c<sup>+</sup> Microglia in CVN-AD mice**

One of the major outstanding questions in AD is whether reactive myeloid cells in the brain are derived from infiltrating blood-derived myeloid cells or brain-resident microglia, as this would greatly impact therapeutic strategies. In histopathologic studies of human AD, there has been very little evidence to suggest that circulating cells drive

pathology. However, technological barriers and the inability to predict the development of AD in people have limited our ability to conduct robust studies in human patients. The CD11c<sup>+</sup> cells in the hippocampus of CVN-AD mice are similar to previously described CD11c<sup>+</sup> cells in human AD, and we believe the CVN-AD mouse is a good model system to investigate origin of the primary immunopathologic cells in AD. CVN CD11c<sup>+</sup> cells have a CD45<sup>low</sup> phenotype (consistent with microglia) with little expression of Ly6C or Ly6G (the canonical markers for inflammatory monocytes and neutrophils). Additionally, we saw no lifelong changes in total brain mRNA expression of *Ccr2* and *Ccl2*, the major chemokine responsible for the recruitment of inflammatory monocytes. These observations lead us to believe that CVN CD11c<sup>+</sup> cells are of microglial origin.

We have begun to address this question in two ways. The first is to develop bone marrow chimeras, where CVN-AD and *Nos2*<sup>-/-</sup> control mice receive *Nos2*<sup>-/-</sup> tdTomato<sup>+</sup> bone marrow after busulfan conditioning. The mice are allowed to age and then assessed for chimerism in the brain after the expected development of AD-like pathology and CD11c<sup>+</sup> microglia. Unfortunately, while *Nos2*<sup>-/-</sup> mice are able to accept the donor bone marrow, CVN-AD mice are unable to accept the graft despite multiple attempts using recipients of various ages. Although both recipient mouse strains are on the same genetic background, we have conducted mixed lymphocyte reactions to rule out MHC mismatch and found no evidence of such responses. These findings imply that the expression of mutated *hAPP* under the *Thy1* promoter in CVN-AD recipient mice

prevents donor bone marrow engraftment. *Thy1* is expressed on many peripheral cells, including lymphocytes. While the effects of APP and A $\beta$  have not been well characterized outside of the CNS, others have demonstrated that A $\beta$  *i.p.* may suppress the activation and proliferation of T cells. A $\beta$  treatment also can prevent and reverse paralysis in experimental autoimmune encephalitis, and may have a therapeutic benefit in multiple sclerosis (Grant et al., 2012; Kurnellas et al., 2013). Our results suggest that transferred bone marrow cells in CVN-AD mice may be unable to proliferate due to the presence of peripherally expressed APP. Further attempts to generate these bone marrow chimeras will explore the use of irradiation with head shielding to prevent breakdown of the blood brain barrier, and parabiosis (Ajami et al., 2011; Ajami et al., 2007).

A parallel strategy that we have pursued to answer this question is the use of the microarray data that were generated from sorted myeloid populations in Chapter 2. In that study, we isolated CD11c<sup>+</sup> microglia from 48-week old CVN-AD mice and compared them to that of CD11c<sup>-</sup> microglia from the same CVN-AD mice, as well as microglia from age-matched *C57BL/6* and *Nos2<sup>-/-</sup>* control mice. We also isolated Ly6C<sup>+</sup> and Ly6C<sup>-</sup> monocytes from *C57BL/6* lung and yolk sac macrophages from E12.5 *C57BL/6* embryos. The direct comparison of gene expression between these cell populations would help us determine if CD11c<sup>+</sup> microglia from CVN-AD mice were similar to control microglia, monocytes, or embryonic yolk sac macrophages.

An analysis by hierarchical clustering reveals that CD11c<sup>+</sup> microglia from CVN-AD mice have a unique gene expression signature (**Figure 20**) that is distinct from control microglia, which are indistinguishable by genotype (detailed tree not shown). CD11c<sup>+</sup> microglia cluster most closely with yolk sac macrophages, followed by control microglia, and are most distinct from both types of monocytes. While these results cannot directly prove the progenitors of CD11c<sup>+</sup> microglia are brain-resident microglia, the gene expression patterns suggest that they are much more related to endogenous microglia and their yolk sac precursors than infiltrating monocytes.

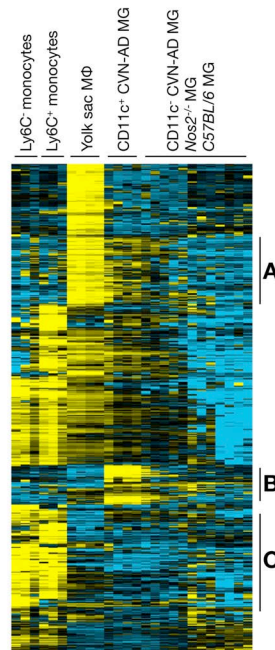


**Figure 20: Fig. 20 Heat map from Agilent microarray analysis of gene expression in monocytes, yolk sac MΦ, and microglia (MG).**

Genes that are upregulated are depicted in yellow by intensity, whereas genes that are downregulated are depicted in blue by intensity. Black = 0 or no change.

**A)** Genes upregulated only in yolk sac MΦ and CD11c<sup>+</sup> CVN-AD MG.

**B) Genes upregulated only in CD11c<sup>+</sup> CVN-AD MG.**

**C) Genes upregulated only in monocytes**

In these studies, we identified several gene clusters of interest. In group A (**Figure 20A**), we found genes that were significantly upregulated only in yolk sac macrophages and CD11c<sup>+</sup> CVN-AD microglia. Using GATHER (Chang and Nevins, 2006), a gene expression analysis annotation tool, we found that the majority of genes in group A are related to cell proliferation, such as DNA and nucleotide synthesis, and cell metabolism. Yolk sac macrophages have high proliferative potential, as they seed the embryo with tissue resident macrophages, and these results suggest that CD11c<sup>+</sup> CVN-AD microglia undergo cell division. Indeed, Ki-67 staining, which stains nuclei in S-phase, in histologic brain sections from CVN-AD mice is predominately seen in the brain regions in which CD11c<sup>+</sup> microglia are found (data not shown). Further co-staining will be required to demonstrate that Ki-67 is co-expressed with CD11c. These data are significant because they suggest that CD11c<sup>+</sup> microglia are proliferating in the late stages of pathology, meaning that therapeutic strategies aiming to block cell recruitment may not be fruitful. They are also significant because there is controversy regarding whether microglia proliferate in human AD (Marlatt et al., 2014). We have obtained human hippocampal samples to pursue this question.

Group B genes (**Figure 20B**) are of the most interest to us, because these ~160 genes are significantly upregulated only in CD11c<sup>+</sup> CVN-AD microglia. GATHER

analysis reveals that many of these genes are related to cell proliferation and increased metabolic demand, including some genes related to amino acid regulation. However, most surprising is that many of these genes are related to immune suppression. We are now using this list of gene targets to verify expression in CVN-AD mice, and more importantly, in human AD. This gene group includes *Itgax* (CD11c), which was one of the selection criteria for these cells, *Spp1*, *ApoE* (allelic differences confer highest single known risk factor in LOAD), and *Pdcd1*.

*Pdcd1* encodes programmed death ligand-1 (PD-L1), a marker of chronic inflammation and inducer of effector T cell death (Butte et al., 2008) and is upregulated ~50-fold in CD11c<sup>+</sup> CVN-AD microglia. We are in the process of verifying the levels and staining pattern of PD-L1 protein expression in CVN-AD mouse. The expression of PD-L1 in Alzheimer's disease has only been studied in the peripheral blood of human patients (Saresella et al., 2012), but protein expression in AD brain is unexplored. We are actively seeking to determine if PD-L1 is expressed in human hippocampal sections from AD patients. This finding would have important relevance to our previous findings that microglia in AD may have an immunosuppressive phenotype and also open future directions for investigating myeloid biology in AD. The expression of PD-L1, which is the ligand for PD-1 on T cells, suggests that T cells may participate in AD pathogenesis, and suggest that anti-PD-1 or anti-PD-L1 inhibitors, which have been used to reverse T cell checkpoint blockade in the treatment of cancer, might have a role in AD

therapy. Others have previously suggested that the co-stimulatory molecule CD40 and its ligand CD40L may play a role in AD (Tan et al., 2002a; Tan et al., 2002b). There are reports suggesting that, in some patients, there may be increased T cells in AD brain, as assessed by histologic staining (Togo et al., 2002). Although more rigorous quantitative studies will be required to determine if this is meaningful or an epiphenomenon, we have also seen that there is a heterogeneous increase in T cell number in the brains of CVN-AD mice (Chapter 2) (Kan et al., 2015).

We have previously examined the whole brain protein expression in CVN-AD mice at various ages using mass spectrometry-based proteomics (Hoos et al., 2013). In examining whole brain proteomics and phospho-proteomics, we found that CVN-AD mice express many protein changes found in post-mortem AD brain, including complement factor C1Q. Future studies will compare the protein changes found in this proteomic screen and the microarray data from CNS microglia.

## **5.5 Applications of *Cx3cr1-CreBT* Mice**

In Chapter 3, I described the *Cx3cr1-CreBT* mouse, in which Cre is expressed under the *Cx3cr1* promoter but the *Cx3cr1* gene is not disrupted. We believe that this mouse will be an invaluable tool for the study of tissue macrophages and brain immunity. As described above, we are currently producing *Cx3cr1-CreBT:Arg1<sup>flox/flox</sup>* mice (El Kasmi et al., 2008) on a CVN-AD background. In these mice, *Arg1* is expected to

be deleted in microglia and the other cell types described in Chapter 3. Our hope is that the cell-specific deletion of *Arg1* in CVN-AD mice will demonstrate that AD-like pathology, memory loss, and neuronal death are dependent on the aberrant overexpression of arginase-1. Cell-specific deletion is expected to have less off-target effects than the use of DFMO, which also inhibits ODC and arginase-2. Secondly, cell-specific deletion would demonstrate that, in CVN-AD mice, arginase-1 is produced by CX3CR1<sup>+</sup> myeloid cells.

*Cx3cr1-CreBT* mice are also being used in other contexts. We and other have previously used Cre-inducible diphtheria toxin receptor mice to ablate tissue macrophages and microglia in adult animals (Kan et al., in submission, (Parkhurst et al., 2013). While this results in successful ablation of the desired cell types, acute apoptosis of large populations of cells leads to side effects that affect the interpretation of the effects of ablation. In an attempt to make a mouse that lacks microglia and certain tissue macrophages throughout development, I generated *Cx3cr1-CreBT:Csf1r<sup>flox/flox</sup>* mice. Colony stimulating factor 1 receptor (CSF1R) is required for the survival of a variety of tissue macrophage populations, as *Csf1r<sup>-/-</sup>* mice lack microglia, tissue macrophages, and osteoclasts, and survive only shortly after birth. Our hypothesis was that cell-lineage specific deletion would result in a mouse with a less severe phenotype and the ability to study tissues that lack certain macrophage populations, such as microglia, which are dependent on CSF1R for survival (Wang et al., 2012).

Surprisingly, *Cx3cr1-CreBT:Csf1<sup>flx/flx</sup>* mice appear to have no obvious development defects or deficits in tissue macrophage populations. However, we have found that these mice appear to lack Ly6C<sup>lo</sup> resident monocytes (**Figure 21**). Unlike Ly6C<sup>hi</sup> inflammatory monocytes, the physiologic roles of resident monocytes are still controversial (Cain and Gunn, 2011). The *Nr4a1<sup>-/-</sup>* mouse strain has been described to lack resident monocytes, these mice revealed that that resident monocytes play a role in patrolling and disposing of damaged endothelial cells (Carlin et al., 2013; Hanna et al., 2011). *Cx3cr1-CreBT:Csf1<sup>flx/flx</sup>* mice, which also lack resident monocytes, may represent a complementary model system to study the role of resident monocytes.

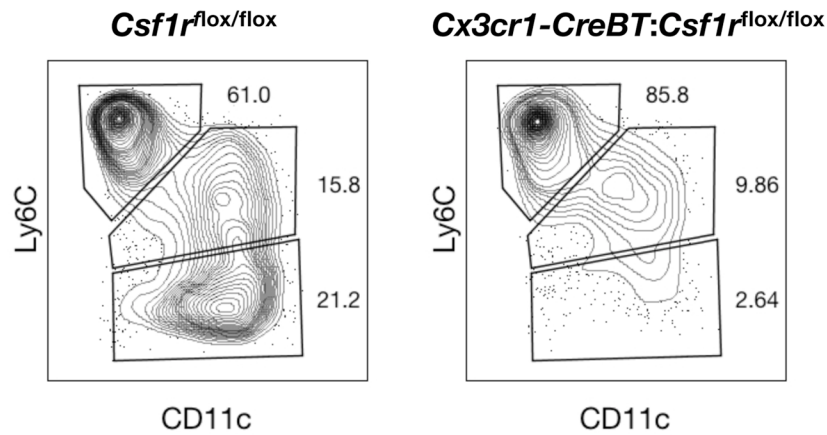


**Figure 21: Figure 21: *Cx3cr1-CreBT:Csf1<sup>flx/flx</sup>* mice lack Ly6C<sup>lo</sup> resident monocytes**

Flow cytometry plots of Ly6C vs CD11c after gating on peripheral blood monocytes (CD11b<sup>+</sup> F4/80<sup>int</sup>) from 12 week-old mice. Representative of 3 mice per genotype.

In the Gunn lab, Dr. Yen-rei Andrea Yu has used *Cx3cr1-CreBT* mice to manipulate the pathogenic hypoxia-sensing cells in a model of pulmonary hypertension. In this setting, pulmonary hypertension is experimentally induced by hypoxia, resulting in the expansion of a previously unidentifiable macrophage population. Using flow cytometry and IHC, she has since demonstrated that these macrophages are interstitial macrophages that express CX3CR1. Hypoxia inducible factors HIF1 $\alpha$  and HIF2 $\alpha$  are required for the development of pulmonary hypertension (Yu et al., 1999), but the cell type that senses hypoxia has not been identified. By generating *Cx3cr1-CreBT:Hif1a<sup>flox/flox</sup>* mice, Dr. Yu has been able to demonstrate that monocytes and interstitial macrophages are the hypoxia-sensing cells that promote pulmonary hypertension, as these mice do not develop pulmonary hypertension or related pathology (unpublished data).

In other collaborations at Duke University, Drs. Tony DeFalco and Blanche Capel have used *Cx3cr1-CreBT:DTR* mice to demonstrate that testes macrophages are required for maintenance of the spermatogonial niche (in submission) (DeFalco et al., 2014). Dr. Daniel Saban is using *Cx3cr1-CreBT:GFP* mice to track the migration of *Cx3cr1<sup>+</sup>* cells in the cornea of the eye (unpublished data). Dr. Staci Bilbo and her lab have utilized *Cx3cr1-CreBT* mice to make cell-specific knockouts of *Myd88* and cytokines that they believe are produced by microglia and contribute to the development of opioid addiction (unpublished data). These studies would not be possible using *Cx3cr1-CreKI* mice, as the phenotypes of the mice generated would be affected by *Cx3cr1*

heterozygosity. These examples illustrate the impact that we hope *Cx3cr1-CreBT* mice will have on future studies of tissue macrophages, microglia, and monocytes.

## **5.6 Applications of Murine Brain Immune Characterization**

In Chapter 4, I described the comprehensive identification of murine brain immune cells. This allows us, for the first time, to be able to identify circulating and infiltrating immune cells, including neutrophils, T cells, B cells, NK cells, inflammatory monocytes, and resident monocytes in brain. It also allows us to identify brain-resident myeloid populations, including microglia, dendritic cells, and two previously populations not identifiable by flow cytometry: F4/80<sup>hi</sup> macrophages and MHC-II<sup>+</sup> macrophages. We show that dendritic cells are derived from bone marrow-derived dendritic cell precursors, whereas microglia and macrophage populations are self-renewing populations. While further studies are required to demonstrate that F4/80<sup>+</sup> macrophages are meningeal macrophages and MHC-II<sup>+</sup> macrophages are perivascular and choroid plexus macrophages, these studies establish a strong foundation to study CNS immune cells. Further work with collaborators studying mouse models of traumatic brain injury, experimental autoimmune encephalitis, and glioblastoma will help us improve upon these tools to delineate cell types in complex models of neuroinflammation.

These findings also provide a basis for translating these findings into studies of the human brain using flow cytometry. Cerebral amyloid angiopathy is a feature sometimes observed in Alzheimer's disease, suggesting a role for dysfunctional endothelial cells or perivascular macrophages in AD pathogenesis. Our studies now provide a basis for isolating and studying these cell types. We have previously translated similar strategies for identifying immune cell types in the mouse lung to clinical samples of human lung (Yu et al., in submission and unpublished). This work has allowed us to describe changes in the frequencies of immune cells present in different lung compartments and lung diseases, including pulmonary fibrosis (Yu et al., unpublished). We believe that these strategies can be someday similarly employed for human brain samples.

Initial steps will include validating that immune cell subsets found in mouse brains are present in human brains. We will also need to identify some species-specific cell surface markers, as certain proteins, such as F4/80, are specific to mice and not present in humans. The human correlate of F4/80<sup>hi</sup> macrophages might be identifiable by CD206, which we have previously used to differentiate human macrophage subsets in the lung. While there are ethical, practical, and safety concerns that make attempting flow cytometry on human brain tissue more difficult than for peripheral tissues, we are hopeful that this will become an established technique in the future, allowing for detailed immunophenotyping of a variety of brain pathologies.

## **5.7 Concluding Thoughts**

I am cautiously optimistic that our novel hypothesis for the pathogenesis of Alzheimer's disease will have relevance and eventual therapeutic potential for this devastating and increasingly widespread disease. However, even if this theory is eventually demonstrated not to be central to AD pathogenesis, we hope that the presentation of a new direction, unique from the amyloid cascade hypothesis, stirs scientific discourse and promotes a reevaluation of the evidence in AD. Lastly, I hope that the tools presented here for the study of neuroinflammation in mice will someday lead to a better understanding of human neurobiology and the pathogenesis of neuroinflammatory, neurodegenerative, and neuropsychiatric disorders.

## References

- Abeloff, M.D., Slavik, M., Luk, G.D., Griffin, C.A., Hermann, J., Blanc, O., Sjoerdsma, A., and Baylin, S.B. (1984). Phase I trial and pharmacokinetic studies of alpha-difluoromethylornithine--an inhibitor of polyamine biosynthesis. *Journal of clinical oncology : official journal of the American Society of Clinical Oncology* 2, 124-130.
- Abram, C.L., Roberge, G.L., Hu, Y., and Lowell, C.A. (2014). Comparative analysis of the efficiency and specificity of myeloid-Cre deleting strains using ROSA-EYFP reporter mice. *J Immunol Methods* 408, 89-100.
- Ajami, B., Bennett, J.L., Krieger, C., McNagny, K.M., and Rossi, F.M. (2011). Infiltrating monocytes trigger EAE progression, but do not contribute to the resident microglia pool. *Nature neuroscience* 14, 1142-1149.
- Ajami, B., Bennett, J.L., Krieger, C., Tetzlaff, W., and Rossi, F.M. (2007). Local self-renewal can sustain CNS microglia maintenance and function throughout adult life. *Nature neuroscience* 10, 1538-1543.
- Akiyama, H., and McGeer, P.L. (1990). Brain microglia constitutively express beta-2 integrins. *J Neuroimmunol* 30, 81-93.
- Alamed, J., Wilcock, D.M., Diamond, D.M., Gordon, M.N., and Morgan, D. (2006). Two-day radial-arm water maze learning and memory task; robust resolution of amyloid-related memory deficits in transgenic mice. *Nat Protoc* 1, 1671-1679.
- Altman, B.J., and Rathmell, J.C. (2012). Metabolic stress in autophagy and cell death pathways. *Cold Spring Harbor perspectives in biology* 4.
- Anandasabapathy, N., Victora, G.D., Meredith, M., Feder, R., Dong, B., Kluger, C., Yao, K., Dustin, M.L., Nussenzweig, M.C., Steinman, R.M., *et al.* (2011). Flt3L controls the development of radiosensitive dendritic cells in the meninges and choroid plexus of the steady-state mouse brain. *J Exp Med* 208, 1695-1705.
- Anthony, R.M., Urban, J.F., Jr., Alem, F., Hamed, H.A., Rozo, C.T., Boucher, J.L., Van Rooijen, N., and Gause, W.C. (2006). Memory T(H)2 cells induce alternatively activated macrophages to mediate protection against nematode parasites. *Nat Med* 12, 955-960.
- Arakawa, J., Uegaki, M., and Ishimizu, T. (2011). Effects of L-arginine on solubilization and purification of plant membrane proteins. *Protein expression and purification* 80, 91-96.

Arm, J.P., Nwankwo, C., and Austen, K.F. (1997). Molecular identification of a novel family of human Ig superfamily members that possess immunoreceptor tyrosine-based inhibition motifs and homology to the mouse gp49B1 inhibitory receptor. *J Immunol* 159, 2342-2349.

Badaut, J., Copin, J.C., Fukuda, A.M., Gasche, Y., Schaller, K., and da Silva, R.F. (2012). Increase of arginase activity in old apolipoprotein-E deficient mice under Western diet associated with changes in neurovascular unit. *J Neuroinflammation* 9, 132.

Baruch, K., Ron-Harel, N., Gal, H., Deczkowska, A., Shifrut, E., Ndifon, W., Mirlas-Neisberg, N., Cardon, M., Vaknin, I., Cahalon, L., *et al.* (2013). CNS-specific immunity at the choroid plexus shifts toward destructive Th2 inflammation in brain aging. *Proceedings of the National Academy of Sciences of the United States of America* 110, 2264-2269.

Baruch, K., and Schwartz, M. (2013). CNS-specific T cells shape brain function via the choroid plexus. *Brain Behav Immun* 34, 11-16.

Becher, B., and Antel, J.P. (1996). Comparison of phenotypic and functional properties of immediately ex vivo and cultured human adult microglia. *Glia* 18, 1-10.

Bechmann, I., Kwidzinski, E., Kovac, A.D., Simburger, E., Horvath, T., Gimsa, U., Dirnagl, U., Priller, J., and Nitsch, R. (2001). Turnover of rat brain perivascular cells. *Exp Neurol* 168, 242-249.

Becker, M., Guttler, S., Bachem, A., Hartung, E., Mora, A., Jakel, A., Hutloff, A., Henn, V., Mages, H.W., Gurka, S., *et al.* (2014). Ontogenic, Phenotypic, and Functional Characterization of XCR1(+) Dendritic Cells Leads to a Consistent Classification of Intestinal Dendritic Cells Based on the Expression of XCR1 and SIRPalpha. *Frontiers in immunology* 5, 326.

Beumer, W., Gibney, S.M., Drexhage, R.C., Pont-Lezica, L., Doorduyn, J., Klein, H.C., Steiner, J., Connor, T.J., Harkin, A., Versnel, M.A., *et al.* (2012). The immune theory of psychiatric diseases: a key role for activated microglia and circulating monocytes. *J Leukoc Biol* 92, 959-975.

Boado, R.J., Li, J.Y., Wise, P., and Pardridge, W.M. (2004). Human LAT1 single nucleotide polymorphism N230K does not alter phenylalanine transport. *Mol Genet Metab* 83, 306-311.

Boche, D., Donald, J., Love, S., Harris, S., Neal, J.W., Holmes, C., and Nicoll, J.A. (2010). Reduction of aggregated Tau in neuronal processes but not in the cell bodies after Abeta42 immunisation in Alzheimer's disease. *Acta neuropathologica* 120, 13-20.

Boucher, J.L., Moali, C., and Tenu, J.P. (1999). Nitric oxide biosynthesis, nitric oxide synthase inhibitors and arginase competition for L-arginine utilization. *Cell Mol Life Sci* 55, 1015-1028.

Braak, H., Thal, D.R., Ghebremedhin, E., and Del Tredici, K. (2011). Stages of the pathologic process in Alzheimer disease: age categories from 1 to 100 years. *J Neuropathol Exp Neurol* 70, 960-969.

Bradshaw, E.M., Chibnik, L.B., Keenan, B.T., Ottoboni, L., Raj, T., Tang, A., Rosenkrantz, L.L., Imboywa, S., Lee, M., Von Korff, A., *et al.* (2013). CD33 Alzheimer's disease locus: altered monocyte function and amyloid biology. *Nat Neurosci* 16, 848-850.

Broer, S. (2002). Adaptation of plasma membrane amino acid transport mechanisms to physiological demands. *Pflugers Archiv : European journal of physiology* 444, 457-466.

Bronte, V., and Zanovello, P. (2005). Regulation of immune responses by L-arginine metabolism. *Nat Rev Immunol* 5, 641-654.

Brown, C.M., Becker, J.O., Wise, P.M., and Hoofnagle, A.N. (2011). Simultaneous determination of 6 L-arginine metabolites in human and mouse plasma by using hydrophilic-interaction chromatography and electrospray tandem mass spectrometry. *Clinical chemistry* 57, 701-709.

Buch, T., Heppner, F.L., Tertilt, C., Heinen, T.J., Kremer, M., Wunderlich, F.T., Jung, S., and Waisman, A. (2005). A Cre-inducible diphtheria toxin receptor mediates cell lineage ablation after toxin administration. *Nature methods* 2, 419-426.

Butovsky, O., Bukshpan, S., Kunis, G., Jung, S., and Schwartz, M. (2007). Microglia can be induced by IFN-gamma or IL-4 to express neural or dendritic-like markers. *Molecular and cellular neurosciences* 35, 490-500.

Butovsky, O., Ziv, Y., Schwartz, A., Landa, G., Talpalar, A.E., Pluchino, S., Martino, G., and Schwartz, M. (2006). Microglia activated by IL-4 or IFN-gamma differentially induce neurogenesis and oligodendrogenesis from adult stem/progenitor cells. *Mol Cell Neurosci* 31, 149-160.

- Buts, J.P., De Keyser, N., Kolanowski, J., Sokal, E., and Van Hoof, F. (1993). Maturation of villus and crypt cell functions in rat small intestine. Role of dietary polyamines. *Digestive diseases and sciences* 38, 1091-1098.
- Butte, M.J., Pena-Cruz, V., Kim, M.J., Freeman, G.J., and Sharpe, A.H. (2008). Interaction of human PD-L1 and B7-1. *Molecular immunology* 45, 3567-3572.
- Cain, D.W., and Gunn, M.D. (2011). NUR who? An orphan transcription factor holds promise for monomaniacs. *Nat Immunol* 12, 727-729.
- Cardona, A.E., Huang, D., Sasse, M.E., and Ransohoff, R.M. (2006a). Isolation of murine microglial cells for RNA analysis or flow cytometry. *Nat Protoc* 1, 1947-1951.
- Cardona, A.E., Pioro, E.P., Sasse, M.E., Kostenko, V., Cardona, S.M., Dijkstra, I.M., Huang, D., Kidd, G., Dombrowski, S., Dutta, R., *et al.* (2006b). Control of microglial neurotoxicity by the fractalkine receptor. *Nature neuroscience* 9, 917-924.
- Carlin, L.M., Stamatiades, E.G., Auffray, C., Hanna, R.N., Glover, L., Vizcay-Barrena, G., Hedrick, C.C., Cook, H.T., Diebold, S., and Geissmann, F. (2013). Nr4a1-dependent Ly6C(low) monocytes monitor endothelial cells and orchestrate their disposal. *Cell* 153, 362-375.
- Carson, M.J., Doose, J.M., Melchior, B., Schmid, C.D., and Ploix, C.C. (2006). CNS immune privilege: hiding in plain sight. *Immunol Rev* 213, 48-65.
- Carter-Dawson, L.D., and LaVail, M.M. (1979). Rods and cones in the mouse retina. II. Autoradiographic analysis of cell generation using tritiated thymidine. *J Comp Neurol* 188, 263-272.
- Chakrabarty, P., Li, A., Ceballos-Diaz, C., Eddy, J.A., Funk, C.C., Moore, B., DiNunno, N., Rosario, A.M., Cruz, P.E., Verbeeck, C., *et al.* (2015). IL-10 alters immunoproteostasis in APP mice, increasing plaque burden and worsening cognitive behavior. *Neuron* 85, 519-533.
- Chang, J.T., and Nevins, J.R. (2006). GATHER: a systems approach to interpreting genomic signatures. *Bioinformatics* 22, 2926-2933.
- Clausen, B.E., Burkhardt, C., Reith, W., Renkawitz, R., and Forster, I. (1999). Conditional gene targeting in macrophages and granulocytes using LysMcre mice. *Transgenic research* 8, 265-277.

- Closs, E.I., Boissel, J.P., Habermeier, A., and Rotmann, A. (2006). Structure and function of cationic amino acid transporters (CATs). *J Membr Biol* 213, 67-77.
- Colton, C., Wilt, S., Gilbert, D., Chernyshev, O., Snell, J., and Dubois-Dalcq, M. (1996). Species differences in the generation of reactive oxygen species by microglia. *Mol Chem Neuropathol* 28, 15-20.
- Colton, C.A., Mott, R.T., Sharpe, H., Xu, Q., Van Nostrand, W.E., and Vitek, M.P. (2006). Expression profiles for macrophage alternative activation genes in AD and in mouse models of AD. *J Neuroinflammation* 3, 27.
- Colton, C.A., Wilcock, D.M., Wink, D.A., Davis, J., Van Nostrand, W.E., and Vitek, M.P. (2008). The effects of NOS2 gene deletion on mice expressing mutated human AbetaPP. *J Alzheimers Dis* 15, 571-587.
- Colton, C.A., Wilson, J.G., Everhart, A., Wilcock, D.M., Puolivali, J., Heikkinen, T., Oksman, J., Jaaskelainen, O., Lehtimaki, K., Laitinen, T., *et al.* (2014). mNos2 deletion and human NOS2 replacement in Alzheimer disease models. *J Neuropathol Exp Neurol* 73, 752-769.
- Colton, C.A., Xu, Q., Burke, J.R., Bae, S.Y., Wakefield, J.K., Nair, A., Strittmatter, W.J., and Vitek, M.P. (2004). Disrupted spermine homeostasis: a novel mechanism in polyglutamine-mediated aggregation and cell death. *J Neurosci* 24, 7118-7127.
- Combadiere, C., Potteaux, S., Gao, J.L., Esposito, B., Casanova, S., Lee, E.J., Debre, P., Tedgui, A., Murphy, P.M., and Mallat, Z. (2003). Decreased atherosclerotic lesion formation in CX3CR1/apolipoprotein E double knockout mice. *Circulation* 107, 1009-1016.
- Comi, C., Carecchio, M., Chiochetti, A., Nicola, S., Galimberti, D., Fenoglio, C., Cappellano, G., Monaco, F., Scarpini, E., and Dianzani, U. (2010). Osteopontin is increased in the cerebrospinal fluid of patients with Alzheimer's disease and its levels correlate with cognitive decline. *J Alzheimers Dis* 19, 1143-1148.
- Cunningham, C.L., Martinez-Cerdeno, V., and Noctor, S.C. (2013). Microglia regulate the number of neural precursor cells in the developing cerebral cortex. *J Neurosci* 33, 4216-4233.
- Curry, H., Alvarez, G.R., Zwilling, B.S., and Lafuse, W.P. (2004). Toll-like receptor 2 stimulation decreases IFN-gamma receptor expression in mouse RAW264.7 macrophages. *J Interferon Cytokine Res* 24, 699-710.

- Date, D., Das, R., Narla, G., Simon, D.I., Jain, M.K., and Mahabeleshwar, G.H. (2014). Kruppel-like transcription factor 6 regulates inflammatory macrophage polarization. *J Biol Chem* 289, 10318-10329.
- Davis, J., Xu, F., Deane, R., Romanov, G., Previti, M.L., Zeigler, K., Zlokovic, B.V., and Van Nostrand, W.E. (2004). Early-onset and robust cerebral microvascular accumulation of amyloid beta-protein in transgenic mice expressing low levels of a vasculotropic Dutch/Iowa mutant form of amyloid beta-protein precursor. *J Biol Chem* 279, 20296-20306.
- Dawson, L.A., Organ, A.J., Winter, P., Lacroix, L.P., Shilliam, C.S., Heidebreder, C., and Shah, A.J. (2004). Rapid high-throughput assay for the measurement of amino acids from microdialysates and brain tissue using monolithic C18-bonded reversed-phase columns. *Journal of chromatography B, Analytical technologies in the biomedical and life sciences* 807, 235-241.
- DeFalco, T., Bhattacharya, I., Williams, A.V., Sams, D.M., and Capel, B. (2014). Yolk-sac-derived macrophages regulate fetal testis vascularization and morphogenesis. *Proc Natl Acad Sci U S A* 111, E2384-2393.
- Denieffe, S., Kelly, R.J., McDonald, C., Lyons, A., and Lynch, M.A. (2013). Classical activation of microglia in CD200-deficient mice is a consequence of blood brain barrier permeability and infiltration of peripheral cells. *Brain Behav Immun* 34, 86-97.
- Dick, A.D., Pell, M., Brew, B.J., Foulcher, E., and Sedgwick, J.D. (1997). Direct ex vivo flow cytometric analysis of human microglial cell CD4 expression: examination of central nervous system biopsy specimens from HIV-seropositive patients and patients with other neurological disease. *Aids* 11, 1699-1708.
- Dickson, D.W., Farlo, J., Davies, P., Crystal, H., Fuld, P., and Yen, S.H. (1988). Alzheimer's disease. A double-labeling immunohistochemical study of senile plaques. *Am J Pathol* 132, 86-101.
- Doody, R.S., Farlow, M., Aisen, P.S., Alzheimer's Disease Cooperative Study Data, A., and Publication, C. (2014). Phase 3 trials of solanezumab and bapineuzumab for Alzheimer's disease. *N Engl J Med* 370, 1460.
- Duffield, J.S. (2010). Macrophages and immunologic inflammation of the kidney. *Seminars in nephrology* 30, 234-254.

Eikelenboom, P., van Exel, E., Hoozemans, J.J., Veerhuis, R., Rozemuller, A.J., and van Gool, W.A. (2010). Neuroinflammation - an early event in both the history and pathogenesis of Alzheimer's disease. *Neurodegener Dis* 7, 38-41.

El Kasmi, K.C., Qualls, J.E., Pesce, J.T., Smith, A.M., Thompson, R.W., Henao-Tamayo, M., Basaraba, R.J., Konig, T., Schleicher, U., Koo, M.S., *et al.* (2008). Toll-like receptor-induced arginase 1 in macrophages thwarts effective immunity against intracellular pathogens. *Nat Immunol* 9, 1399-1406.

El Khoury, J., Toft, M., Hickman, S.E., Means, T.K., Terada, K., Geula, C., and Luster, A.D. (2007). Ccr2 deficiency impairs microglial accumulation and accelerates progression of Alzheimer-like disease. *Nat Med* 13, 432-438.

Elahi, S., Ertelt, J.M., Kinder, J.M., Jiang, T.T., Zhang, X., Xin, L., Chaturvedi, V., Strong, B.S., Qualls, J.E., Steinbrecher, K.A., *et al.* (2013). Immunosuppressive CD71+ erythroid cells compromise neonatal host defence against infection. *Nature* 504, 158-162.

Ellmeier, W., Jung, S., Sunshine, M.J., Hatam, F., Xu, Y., Baltimore, D., Mano, H., and Littman, D.R. (2000). Severe B cell deficiency in mice lacking the tec kinase family members Tec and Btk. *J Exp Med* 192, 1611-1624.

Engler, H., Forsberg, A., Almkvist, O., Blomquist, G., Larsson, E., Savitcheva, I., Wall, A., Ringheim, A., Langstrom, B., and Nordberg, A. (2006). Two-year follow-up of amyloid deposition in patients with Alzheimer's disease. *Brain* 129, 2856-2866.

Erdely, A., Kepka-Lenhart, D., Salmen-Muniz, R., Chapman, R., Hulderman, T., Kashon, M., Simeonova, P.P., and Morris, S.M., Jr. (2010). Arginase activities and global arginine bioavailability in wild-type and ApoE-deficient mice: responses to high fat and high cholesterol diets. *PLoS One* 5, e15253.

Fuhrmann, M., Bittner, T., Jung, C.K., Burgold, S., Page, R.M., Mitteregger, G., Haass, C., LaFerla, F.M., Kretzschmar, H., and Herms, J. (2010). Microglial Cx3cr1 knockout prevents neuron loss in a mouse model of Alzheimer's disease. *Nature neuroscience* 13, 411-413.

Gabrilovich, D.I., and Nagaraj, S. (2009). Myeloid-derived suppressor cells as regulators of the immune system. *Nat Rev Immunol* 9, 162-174.

Galea, I., Palin, K., Newman, T.A., Van Rooijen, N., Perry, V.H., and Boche, D. (2005). Mannose receptor expression specifically reveals perivascular macrophages in normal, injured, and diseased mouse brain. *Glia* 49, 375-384.

- Ganster, R.W., Taylor, B.S., Shao, L., and Geller, D.A. (2001). Complex regulation of human inducible nitric oxide synthase gene transcription by Stat 1 and NF-kappa B. *Proc Natl Acad Sci U S A* 98, 8638-8643.
- Garcia, J.A., Cardona, S.M., and Cardona, A.E. (2014). Isolation and analysis of mouse microglial cells. *Current protocols in immunology / edited by John E Coligan [et al]* 104, Unit 14 35.
- Geller, D.A., and Billiar, T.R. (1998). Molecular biology of nitric oxide synthases. *Cancer Metastasis Rev* 17, 7-23.
- Genin, E., Hannequin, D., Wallon, D., Sleegers, K., Hiltunen, M., Combarros, O., Bullido, M.J., Engelborghs, S., De Deyn, P., Berr, C., *et al.* (2011). APOE and Alzheimer disease: a major gene with semi-dominant inheritance. *Mol Psychiatry* 16, 903-907.
- Ginhoux, F., Greter, M., Leboeuf, M., Nandi, S., See, P., Gokhan, S., Mehler, M.F., Conway, S.J., Ng, L.G., Stanley, E.R., *et al.* (2010). Fate mapping analysis reveals that adult microglia derive from primitive macrophages. *Science* 330, 841-845.
- Glenner, G.G., and Wong, C.W. (1984). Alzheimer's disease: initial report of the purification and characterization of a novel cerebrovascular amyloid protein. *Biochem Biophys Res Commun* 120, 885-890.
- Gobert, A.P., Daulouede, S., Lepoivre, M., Boucher, J.L., Bouteille, B., Buguet, A., Cespuglio, R., Veyret, B., and Vincendeau, P. (2000). L-Arginine availability modulates local nitric oxide production and parasite killing in experimental trypanosomiasis. *Infect Immun* 68, 4653-4657.
- Golanska, E., Sieruta, M., Gresner, S.M., Pfeffer, A., Chodakowska-Zebrowska, M., Sobow, T.M., Klich, I., Mossakowska, M., Szybinska, A., Barcikowska, M., *et al.* (2013). APBB2 genetic polymorphisms are associated with severe cognitive impairment in centenarians. *Exp Gerontol* 48, 391-394.
- Gong, S., Zheng, C., Doughty, M.L., Losos, K., Didkovsky, N., Schambra, U.B., Nowak, N.J., Joyner, A., Leblanc, G., Hatten, M.E., *et al.* (2003). A gene expression atlas of the central nervous system based on bacterial artificial chromosomes. *Nature* 425, 917-925.
- Goren, I., Allmann, N., Yogev, N., Schurmann, C., Linke, A., Holdener, M., Waisman, A., Pfeilschifter, J., and Frank, S. (2009). A transgenic mouse model of inducible macrophage depletion: effects of diphtheria toxin-driven lysozyme M-specific cell lineage ablation on wound inflammatory, angiogenic, and contractive processes. *Am J Pathol* 175, 132-147.

- Grant, J.L., Ghosn, E.E., Axtell, R.C., Herges, K., Kuipers, H.F., Woodling, N.S., Andreasson, K., Herzenberg, L.A., and Steinman, L. (2012). Reversal of paralysis and reduced inflammation from peripheral administration of beta-amyloid in TH1 and TH17 versions of experimental autoimmune encephalomyelitis. *Sci Transl Med* 4, 145ra105.
- Grupe, A., Li, Y., Rowland, C., Nowotny, P., Hinrichs, A.L., Smemo, S., Kauwe, J.S., Maxwell, T.J., Cherny, S., Doil, L., *et al.* (2006). A scan of chromosome 10 identifies a novel locus showing strong association with late-onset Alzheimer disease. *American journal of human genetics* 78, 78-88.
- Gueli, M.C., and Taibi, G. (2013). Alzheimer's disease: amino acid levels and brain metabolic status. *Neurol Sci* 34, 1575-1579.
- Guerreiro, R., Wojtas, A., Bras, J., Carrasquillo, M., Rogaeva, E., Majounie, E., Cruchaga, C., Sassi, C., Kauwe, J.S., Younkin, S., *et al.* (2013). TREM2 variants in Alzheimer's disease. *N Engl J Med* 368, 117-127.
- Guillot-Sestier, M.V., Doty, K.R., Gate, D., Rodriguez, J., Jr., Leung, B.P., Rezai-Zadeh, K., and Town, T. (2015). Il10 deficiency rebalances innate immunity to mitigate Alzheimer-like pathology. *Neuron* 85, 534-548.
- Guo, Z., Shao, L., Zheng, L., Du, Q., Li, P., John, B., and Geller, D.A. (2012). miRNA-939 regulates human inducible nitric oxide synthase posttranscriptional gene expression in human hepatocytes. *Proceedings of the National Academy of Sciences of the United States of America* 109, 5826-5831.
- Halks-Miller, M., Schroeder, M.L., Haroutunian, V., Moenning, U., Rossi, M., Achim, C., Purohit, D., Mahmoudi, M., and Horuk, R. (2003). CCR1 is an early and specific marker of Alzheimer's disease. *Ann Neurol* 54, 638-646.
- Hanna, R.N., Carlin, L.M., Hubbeling, H.G., Nackiewicz, D., Green, A.M., Punt, J.A., Geissmann, F., and Hedrick, C.C. (2011). The transcription factor NR4A1 (Nur77) controls bone marrow differentiation and the survival of Ly6C- monocytes. *Nat Immunol* 12, 778-785.
- Hansmannel, F., Sillaire, A., Kamboh, M.I., Lendon, C., Pasquier, F., Hannequin, D., Laumet, G., Mounier, A., Ayrat, A.M., DeKosky, S.T., *et al.* (2010). Is the urea cycle involved in Alzheimer's disease? *J Alzheimers Dis* 21, 1013-1021.
- Hawkins, R.A., Mokashi, A., and Simpson, I.A. (2005). An active transport system in the blood-brain barrier may reduce levodopa availability. *Exp Neurol* 195, 267-271.

- Hawkins, R.A., O'Kane, R.L., Simpson, I.A., and Vina, J.R. (2006). Structure of the blood-brain barrier and its role in the transport of amino acids. *J Nutr* 136, 218S-226S.
- Hebert, L.E., Weuve, J., Scherr, P.A., and Evans, D.A. (2013). Alzheimer disease in the United States (2010-2050) estimated using the 2010 census. *Neurology* 80, 1778-1783.
- Hesse, M., Modolell, M., La Flamme, A.C., Schito, M., Fuentes, J.M., Cheever, A.W., Pearce, E.J., and Wynn, T.A. (2001). Differential regulation of nitric oxide synthase-2 and arginase-1 by type 1/type 2 cytokines in vivo: granulomatous pathology is shaped by the pattern of L-arginine metabolism. *J Immunol* 167, 6533-6544.
- Hickey, W.F., and Kimura, H. (1988). Perivascular microglial cells of the CNS are bone marrow-derived and present antigen in vivo. *Science* 239, 290-292.
- Hickman, S.E., Kingery, N.D., Ohsumi, T.K., Borowsky, M.L., Wang, L.C., Means, T.K., and El Khoury, J. (2013). The microglial sensome revealed by direct RNA sequencing. *Nat Neurosci* 16, 1896-1905.
- Hoane, M.R., Kaufman, N., Vitek, M.P., and McKenna, S.E. (2009). COG1410 improves cognitive performance and reduces cortical neuronal loss in the traumatically injured brain. *Journal of neurotrauma* 26, 121-129.
- Hoane, M.R., Pierce, J.L., Holland, M.A., Birky, N.D., Dang, T., Vitek, M.P., and McKenna, S.E. (2007). The novel apolipoprotein E-based peptide COG1410 improves sensorimotor performance and reduces injury magnitude following cortical contusion injury. *Journal of neurotrauma* 24, 1108-1118.
- Hoos, M.D., Richardson, B.M., Foster, M.W., Everhart, A., Thompson, J.W., Moseley, M.A., and Colton, C.A. (2013). Longitudinal study of differential protein expression in an Alzheimer's mouse model lacking inducible nitric oxide synthase. *Journal of proteome research* 12, 4462-4477.
- Hosokawa, H., Ninomiya, H., Sawamura, T., Sugimoto, Y., Ichikawa, A., Fujiwara, K., and Masaki, T. (1999). Neuron-specific expression of cationic amino acid transporter 3 in the adult rat brain. *Brain Res* 838, 158-165.
- Hyatt, S.L., Aulak, K.S., Malandro, M., Kilberg, M.S., and Hatzoglou, M. (1997). Adaptive regulation of the cationic amino acid transporter-1 (Cat-1) in Fao cells. *J Biol Chem* 272, 19951-19957.
- Ingelsson, M., Fukumoto, H., Newell, K.L., Growdon, J.H., Hedley-Whyte, E.T., Frosch, M.P., Albert, M.S., Hyman, B.T., and Irizarry, M.C. (2004). Early Abeta accumulation and

progressive synaptic loss, gliosis, and tangle formation in AD brain. *Neurology* 62, 925-931.

Inoue, K., Tsutsui, H., Akatsu, H., Hashizume, Y., Matsukawa, N., Yamamoto, T., and Toyo'oka, T. (2013). Metabolic profiling of Alzheimer's disease brains. *Scientific reports* 3, 2364.

Irizarry, M.C., McNamara, M., Fedorchak, K., Hsiao, K., and Hyman, B.T. (1997a). APPSw transgenic mice develop age-related A beta deposits and neuropil abnormalities, but no neuronal loss in CA1. *J Neuropathol Exp Neurol* 56, 965-973.

Irizarry, M.C., Soriano, F., McNamara, M., Page, K.J., Schenk, D., Games, D., and Hyman, B.T. (1997b). Abeta deposition is associated with neuropil changes, but not with overt neuronal loss in the human amyloid precursor protein V717F (PDAPP) transgenic mouse. *J Neurosci* 17, 7053-7059.

Iyer, R., Jenkinson, C.P., Vockley, J.G., Kern, R.M., Grody, W.W., and Cederbaum, S. (1998). The human arginases and arginase deficiency. *Journal of inherited metabolic disease* 21 Suppl 1, 86-100.

Jay, T.R., Miller, C.M., Cheng, P.J., Graham, L.C., Bemiller, S., Broihier, M.L., Xu, G., Margevicius, D., Karlo, J.C., Sousa, G.L., *et al.* (2015). TREM2 deficiency eliminates TREM2+ inflammatory macrophages and ameliorates pathology in Alzheimer's disease mouse models. *J Exp Med* 212, 287-295.

Jenkinson, C.P., Grody, W.W., and Cederbaum, S.D. (1996). Comparative properties of arginases. *Comp Biochem Physiol B Biochem Mol Biol* 114, 107-132.

Jonsson, T., Stefansson, H., Steinberg, S., Jonsdottir, I., Jonsson, P.V., Snaedal, J., Bjornsson, S., Huttenlocher, J., Levey, A.I., Lah, J.J., *et al.* (2013a). Variant of TREM2 associated with the risk of Alzheimer's disease. *N Engl J Med* 368, 107-116.

Jonsson, T., Stefansson, H., Steinberg, S., Jonsdottir, I., Jonsson, P.V., Snaedal, J., Bjornsson, S., Huttenlocher, J., Levey, A.I., Lah, J.J., *et al.* (2013b). Variant of TREM2 associated with the risk of Alzheimer's disease. *N Engl J Med* 368, 107-116.

Jung, S., Aliberti, J., Graemmel, P., Sunshine, M.J., Kreutzberg, G.W., Sher, A., and Littman, D.R. (2000). Analysis of fractalkine receptor CX(3)CR1 function by targeted deletion and green fluorescent protein reporter gene insertion. *Mol Cell Biol* 20, 4106-4114.

- Kamboh, M.I., Barmada, M.M., Demirci, F.Y., Minster, R.L., Carrasquillo, M.M., Pankratz, V.S., Younkin, S.G., Saykin, A.J., Alzheimer's Disease Neuroimaging, I., Sweet, R.A., *et al.* (2012a). Genome-wide association analysis of age-at-onset in Alzheimer's disease. *Mol Psychiatry* 17, 1340-1346.
- Kamboh, M.I., Demirci, F.Y., Wang, X., Minster, R.L., Carrasquillo, M.M., Pankratz, V.S., Younkin, S.G., Saykin, A.J., Jun, G., Baldwin, C., *et al.* (2012b). Genome-wide association study of Alzheimer's disease. *Translational psychiatry* 2, e117.
- Kameji, T., Murakami, Y., and Hayashi, S. (1979). Effect of diaminobutene and diaminopropane on diet-stimulated polyamine synthesis and cell proliferation in rat liver. *J Biochem* 86, 191-197.
- Kan, M.J., Lee, J.E., Wilson, J.G., Everhart, A.L., Brown, C.M., Hoofnagle, A.N., Jansen, M., Vitek, M.P., Gunn, M.D., and Colton, C.A. (2015). Arginine deprivation and immune suppression in a mouse model of Alzheimer's disease. *J Neurosci* 35, 5969-5982.
- Kanazawa, N., Nakamura, T., Tashiro, K., Muramatsu, M., Morita, K., Yoneda, K., Inaba, K., Imamura, S., and Honjo, T. (1999). Fractalkine and macrophage-derived chemokine: T cell-attracting chemokines expressed in T cell area dendritic cells. *Eur J Immunol* 29, 1925-1932.
- Karlstetter, M., Walczak, Y., Weigelt, K., Ebert, S., Van den Brulle, J., Schwer, H., Fuchshofer, R., and Langmann, T. (2010). The novel activated microglia/macrophage WAP domain protein, AMWAP, acts as a counter-regulator of proinflammatory response. *J Immunol* 185, 3379-3390.
- Kaufman, N.A., Beare, J.E., Tan, A.A., Vitek, M.P., McKenna, S.E., and Hoane, M.R. (2010). COG1410, an apolipoprotein E-based peptide, improves cognitive performance and reduces cortical loss following moderate fluid percussion injury in the rat. *Behav Brain Res* 214, 395-401.
- Kearney, S.J., Delgado, C., Eshleman, E.M., Hill, K.K., O'Connor, B.P., and Lenz, L.L. (2013). Type I IFNs downregulate myeloid cell IFN-gamma receptor by inducing recruitment of an early growth response 3/NGFI-A binding protein 1 complex that silences *ifngr1* transcription. *J Immunol* 191, 3384-3392.
- Kierdorf, K., Katzmarski, N., Haas, C.A., and Prinz, M. (2013). Bone marrow cell recruitment to the brain in the absence of irradiation or parabiosis bias. *PLoS One* 8, e58544.

Kipnis, J., Gadani, S., and Derecki, N.C. (2012). Pro-cognitive properties of T cells. *Nat Rev Immunol* 12, 663-669.

Krempski, J., Karyampudi, L., Behrens, M.D., Erskine, C.L., Hartmann, L., Dong, H., Goode, E.L., Kalli, K.R., and Knutson, K.L. (2011a). Tumor-infiltrating programmed death receptor-1+ dendritic cells mediate immune suppression in ovarian cancer. *J Immunol* 186, 6905-6913.

Krempski, J., Karyampudi, L., Behrens, M.D., Erskine, C.L., Hartmann, L., Dong, H., Goode, E.L., Kalli, K.R., and Knutson, K.L. (2011b). Tumor-infiltrating programmed death receptor-1+ dendritic cells mediate immune suppression in ovarian cancer. *Journal of immunology* 186, 6905-6913.

Kudou, M., Ejima, D., Sato, H., Yumioka, R., Arakawa, T., and Tsumoto, K. (2011). Refolding single-chain antibody (scFv) using lauroyl-L-glutamate as a solubilization detergent and arginine as a refolding additive. *Protein expression and purification* 77, 68-74.

Kuma, A., and Mizushima, N. (2010). Physiological role of autophagy as an intracellular recycling system: with an emphasis on nutrient metabolism. *Seminars in cell & developmental biology* 21, 683-690.

Kung, J.T., Brooks, S.B., Jakway, J.P., Leonard, L.L., and Talmage, D.W. (1977). Suppression of in vitro cytotoxic response by macrophages due to induced arginase. *J Exp Med* 146, 665-672.

Kurnellas, M.P., Adams, C.M., Sobel, R.A., Steinman, L., and Rothbard, J.B. (2013). Amyloid fibrils composed of hexameric peptides attenuate neuroinflammation. *Sci Transl Med* 5, 179ra142.

Lambert, J.C., Ibrahim-Verbaas, C.A., Harold, D., Naj, A.C., Sims, R., Bellenguez, C., DeStafano, A.L., Bis, J.C., Beecham, G.W., Grenier-Boley, B., *et al.* (2013). Meta-analysis of 74,046 individuals identifies 11 new susceptibility loci for Alzheimer's disease. *Nat Genet* 45, 1452-1458.

Langlet, C., Tamoutounour, S., Henri, S., Luche, H., Ardouin, L., Gregoire, C., Malissen, B., and Guillemins, M. (2012). CD64 expression distinguishes monocyte-derived and conventional dendritic cells and reveals their distinct role during intramuscular immunization. *J Immunol* 188, 1751-1760.

- Larson, K.C., Lipko, M., Dabrowski, M., and Draper, M.P. (2010). Gng12 is a novel negative regulator of LPS-induced inflammation in the microglial cell line BV-2. *Inflamm Res* 59, 15-22.
- Laskowitz, D.T., Goel, S., Bennett, E.R., and Matthew, W.D. (1997). Apolipoprotein E suppresses glial cell secretion of TNF alpha. *J Neuroimmunol* 76, 70-74.
- Laskowitz, D.T., Lei, B., Dawson, H.N., Wang, H., Bellows, S.T., Christensen, D.J., Vitek, M.P., and James, M.L. (2012). The apoE-mimetic peptide, COG1410, improves functional recovery in a murine model of intracerebral hemorrhage. *Neurocrit Care* 16, 316-326.
- Laskowitz, D.T., McKenna, S.E., Song, P., Wang, H., Durham, L., Yeung, N., Christensen, D., and Vitek, M.P. (2007). COG1410, a novel apolipoprotein E-based peptide, improves functional recovery in a murine model of traumatic brain injury. *Journal of neurotrauma* 24, 1093-1107.
- Laubach, V.E., Foley, P.L., Shockey, K.S., Tribble, C.G., and Kron, I.L. (1998). Protective roles of nitric oxide and testosterone in endotoxemia: evidence from NOS-2-deficient mice. *Am J Physiol* 275, H2211-2218.
- Levy-Lahad, E., Wasco, W., Poorkaj, P., Romano, D.M., Oshima, J., Pettingell, W.H., Yu, C.E., Jondro, P.D., Schmidt, S.D., Wang, K., *et al.* (1995a). Candidate gene for the chromosome 1 familial Alzheimer's disease locus. *Science* 269, 973-977.
- Levy-Lahad, E., Wijsman, E.M., Nemens, E., Anderson, L., Goddard, K.A., Weber, J.L., Bird, T.D., and Schellenberg, G.D. (1995b). A familial Alzheimer's disease locus on chromosome 1. *Science* 269, 970-973.
- Lio, D., Licastro, F., Scola, L., Chiappelli, M., Grimaldi, L.M., Crivello, A., Colonna-Romano, G., Candore, G., Franceschi, C., and Caruso, C. (2003). Interleukin-10 promoter polymorphism in sporadic Alzheimer's disease. *Genes and immunity* 4, 234-238.
- Liu, P., Fleete, M.S., Jing, Y., Collie, N.D., Curtis, M.A., Waldvogel, H.J., Faull, R.L., Abraham, W.C., and Zhang, H. (2014). Altered arginine metabolism in Alzheimer's disease brains. *Neurobiol Aging* 35, 1992-2003.
- Liu, P., Jing, Y., Collie, N.D., Campbell, S.A., and Zhang, H. (2011). Pre-aggregated Abeta(25-35) alters arginine metabolism in the rat hippocampus and prefrontal cortex. *Neuroscience* 193, 269-282.

- Liu, Y., Yu, Y., Yang, S., Zeng, B., Zhang, Z., Jiao, G., Zhang, Y., Cai, L., and Yang, R. (2009). Regulation of arginase I activity and expression by both PD-1 and CTLA-4 on the myeloid-derived suppressor cells. *Cancer Immunol Immunother* 58, 687-697.
- Livak, K.J., and Schmittgen, T.D. (2001). Analysis of relative gene expression data using real-time quantitative PCR and the 2(-Delta Delta C(T)) Method. *Methods* 25, 402-408.
- Loser, C., Eisel, A., Harms, D., and Folsch, U.R. (1999). Dietary polyamines are essential luminal growth factors for small intestinal and colonic mucosal growth and development. *Gut* 44, 12-16.
- Ma, T., Trinh, M.A., Wexler, A.J., Bourbon, C., Gatti, E., Pierre, P., Cavener, D.R., and Klann, E. (2013a). Suppression of eIF2alpha kinases alleviates Alzheimer's disease-related plasticity and memory deficits. *Nat Neurosci* 16, 1299-1305.
- Ma, T., Trinh, M.A., Wexler, A.J., Bourbon, C., Gatti, E., Pierre, P., Cavener, D.R., and Klann, E. (2013b). Suppression of eIF2alpha kinases alleviates Alzheimer's disease-related plasticity and memory deficits. *Nature neuroscience*.
- Macewan, S.R., and Chilkoti, A. (2012). Digital switching of local arginine density in a genetically encoded self-assembled polypeptide nanoparticle controls cellular uptake. *Nano letters* 12, 3322-3328.
- MacIver, N.J., Michalek, R.D., and Rathmell, J.C. (2013). Metabolic regulation of T lymphocytes. *Annu Rev Immunol* 31, 259-283.
- Madisen, L., Zwingman, T.A., Sunkin, S.M., Oh, S.W., Zariwala, H.A., Gu, H., Ng, L.L., Palmiter, R.D., Hawrylycz, M.J., Jones, A.R., *et al.* (2010). A robust and high-throughput Cre reporting and characterization system for the whole mouse brain. *Nature neuroscience* 13, 133-140.
- Marlatt, M.W., Bauer, J., Aronica, E., van Haastert, E.S., Hoozemans, J.J., Joels, M., and Lucassen, P.J. (2014). Proliferation in the Alzheimer hippocampus is due to microglia, not astroglia, and occurs at sites of amyloid deposition. *Neural plasticity* 2014, 693851.
- Masters, C.L. (1984). Etiology and pathogenesis of Alzheimer's disease. *Pathology* 16, 233-234.
- Mattapallil, M.J., Wawrousek, E.F., Chan, C.C., Zhao, H., Roychoudhury, J., Ferguson, T.A., and Caspi, R.R. (2012). The Rd8 mutation of the *Crb1* gene is present in vendor lines of C57BL/6N mice and embryonic stem cells, and confounds ocular induced mutant phenotypes. *Invest Ophthalmol Vis Sci* 53, 2921-2927.

Maus, U., Herold, S., Muth, H., Maus, R., Ermert, L., Ermert, M., Weissmann, N., Rosseau, S., Seeger, W., Grimminger, F., *et al.* (2001). Monocytes recruited into the alveolar air space of mice show a monocytic phenotype but upregulate CD14. *American journal of physiology Lung cellular and molecular physiology* 280, L58-68.

Mazzini, E., Massimiliano, L., Penna, G., and Rescigno, M. (2014). Oral tolerance can be established via gap junction transfer of fed antigens from CX3CR1(+) macrophages to CD103(+) dendritic cells. *Immunity* 40, 248-261.

McCormick, M.J., Castells, M.C., Austen, K.F., and Katz, H.R. (1999). The gp49A gene has extensive sequence conservation with the gp49B gene and provides gp49A protein, a unique member of a large family of activating and inhibitory receptors of the immunoglobulin superfamily. *Immunogenetics* 50, 286-294.

McGeer, P.L., Itagaki, S., Tago, H., and McGeer, E.G. (1987). Reactive microglia in patients with senile dementia of the Alzheimer type are positive for the histocompatibility glycoprotein HLA-DR. *Neurosci Lett* 79, 195-200.

Mellor, A.L., and Munn, D.H. (2008). Creating immune privilege: active local suppression that benefits friends, but protects foes. *Nat Rev Immunol* 8, 74-80.

Mestas, J., and Hughes, C.C. (2004a). Of mice and not men: differences between mouse and human immunology. *J Immunol* 172, 2731-2738.

Mestas, J., and Hughes, C.C. (2004b). Of mice and not men: differences between mouse and human immunology. *J Immunol* 172, 2731-2738.

Miki, K., Kumar, A., Yang, R., Killeen, M.E., and Delude, R.L. (2009). Extracellular activation of arginase-1 decreases enterocyte inducible nitric oxide synthase activity during systemic inflammation. *American journal of physiology Gastrointestinal and liver physiology* 297, G840-848.

Mildner, A., Schlevogt, B., Kierdorf, K., Bottcher, C., Erny, D., Kummer, M.P., Quinn, M., Bruck, W., Bechmann, I., Heneka, M.T., *et al.* (2011). Distinct and non-redundant roles of microglia and myeloid subsets in mouse models of Alzheimer's disease. *J Neurosci* 31, 11159-11171.

Mildner, A., Schmidt, H., Nitsche, M., Merkler, D., Hanisch, U.K., Mack, M., Heikenwalder, M., Bruck, W., Priller, J., and Prinz, M. (2007). Microglia in the adult brain arise from Ly-6ChiCCR2+ monocytes only under defined host conditions. *Nat Neurosci* 10, 1544-1553.

- Misharin, A.V., Morales-Nebreda, L., Mutlu, G.M., Budinger, G.R., and Perlman, H. (2013). Flow cytometric analysis of macrophages and dendritic cell subsets in the mouse lung. *American journal of respiratory cell and molecular biology* 49, 503-510.
- Mizutani, M., Pino, P.A., Saederup, N., Charo, I.F., Ransohoff, R.M., and Cardona, A.E. (2012). The fractalkine receptor but not CCR2 is present on microglia from embryonic development throughout adulthood. *J Immunol* 188, 29-36.
- Moatti, D., Faure, S., Fumeron, F., Amara Mel, W., Seknadji, P., McDermott, D.H., Debre, P., Aumont, M.C., Murphy, P.M., de Prost, D., *et al.* (2001). Polymorphism in the fractalkine receptor CX3CR1 as a genetic risk factor for coronary artery disease. *Blood* 97, 1925-1928.
- Morris, G.P., Clark, I.A., and Vissel, B. (2014). Inconsistencies and controversies surrounding the amyloid hypothesis of Alzheimer's disease. *Acta neuropathologica communications* 2, 135.
- Morris, S.M., Jr. (2007). Arginine metabolism: boundaries of our knowledge. *J Nutr* 137, 1602S-1609S.
- Morris, S.M., Jr. (2012). Arginases and arginine deficiency syndromes. *Curr Opin Clin Nutr Metab Care* 15, 64-70.
- Mrak, R.E., and Griffin, W.S. (2005). Glia and their cytokines in progression of neurodegeneration. *Neurobiol Aging* 26, 349-354.
- Munder, M., Eichmann, K., Moran, J.M., Centeno, F., Soler, G., and Modolell, M. (1999). Th1/Th2-regulated expression of arginase isoforms in murine macrophages and dendritic cells. *J Immunol* 163, 3771-3777.
- Mussai, F., De Santo, C., Abu-Dayyeh, I., Booth, S., Quek, L., McEwen-Smith, R.M., Qureshi, A., Dazzi, F., Vyas, P., and Cerundolo, V. (2013). Acute myeloid leukemia creates an arginase-dependent immunosuppressive microenvironment. *Blood* 122, 749-758.
- Naert, G., and Rivest, S. (2011). CC chemokine receptor 2 deficiency aggravates cognitive impairments and amyloid pathology in a transgenic mouse model of Alzheimer's disease. *J Neurosci* 31, 6208-6220.
- Nasreddine, Z.S., Phillips, N.A., Bedirian, V., Charbonneau, S., Whitehead, V., Collin, I., Cummings, J.L., and Chertkow, H. (2005). The Montreal Cognitive Assessment, MoCA: a brief screening tool for mild cognitive impairment. *J Am Geriatr Soc* 53, 695-699.

- Nguyen, H.X., Beck, K.D., and Anderson, A.J. (2011). Quantitative assessment of immune cells in the injured spinal cord tissue by flow cytometry: a novel use for a cell purification method. *J Vis Exp*.
- Nichol, K.E., Poon, W.W., Parachikova, A.I., Cribbs, D.H., Glabe, C.G., and Cotman, C.W. (2008). Exercise alters the immune profile in Tg2576 Alzheimer mice toward a response coincident with improved cognitive performance and decreased amyloid. *J Neuroinflammation* 5, 13.
- Ostrowitzki, S., Deptula, D., Thurffjell, L., Barkhof, F., Bohrmann, B., Brooks, D.J., Klunk, W.E., Ashford, E., Yoo, K., Xu, Z.X., *et al.* (2012). Mechanism of amyloid removal in patients with Alzheimer disease treated with gantenerumab. *Arch Neurol* 69, 198-207.
- Papadopoulos, E.J., Sasseti, C., Saeki, H., Yamada, N., Kawamura, T., Fitzhugh, D.J., Saraf, M.A., Schall, T., Blauvelt, A., Rosen, S.D., *et al.* (1999). Fractalkine, a CX3C chemokine, is expressed by dendritic cells and is up-regulated upon dendritic cell maturation. *Eur J Immunol* 29, 2551-2559.
- Parkhurst, C.N., Yang, G., Ninan, I., Savas, J.N., Yates, J.R., 3rd, Lafaille, J.J., Hempstead, B.L., Littman, D.R., and Gan, W.B. (2013). Microglia promote learning-dependent synapse formation through brain-derived neurotrophic factor. *Cell* 155, 1596-1609.
- Pepin, J., Milord, F., Guern, C., and Schechter, P.J. (1987). Difluoromethylornithine for arseno-resistant *Trypanosoma brucei gambiense* sleeping sickness. *Lancet* 2, 1431-1433.
- Perry, V.H. (1998). A revised view of the central nervous system microenvironment and major histocompatibility complex class II antigen presentation. *J Neuroimmunol* 90, 113-121.
- Pesce, J.T., Ramalingam, T.R., Mentink-Kane, M.M., Wilson, M.S., El Kasmi, K.C., Smith, A.M., Thompson, R.W., Cheever, A.W., Murray, P.J., and Wynn, T.A. (2009). Arginase-1-expressing macrophages suppress Th2 cytokine-driven inflammation and fibrosis. *PLoS Pathog* 5, e1000371.
- Pettem, K.L., Yokomaku, D., Takahashi, H., Ge, Y., and Craig, A.M. (2013). Interaction between autism-linked MDGAs and neuroligins suppresses inhibitory synapse development. *J Cell Biol* 200, 321-336.
- Price, J.L., McKeel, D.W., Jr., Buckles, V.D., Roe, C.M., Xiong, C., Grundman, M., Hansen, L.A., Petersen, R.C., Parisi, J.E., Dickson, D.W., *et al.* (2009). Neuropathology of nondemented aging: presumptive evidence for preclinical Alzheimer disease. *Neurobiol Aging* 30, 1026-1036.

Prodinger, C., Bunse, J., Kruger, M., Schiefenhover, F., Brandt, C., Laman, J.D., Greter, M., Immig, K., Heppner, F., Becher, B., *et al.* (2011). CD11c-expressing cells reside in the juxtavascular parenchyma and extend processes into the glia limitans of the mouse nervous system. *Acta neuropathologica* 121, 445-458.

Radde, R., Duma, C., Goedert, M., and Jucker, M. (2008a). The value of incomplete mouse models of Alzheimer's disease. *Eur J Nucl Med Mol Imaging* 35 *Suppl* 1, S70-74.

Radde, R., Duma, C., Goedert, M., and Jucker, M. (2008b). The value of incomplete mouse models of Alzheimer's disease. *Eur J Nucl Med Mol Imaging* 35 *Suppl* 1, S70-74.

Ransohoff, R.M., and Cardona, A.E. (2010). The myeloid cells of the central nervous system parenchyma. *Nature* 468, 253-262.

Raychaudhuri, B., Rayman, P., Ireland, J., Ko, J., Rini, B., Borden, E.C., Garcia, J., Vogelbaum, M.A., and Finke, J. (2011). Myeloid-derived suppressor cell accumulation and function in patients with newly diagnosed glioblastoma. *Neuro-oncology* 13, 591-599.

Reeds, P.J. (2000). Dispensable and indispensable amino acids for humans. *J Nutr* 130, 1835S-1840S.

Rentz, D.M., Locascio, J.J., Becker, J.A., Moran, E.K., Eng, E., Buckner, R.L., Sperling, R.A., and Johnson, K.A. (2010). Cognition, reserve, and amyloid deposition in normal aging. *Ann Neurol* 67, 353-364.

Ridnour, L.A., Windhausen, A.N., Isenberg, J.S., Yeung, N., Thomas, D.D., Vitek, M.P., Roberts, D.D., and Wink, D.A. (2007). Nitric oxide regulates matrix metalloproteinase-9 activity by guanylyl-cyclase-dependent and -independent pathways. *Proc Natl Acad Sci U S A* 104, 16898-16903.

Rogers, J., Strohmeyer, R., Kovelowski, C.J., and Li, R. (2002). Microglia and inflammatory mechanisms in the clearance of amyloid beta peptide. *Glia* 40, 260-269.

Rogers, J.T., Morganti, J.M., Bachstetter, A.D., Hudson, C.E., Peters, M.M., Grimmig, B.A., Weeber, E.J., Bickford, P.C., and Gemma, C. (2011). CX3CR1 deficiency leads to impairment of hippocampal cognitive function and synaptic plasticity. *J Neurosci* 31, 16241-16250.

Rozemuller, J.M., Eikelenboom, P., and Stam, F.C. (1986). Role of microglia in plaque formation in senile dementia of the Alzheimer type. An immunohistochemical study. *Virchows Archiv B, Cell pathology including molecular pathology* 51, 247-254.

- Salminen, A., Ojala, J., Kauppinen, A., Kaarniranta, K., and Suuronen, T. (2009). Inflammation in Alzheimer's disease: amyloid-beta oligomers trigger innate immunity defence via pattern recognition receptors. *Prog Neurobiol* 87, 181-194.
- Sangaletti, S., Tripodo, C., Sandri, S., Torselli, I., Vitali, C., Ratti, C., Botti, L., Burocchi, A., Porcasi, R., Tomirotti, A., *et al.* (2014). Osteopontin shapes immunosuppression in the metastatic niche. *Cancer Res* 74, 4706-4719.
- Santiago, M.L., Montano, M., Benitez, R., Messer, R.J., Yonemoto, W., Chesebro, B., Hasenkrug, K.J., and Greene, W.C. (2008). Apobec3 encodes Rfv3, a gene influencing neutralizing antibody control of retrovirus infection. *Science* 321, 1343-1346.
- Saresella, M., Calabrese, E., Marventano, I., Piancone, F., Gatti, A., Farina, E., Alberoni, M., and Clerici, M. (2012). A potential role for the PD1/PD-L1 pathway in the neuroinflammation of Alzheimer's disease. *Neurobiol Aging* 33, 624 e611-622.
- Sasaki, A., Nakazato, Y., Ogawa, A., and Sugihara, S. (1996). The immunophenotype of perivascular cells in the human brain. *Pathol Int* 46, 15-23.
- Saunders, A.M., Hulette, O., Welsh-Bohmer, K.A., Schmechel, D.E., Crain, B., Burke, J.R., Alberts, M.J., Strittmatter, W.J., Breitner, J.C., and Rosenberg, C. (1996). Specificity, sensitivity, and predictive value of apolipoprotein-E genotyping for sporadic Alzheimer's disease. *Lancet* 348, 90-93.
- Schneider, E., and Dy, M. (1985). The role of arginase in the immune response. *Immunol Today* 6, 136-140.
- Schulz, C., Gomez Perdiguero, E., Chorro, L., Szabo-Rogers, H., Cagnard, N., Kierdorf, K., Prinz, M., Wu, B., Jacobsen, S.E., Pollard, J.W., *et al.* (2012). A Lineage of Myeloid Cells Independent of Myb and Hematopoietic Stem Cells. *Science*.
- Seiler, N. (2003). Thirty years of polyamine-related approaches to cancer therapy. Retrospect and prospect. Part 2. Structural analogues and derivatives. *Current drug targets* 4, 565-585.
- Selamnia, M., Mayeur, C., Robert, V., and Blachier, F. (1998). Alpha-difluoromethylornithine (DFMO) as a potent arginase activity inhibitor in human colon carcinoma cells. *Biochem Pharmacol* 55, 1241-1245.
- Seok, J., Warren, H.S., Cuenca, A.G., Mindrinos, M.N., Baker, H.V., Xu, W., Richards, D.R., McDonald-Smith, G.P., Gao, H., Hennessy, L., *et al.* (2013). Genomic responses in

mouse models poorly mimic human inflammatory diseases. *Proceedings of the National Academy of Sciences of the United States of America* 110, 3507-3512.

Serafini, P., Borrello, I., and Bronte, V. (2006). Myeloid suppressor cells in cancer: recruitment, phenotype, properties, and mechanisms of immune suppression. *Seminars in cancer biology* 16, 53-65.

Sherrington, R., Rogaev, E.I., Liang, Y., Rogaeva, E.A., Levesque, G., Ikeda, M., Chi, H., Lin, C., Li, G., Holman, K., *et al.* (1995). Cloning of a gene bearing missense mutations in early-onset familial Alzheimer's disease. *Nature* 375, 754-760.

Strittmatter, W.J., Saunders, A.M., Schmechel, D., Pericak-Vance, M., Enghild, J., Salvesen, G.S., and Roses, A.D. (1993). Apolipoprotein E: high-avidity binding to beta-amyloid and increased frequency of type 4 allele in late-onset familial Alzheimer disease. *Proc Natl Acad Sci U S A* 90, 1977-1981.

Tambuyzer, B.R., Ponsaerts, P., and Nouwen, E.J. (2009). Microglia: gatekeepers of central nervous system immunology. *J Leukoc Biol* 85, 352-370.

Tamoutounour, S., Henri, S., Lelouard, H., de Bovis, B., de Haar, C., van der Woude, C.J., Woltman, A.M., Reyat, Y., Bonnet, D., Sichien, D., *et al.* (2012). CD64 distinguishes macrophages from dendritic cells in the gut and reveals the Th1-inducing role of mesenteric lymph node macrophages during colitis. *Eur J Immunol* 42, 3150-3166.

Tan, J., Town, T., Crawford, F., Mori, T., DelleDonne, A., Crescentini, R., Obregon, D., Flavell, R.A., and Mullan, M.J. (2002a). Role of CD40 ligand in amyloidosis in transgenic Alzheimer's mice. *Nat Neurosci* 5, 1288-1293.

Tan, J., Town, T., Mori, T., Wu, Y., Saxe, M., Crawford, F., and Mullan, M. (2000). CD45 opposes beta-amyloid peptide-induced microglial activation via inhibition of p44/42 mitogen-activated protein kinase. *J Neurosci* 20, 7587-7594.

Tan, J., Town, T., and Mullan, M. (2002b). CD40-CD40L interaction in Alzheimer's disease. *Current opinion in pharmacology* 2, 445-451.

Tang, W.H., Wang, Z., Cho, L., Brennan, D.M., and Hazen, S.L. (2009). Diminished global arginine bioavailability and increased arginine catabolism as metabolic profile of increased cardiovascular risk. *J Am Coll Cardiol* 53, 2061-2067.

Tenu, J.P., Lepoivre, M., Moali, C., Brollo, M., Mansuy, D., and Boucher, J.L. (1999). Effects of the new arginase inhibitor N(omega)-hydroxy-nor-L-arginine on NO synthase activity in murine macrophages. *Nitric Oxide* 3, 427-438.

Togo, T., Akiyama, H., Iseki, E., Kondo, H., Ikeda, K., Kato, M., Oda, T., Tsuchiya, K., and Kosaka, K. (2002). Occurrence of T cells in the brain of Alzheimer's disease and other neurological diseases. *J Neuroimmunol* 124, 83-92.

Tooyama, I., Kimura, H., Akiyama, H., and McGeer, P.L. (1990). Reactive microglia express class I and class II major histocompatibility complex antigens in Alzheimer's disease. *Brain Res* 523, 273-280.

Trueba-Saiz, A., Cavada, C., Fernandez, A.M., Leon, T., Gonzalez, D.A., Fortea Ormaechea, J., Lleo, A., Del Ser, T., Nunez, A., and Torres-Aleman, I. (2013). Loss of serum IGF-I input to the brain as an early biomarker of disease onset in Alzheimer mice. *Translational psychiatry* 3, e330.

Tukhovskaya, E.A., Yukin, A.Y., Khokhlova, O.N., Murashev, A.N., and Vitek, M.P. (2009). COG1410, a novel apolipoprotein-E mimetic, improves functional and morphological recovery in a rat model of focal brain ischemia. *J Neurosci Res* 87, 677-682.

Vitek, M.P., Brown, C.M., and Colton, C.A. (2009). APOE genotype-specific differences in the innate immune response. *Neurobiol Aging* 30, 1350-1360.

Vitek, M.P., Christensen, D.J., Wilcock, D., Davis, J., Van Nostrand, W.E., Li, F.Q., and Colton, C.A. (2012). APOE-mimetic peptides reduce behavioral deficits, plaques and tangles in Alzheimer's disease transgenics. *Neuro-degenerative diseases* 10, 122-126.

Vitek, M.P., Snell, J., Dawson, H., and Colton, C.A. (1997). Modulation of nitric oxide production in human macrophages by apolipoprotein-E and amyloid-beta peptide. *Biochem Biophys Res Commun* 240, 391-394.

Vockley, J.G., Jenkinson, C.P., Shukla, H., Kern, R.M., Grody, W.W., and Cederbaum, S.D. (1996). Cloning and characterization of the human type II arginase gene. *Genomics* 38, 118-123.

Walker, D.G., and Lue, L.F. (2005). Investigations with cultured human microglia on pathogenic mechanisms of Alzheimer's disease and other neurodegenerative diseases. *J Neurosci Res* 81, 412-425.

Walker, D.G., and Lue, L.F. (2013). Understanding the neurobiology of CD200 and the CD200 receptor: a therapeutic target for controlling inflammation in human brains? *Future neurology* 8.

- Wang, H., Christensen, D.J., Vitek, M.P., Sullivan, P.M., and Laskowitz, D.T. (2009). APOE genotype affects outcome in a murine model of sepsis: implications for a new treatment strategy. *Anaesthesia and intensive care* 37, 38-45.
- Wang, J., Yu, J.T., Wang, H.F., Meng, X.F., Wang, C., Tan, C.C., and Tan, L. (2015). Pharmacological treatment of neuropsychiatric symptoms in Alzheimer's disease: a systematic review and meta-analysis. *J Neurol Neurosurg Psychiatry* 86, 101-109.
- Wang, Y., Szretter, K.J., Vermi, W., Gilfillan, S., Rossini, C., Cella, M., Barrow, A.D., Diamond, M.S., and Colonna, M. (2012). IL-34 is a tissue-restricted ligand of CSF1R required for the development of Langerhans cells and microglia. *Nat Immunol* 13, 753-760.
- Webster, S.J., Bachstetter, A.D., Nelson, P.T., Schmitt, F.A., and Van Eldik, L.J. (2014). Using mice to model Alzheimer's dementia: an overview of the clinical disease and the preclinical behavioral changes in 10 mouse models. *Frontiers in genetics* 5, 88.
- Weinberg, J.B. (1998). Nitric oxide production and nitric oxide synthase type 2 expression by human mononuclear phagocytes: a review. *Mol Med* 4, 557-591.
- Weinberg, J.B., Lopansri, B.K., Mwaikambo, E., and Granger, D.L. (2008). Arginine, nitric oxide, carbon monoxide, and endothelial function in severe malaria. *Curr Opin Infect Dis* 21, 468-475.
- Weinberg, J.B., Misukonis, M.A., Shami, P.J., Mason, S.N., Sauls, D.L., Dittman, W.A., Wood, E.R., Smith, G.K., McDonald, B., Bachus, K.E., *et al.* (1995). Human mononuclear phagocyte inducible nitric oxide synthase (iNOS): analysis of iNOS mRNA, iNOS protein, biopterin, and nitric oxide production by blood monocytes and peritoneal macrophages. *Blood* 86, 1184-1195.
- Wilcock, D.M., and Colton, C.A. (2008). Anti-amyloid-beta immunotherapy in Alzheimer's disease: relevance of transgenic mouse studies to clinical trials. *J Alzheimers Dis* 15, 555-569.
- Wilcock, D.M., Lewis, M.R., Van Nostrand, W.E., Davis, J., Previti, M.L., Gharkholonarehe, N., Vitek, M.P., and Colton, C.A. (2008). Progression of amyloid pathology to Alzheimer's disease pathology in an amyloid precursor protein transgenic mouse model by removal of nitric oxide synthase 2. *The Journal of neuroscience : the official journal of the Society for Neuroscience* 28, 1537-1545.
- Wilcock, D.M., Morgan, D., Gordon, M.N., Taylor, T.L., Ridnour, L.A., Wink, D.A., and Colton, C.A. (2011a). Activation of matrix metalloproteinases following anti-Abeta

immunotherapy; implications for microhemorrhage occurrence. *J Neuroinflammation* 8, 115.

Wilcock, D.M., Zhao, Q., Morgan, D., Gordon, M.N., Everhart, A., Wilson, J.G., Lee, J.E., and Colton, C.A. (2011b). Diverse inflammatory responses in transgenic mouse models of Alzheimer's disease and the effect of immunotherapy on these responses. *ASN neuro* 3, 249-258.

Wink, D.A., Hines, H.B., Cheng, R.Y., Switzer, C.H., Flores-Santana, W., Vitek, M.P., Ridnour, L.A., and Colton, C.A. (2011). Nitric oxide and redox mechanisms in the immune response. *J Leukoc Biol* 89, 873-891.

Wolf, Y., Yona, S., Kim, K.W., and Jung, S. (2013). Microglia, seen from the CX3CR1 angle. *Frontiers in cellular neuroscience* 7, 26.

Wright, K.O., Murray, D.A., Crispe, N.I., and Pierce, R.H. (2005). Quantitative PCR for detection of the OT-1 transgene. *BMC immunology* 6, 20.

Wu, G., Bazer, F.W., Davis, T.A., Kim, S.W., Li, P., Marc Rhoads, J., Carey Satterfield, M., Smith, S.B., Spencer, T.E., and Yin, Y. (2009). Arginine metabolism and nutrition in growth, health and disease. *Amino Acids* 37, 153-168.

Wyss-Coray, T. (2006). Inflammation in Alzheimer disease: driving force, bystander or beneficial response? *Nat Med* 12, 1005-1015.

Yao, A., Liu, F., Chen, K., Tang, L., Liu, L., Zhang, K., Yu, C., Bian, G., Guo, H., Zheng, J., *et al.* (2014). Programmed Death 1 Deficiency Induces the Polarization of Macrophages/Microglia to the M1 Phenotype After Spinal Cord Injury in Mice. *Neurotherapeutics*.

Yeo, T.W., Lampah, D.A., Gitawati, R., Tjitra, E., Kenangalem, E., Granger, D.L., Weinberg, J.B., Lopansri, B.K., Price, R.N., Celermajer, D.S., *et al.* (2008a). Safety profile of L-arginine infusion in moderately severe falciparum malaria. *PLoS One* 3, e2347.

Yeo, T.W., Lampah, D.A., Gitawati, R., Tjitra, E., Kenangalem, E., McNeil, Y.R., Darcy, C.J., Granger, D.L., Weinberg, J.B., Lopansri, B.K., *et al.* (2008b). Recovery of endothelial function in severe falciparum malaria: relationship with improvement in plasma L-arginine and blood lactate concentrations. *J Infect Dis* 198, 602-608.

Yi, J., Horvay, L.L., Friedlich, A.L., Shi, Y., Rogers, J.T., and Huang, X. (2009). L-arginine and Alzheimer's disease. *Int J Clin Exp Pathol* 2, 211-238.

- Yona, S., Kim, K.W., Wolf, Y., Mildner, A., Varol, D., Breker, M., Strauss-Ayali, D., Viukov, S., Guilliams, M., Misharin, A., *et al.* (2013). Fate mapping reveals origins and dynamics of monocytes and tissue macrophages under homeostasis. *Immunity* 38, 79-91.
- Young, J.E., Martinez, R.A., and La Spada, A.R. (2009). Nutrient deprivation induces neuronal autophagy and implicates reduced insulin signaling in neuroprotective autophagy activation. *The Journal of biological chemistry* 284, 2363-2373.
- Yu, A.Y., Shimoda, L.A., Iyer, N.V., Huso, D.L., Sun, X., McWilliams, R., Beaty, T., Sham, J.S., Wiener, C.M., Sylvester, J.T., *et al.* (1999). Impaired physiological responses to chronic hypoxia in mice partially deficient for hypoxia-inducible factor 1alpha. *J Clin Invest* 103, 691-696.
- Yu, H., Iyer, R.K., Kern, R.M., Rodriguez, W.I., Grody, W.W., and Cederbaum, S.D. (2001). Expression of arginase isozymes in mouse brain. *J Neurosci Res* 66, 406-422.
- Zaynagetdinov, R., Sherrill, T.P., Kendall, P.L., Segal, B.H., Weller, K.P., Tighe, R.M., and Blackwell, T.S. (2013). Identification of myeloid cell subsets in murine lungs using flow cytometry. *American journal of respiratory cell and molecular biology* 49, 180-189.
- Zhang, B., Gaiteri, C., Bodea, L.G., Wang, Z., McElwee, J., Podtelezhnikov, A.A., Zhang, C., Xie, T., Tran, L., Dobrin, R., *et al.* (2013a). Integrated systems approach identifies genetic nodes and networks in late-onset Alzheimer's disease. *Cell* 153, 707-720.
- Zhang, R., Miller, R.G., Madison, C., Jin, X., Honrada, R., Harris, W., Katz, J., Forshe, D.A., and McGrath, M.S. (2013b). Systemic immune system alterations in early stages of Alzheimer's disease. *J Neuroimmunol* 256, 38-42.
- Zigman, W.B., Devenny, D.A., Krinsky-McHale, S.J., Jenkins, E.C., Urv, T.K., Wegiel, J., Schupf, N., and Silverman, W. (2008). Alzheimer's Disease in Adults with Down Syndrome. *International review of research in mental retardation* 36, 103-145.
- Ziv, Y., Ron, N., Butovsky, O., Landa, G., Sudai, E., Greenberg, N., Cohen, H., Kipnis, J., and Schwartz, M. (2006). Immune cells contribute to the maintenance of neurogenesis and spatial learning abilities in adulthood. *Nat Neurosci* 9, 268-275.

## Biography

Matthew Kan was born on April 19, 1985 in Poughkeepsie, New York to John Kan and Yin Liu. He and his younger sister, Caroline, grew up in Poughkeepsie, and Danville, California. Matthew attended Harvard College, where he studied Biology, and graduated with an A.B. *cum laude* in 2007. He became a medical and graduate student at Duke University School of Medicine in 2008. In 2015, he and his colleagues published a research article, "Arginine deprivation and immune suppression in a mouse model of Alzheimer's Disease" in *The Journal of Neuroscience* outlining a novel mechanism for neuronal death in Alzheimer's disease.

Matthew is a recipient of a 2011 Chrysalis Award from the American Association of Asthma, Allergy, and Immunology, a Kenan-Biddle Partnership Grant from the William R. Kenan Charitable Trust and the Mary Duke Biddle Foundation in 2012, second place in the 2013 annual Duke Immunology D. Bernard Amos Research Award, and a Junior Scientist Travel Fellowship from the 2014 FASEB Summer Research Conference on Translational Neuroimmunology. He is a member of the American Association of Immunologists and the International Society for Neurochemistry.